AD-A080 158 AIR FORCE INST OF TECH WRIGHT-PATTERSON AFB OH SCHOO--ETC F/G 17/2.1
PULSE-WIDTH MODULATION OF SPREAD SPECTRUM CARRIERS.(U)
DEC 79 F D TILLER
UNCLASSIFIED AFIT/GE/EE/79-39 NL

1 OF 2
AD-
A080158

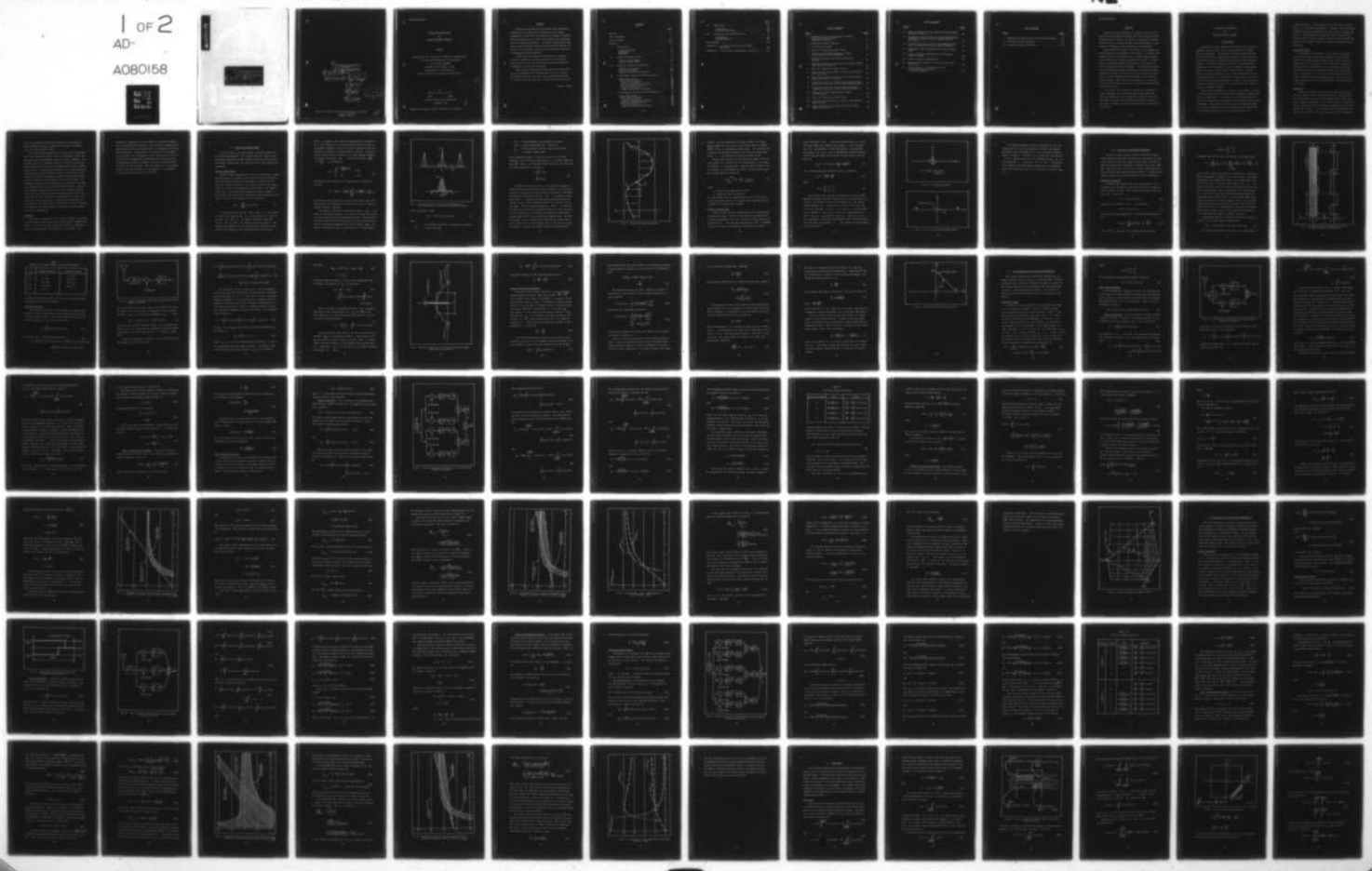

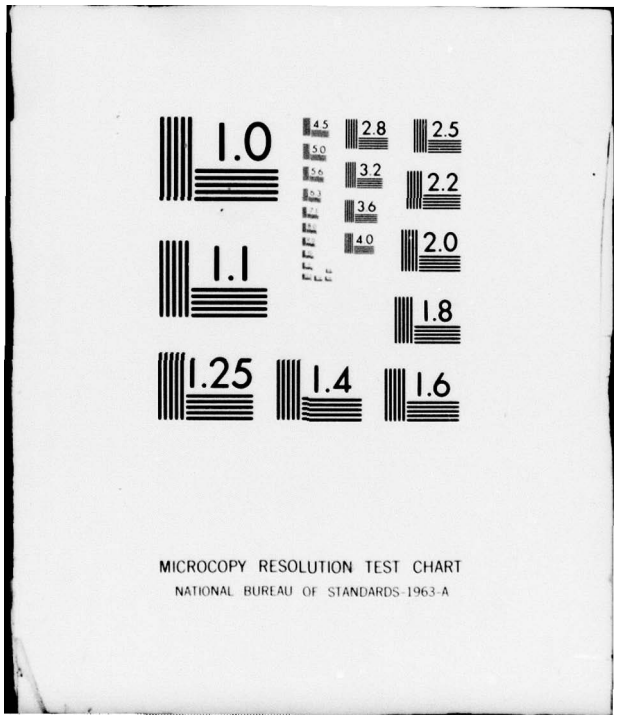
1.0
1.1
1.25
1.4
1.6
1.8
2.0
2.2
2.5
2.8
3.2
3.6
4.0
4.5
5.0
5.6
MICROCOPY RESOLUTION TEST CHART
NATIONAL BUREAU OF STANDARDS-1963-A

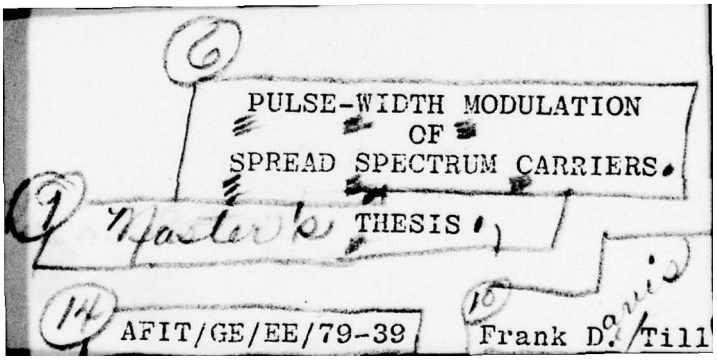
PULSE-WIDTH MODULATION
OF
SPREAD SPECTRUM CARRIERS.
Master's THESIS
AFIT/GE/EE/79-39
Frank D. Till

(6) PULSE-WIDTH MODULATION OF SPREAD SPECTRUM CARRIERS.

(9) Master's THESIS,

(14) AFIT/GE/EE/79-39

(10) Frank D. Tiller
Capt USAF

(11) Dec 79

(12) 121

(16) 2277

Approved for public release; distribution unlimited

AFIT/GE/EE/79-39

PULSE-WIDTH MODULATION
OF
SPREAD SPECTRUM CARRIERS

THESIS

Presented to the Faculty of the School of Engineering
of the Air Force Institute of Technolody
Air Training Command
in Partial Fulfillment of the
Requirements for the Degree of
Master of Science in Electrical Engineering

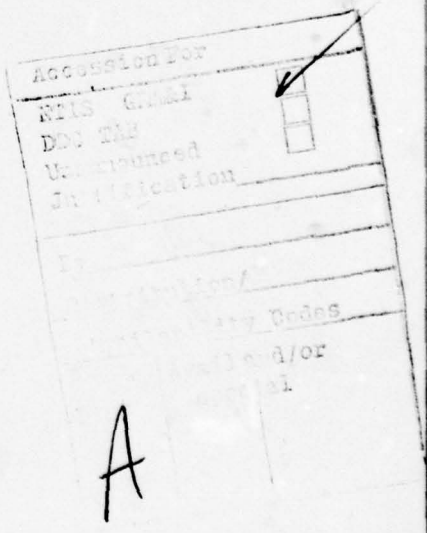

by
Frank D. Tiller, B.S.E.E.
Capt USAF
Graduate Electrical Engineering
December 1979

Preface

Situations involving both intentional and inadvertent interference in communication systems are very common. Consequently, there has been substantial interest in spread spectrum modulation as a method of mitigating the resulting impact on system performance. This paper investigates three linear spread spectrum formats that provide the inherent advantage of interference rejection with the unique capability to superimpose desired signals.

I would like to express my appreciation to Captain Stanley R. Robinson, my thesis advisor, for his patient guidance and for the many stimulating discussions offered throughout the course of this work.

This project would not have been possible without the help, encouragement and understanding of my wife, Jackie. Her unselfishness for the past two years has permitted me to achieve a personal goal that I have wanted for some time.

Frank D. Tiller

Contents

List of Figures

List of Figures

List of Tables

Abstract

Spread spectrum techniques can produce results in communication and navigation systems that are not possible with standard signal formats. The results of particular interest are the ability to screen messages from eavesdroppers, high resolution ranging and the rejection of interference.

Three modulation schemes that exploit these spread spectrum properties are analyzed in this thesis. All three techniques use pulse-width modulation to encode sampled analog voice signals onto a digital phase coded carrier. The performance analysis assumes transmission in the presence of white Gaussian noise and CW jamming. The performance analysis uses maximum likelihood estimation to define the sample parameter estimate and associated error variance when probability density functions can be defined for the receiver sample outputs. When the density function is not available a second moment analysis is used to define the expected signal-to-noise ratio.

The results are extended to include the introduction of signal dependent code noise into the receiver resulting from the degradation of the orthogonal code word structure. The impact of code noise on system performance is seen to grow with the number of users squared and the received signal energy.

PULSE-WIDTH MODULATION
OF
SPREAD SPECTRUM CARRIERS

I. Introduction

The need for robust communication systems has caused considerable interest within the last several years in spread spectrum techniques. The application of spread spectrum modulation techniques to communication systems provides capabilities which cannot be obtained through conventional modulation formats. The primary advantage provided by spread spectrum modulation is the capability to reject jamming by interfering signals in order that the desired signal can be recovered. This anti-jam (AJ) capability is of great significance to military communications as it provides a large measure of protection from active countermeasures by an enemy. This signal discrimination capability also allows multiple access by many signals in a common RF channel.

Spread spectrum modulation results in a wideband, low-power density signal which has statistical properties somewhat similar to random noise. As a result, the transmitted signal is not readily detected or recognized by conventional surveillance techniques. When detected, recovery of the baseband information from the wideband transmitted signal can be accomplished only through correlation with an exact replica of the

transmitted signal. This property denies the casual listener access to the baseband information. Therefore, spread spectrum modulation provides message privacy and selective calling capability. The additional inherent navigation capability and high multipath tolerance coupled with the features already mentioned are the salient reasons for employing spread spectrum modulation.

Problem Statement

The purpose of this thesis is to examine and evaluate three direct sequence modulation schemes that pulse-width modulate the pseudo-noise codewords (Dixon, 1976: 121) with sampled analog voice signals. These modulation schemes are antipodal pulse-width modulation, bi-orthogonal word pulse-width modulation and tri-orthogonal word pulse-width modulation. The analysis is to be made with the objective of providing a mutual system performance measure for the three encoding schemes that can be considered when choosing a modulation format.

Background

There are four basic techniques for generating spread spectrum signals: direct sequence modulation, frequency hopping, pulsed-FM or chirp and time hopping (Dixon, 1976: 14). Direct sequence modulation, as the name implies, is generated when a binary code sequence directly modulates the radio frequency (RF) carrier. In the general case the modulation format may be AM, FM or any other amplitude or angle modulation

form. The modulation techniques examined in this paper all use the direct sequence or pseudo-noise format to bi-phase shift key (PSK) the RF carrier.

The binary code sequences to be studied can be classified into four categories: maximal linear, non-maximal linear, maximal nonlinear and nonmaximal nonlinear (Judge, 1962:81). The maximal linear or m sequences exhibit a two-valued autocorrelation structure for whole bit increments which closely approximates that of a random binary sequence. The maximal nonlinear sequences have an autocorrelation which is a function of the relative time shift and produce a many valued autocorrelation structure similar to that produced by the linear codes. The nonmaximal sequences have autocorrelation properties that make them inappropriate for most practical applications. The nonlinear maximal sequences are used in most practical systems since their autocorrelation structure approximates that of an m sequence and they offer greatly improved privacy due to the nonlinear nature of the code. Linear maximal sequences will be assumed in this paper because they provide an upper performance bound for non-linear maximal sequences and their properties are well understood.

Approach

The thesis is organized into six main sections. The first section develops the notation and structure used throughout the paper. In each of the next three main sections, a modulation format is analyzed and its performance is predicted. The

sequence of presentation will be based on increasing complexity of the modulation technique, starting with antipodal pulse-width modulation and concluding with tri-orthogonal word pulse-width modulation. Performance in the multi-user environment and code noise will be analyzed in the sixth section, with conclusions and recommendations presented in the final section. The appendices contain a summary of the more involved issues necessary for the analysis. When the results of a calculation or derivation are included in the appendix, it is mentioned in the corresponding section of the text.

II. Signal and Channel Model

In this chapter, the basic signal and channel model will be defined and analyzed. The channel model will apply to all pulse-width modulation formats and with additional definition the general signal model can yield any of the three modulation techniques.

General Signal Model

Maximal linear sequences will be used to analyze all spread spectrum modulation formats since their performance provides a very tight upper bound on the performance of more practical nonlinear maximal sequences. The linear sequences also approximate very closely the benchmark characteristics of a random binary wave. The pulse-width modulation formats require at most three linear pseudo-noise sequences that are mutually orthogonal. The ith code waveform will be written as

$$C_i(t) = \sum_{j=-\infty}^{\infty} a_j P_{T_c}(t-jT_c) \qquad (1)$$

All sequences have periods $T=NT_c$ where N is the number of "chips" per codeword and T_c is the duration of a chip in seconds. The terms a_j are sequence elements taken from $\{+1,-1\}$ and $P_{T_c}(t)=1$ for $0\leq t\leq T_c$ and zero otherwise. The pseudonoise sequences are thus deterministic waveforms known only to the transmitter and intended receiver that repeat

every T seconds. The principle characteristic of interest for a code sequence is its autocorrelation function which is discussed in Appendix A and the Fourier transform of the autocorrelation function, its power spectral density. The normalized autocorrelation function of a linear maximal sequence is periodic with period NT_c . During the interval $\frac{-NT_c}{2} \leq \tau \leq \frac{NT_c}{2}$ it is defined by

$$R(\tau) = \begin{cases} \left[1 - \left(\frac{N+1}{NT_c}\right)(|\tau|)\right] , & |\tau| \leq T_c \\ -\frac{1}{N} , & |\tau| > T_c \end{cases} \quad (2)$$

The power spectral density of a linear maximal sequence is given by

$$S(f) = \frac{1}{N^2}\delta(f) + \left(\frac{1+N}{N^2}\right) \sum_{\substack{k=-\infty \\ k\neq 0}}^{\infty} \operatorname{sinc}^2\left(\frac{k}{N}\right) \delta\left(f - \frac{k}{NT_c}\right) \quad (3)$$

The periodic autocorrelation function and discrete power spectral density of a pseudonoise sequence with $N=7$ is shown in Figure 1 (Haykin, 1978:187).

The heart of the general transmitted signal, $x(t)$, is a generic pseudonoise waveform $c(t)$ which is structured to satisfy the desired pulse-width modulation format. The waveform structure ranges from the continuous use of one selected waveform to interleaving segments from three separate codes. The general transmitted signal is represented by a binary phase-

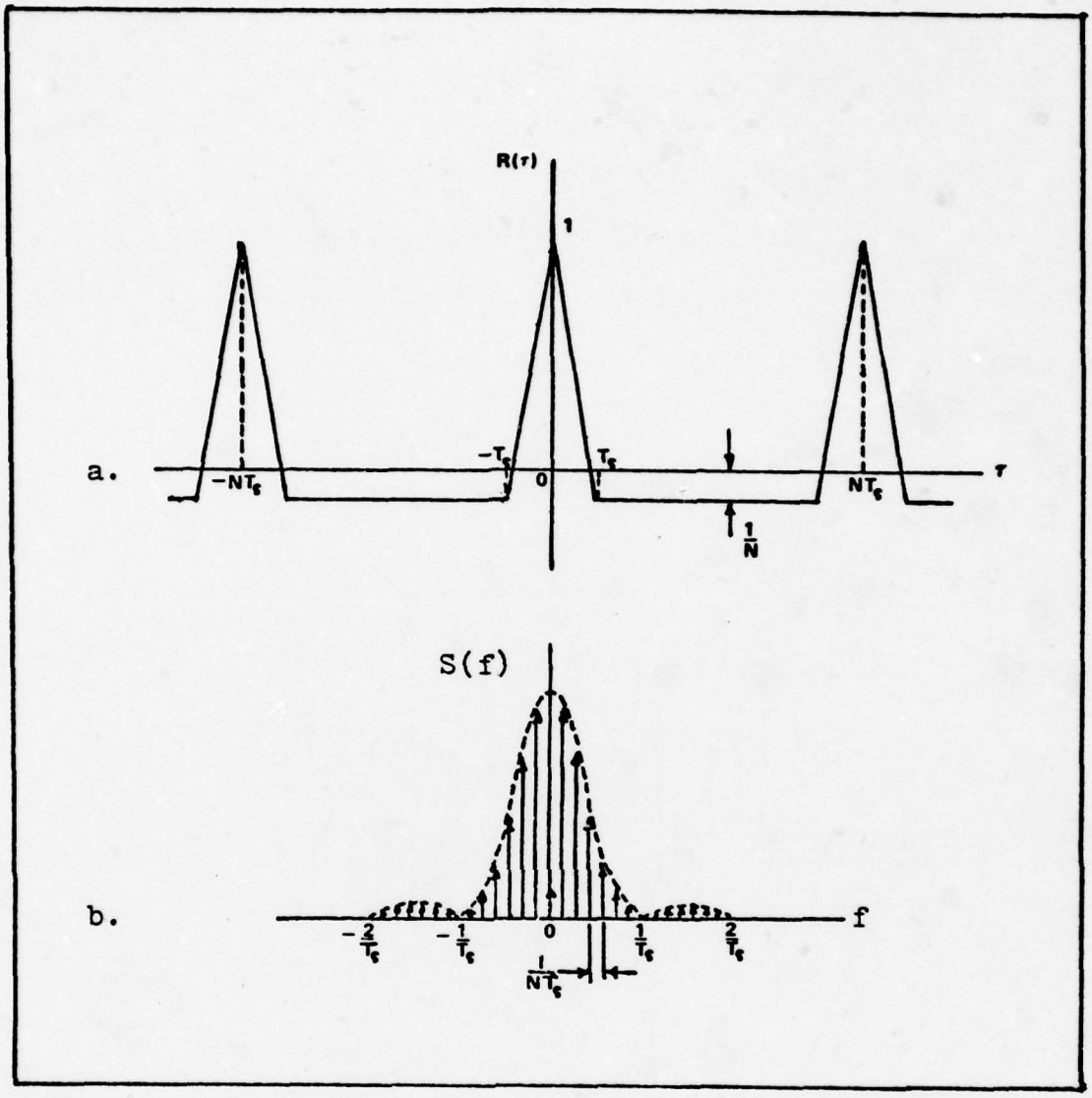

Fig 1. Characteristics of Linear Maximal Sequence
(a) Autocorrelation Function (b) Spectral Density

shift keyed (PSK) format

$$x(t) = \sqrt{P}\, p(m,t)c(t)\cos(\omega_0 t) \qquad (4)$$

where

ω_0 = the transmit frequency in radian/sec.($\omega_0 = 2\pi f_0$)

$\sqrt{P}$ = signal amplitude

$c(t)$ = the pseudonoise code waveform $|c(t)|=1$

$p(m,t)$ = pulse-width modulation $|p(m,t)|=1$

m_k = the kth sample from the input waveform $m(t)$

m = a generic sample value

This transmitted signal is limited in power to P/2 watts; therefore the total energy dissipated in T seconds cannot exceed $\frac{PT}{2}$ joules. The maximum energy associated with each sample value transmitted is given by

$$E = \int_0^T x^2(t)dt = \frac{PT}{2} \text{ joules} \tag{5}$$

A geometric interpretation of the transmitted signal associated with each modulation scheme analyzed in this thesis is available through signal space concepts (Wozencraft, 1965:225). The generic pseudonoise waveform, $c(t)$, is composed of segments from k orthogonal pseudonoise waveforms which can be thought of as a set of orthonormal base functions for the signal space. The pulse-width modulation, $p(m,t)$, is used to determine the coefficients associated with each bases function in the k-dimensional signal space and therefore determines a unique signal vector for each possible sample value. The sample values m_i are obtained from sampling the normalized input waveform $m(t)$ at the Nyquist rate of $\frac{1}{T}$ Hertz as shown in Figure 2. Because the sample values are constrained to

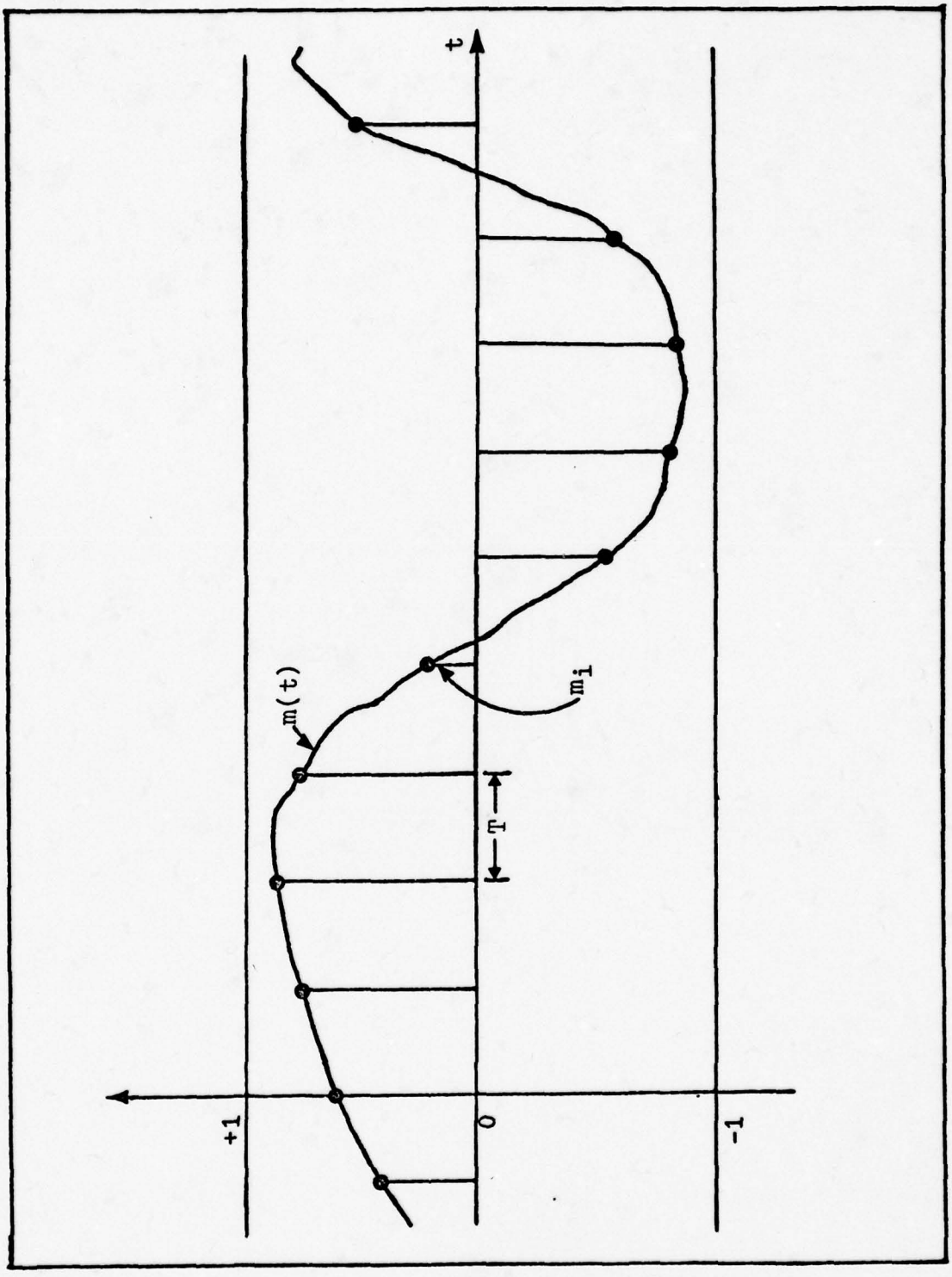

Fig. 2. Normalized Message Sampling

$-1 \leq m_i \leq +1$ and the transmitter is power limited, the transmitted signal will lie within an Euclidean sphere of radius $\sqrt{PT/2}$ in the k dimensional signal space. The receiver will correlate the transmitted signal vector with the bases functions, ζ_i, to obtain the transmitted sample value.

In an actual receiver the reconstructed sample value can only assume $N-1$ discrete values corresponding to the number of chips per T second period. When the input waveform $m(t)$ is assumed to be distributed uniformly, the mean square error due to quantization is given by

$$\varepsilon^2 = \frac{1}{\Delta}\int_{-\Delta/2}^{\Delta/2} x^2 dx = \frac{\Delta^2}{12} = \frac{1}{12(N-1)^2} \qquad (6)$$

where

Δ = width of one quantization level.

N = number of chips per period.

The code period will be assumed sufficiently long to allow this quantization error to be ignored when computing the performance of all modulation schemes.

General Channel Model

Using a tilde to denote random quantities, transmission through the channel results in the additive introduction of the noise processes $\tilde{n}(t)$ and $\tilde{J}(t)\cos(\omega_0 t - \tilde{\theta}) = \tilde{J}_x(t)\cos(\omega_0 t) + \tilde{J}_y(t)\sin(\omega_0 t)$. The channel noise process $\tilde{n}(t)$ is assumed to be a zero mean white Gaussian process with two-sided

spectral density $N_0/2$. The second noise process is a narrow-band jammer with random uniform phase $\underset{\sim}{\theta}$ and the envelope $\underset{\sim}{J}(t)$ is modeled as a Rayleigh process. In quadrature form $\underset{\sim}{J}_x(t)$ and $\underset{\sim}{J}_y(t)$ are two independent Gaussian processes with the zero means and the same autocorrelation function given by

$$R_{J_0}(\tau) = J_0 \text{sinc}(B\tau) = \left(\frac{J_0}{B}\right) \frac{\sin(\pi B\tau)}{\pi\tau} \tag{7}$$

the corresponding power spectral density is given by

$$S_{J_0}(f) = \left(\frac{J_0}{B}\right) \Pi \left(\frac{f}{B}\right) \tag{8}$$

where

$$\Pi(t) = \begin{cases} 1, & |t| \leq \frac{1}{2} \\ 0, & |t| > \frac{1}{2} \end{cases} \tag{9}$$

The channel model then can be defined as a discrete-time memoryless additive Gaussian channel with an average power constraint. The channel has an input alphabet A_x and channel output alphabet A_z , both equal to the set of all real numbers in the interval $[-1,+1]$. If $x_1, x_2, x_3, \ldots$ are the inputs to the channel at times $1,2,3,\ldots$ then the corresponding outputs $z_1, z_2, z_3, \ldots$ are given by $z_i = x_i + y_i$, where $y_1, y_2, y_3, \ldots$ are independent, identically distributed normal random variables with mean zero and variance σ^2 . This channel is often depicted as in Figure 3.

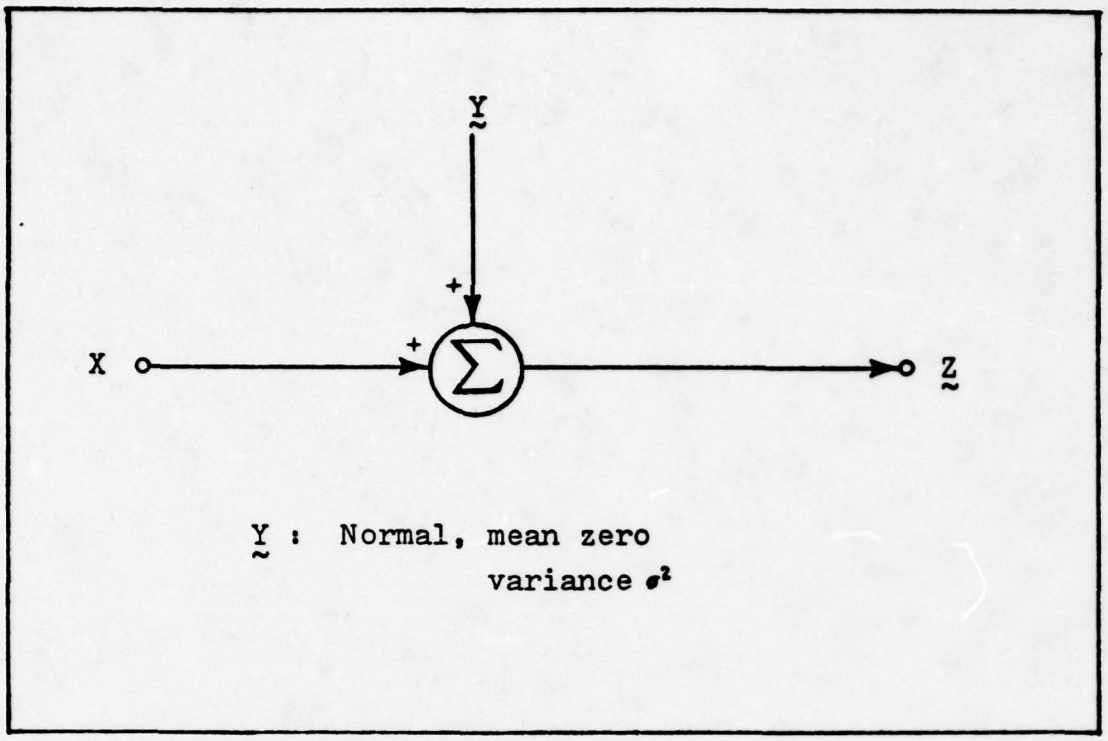

Fig 3. The Gaussian Channel

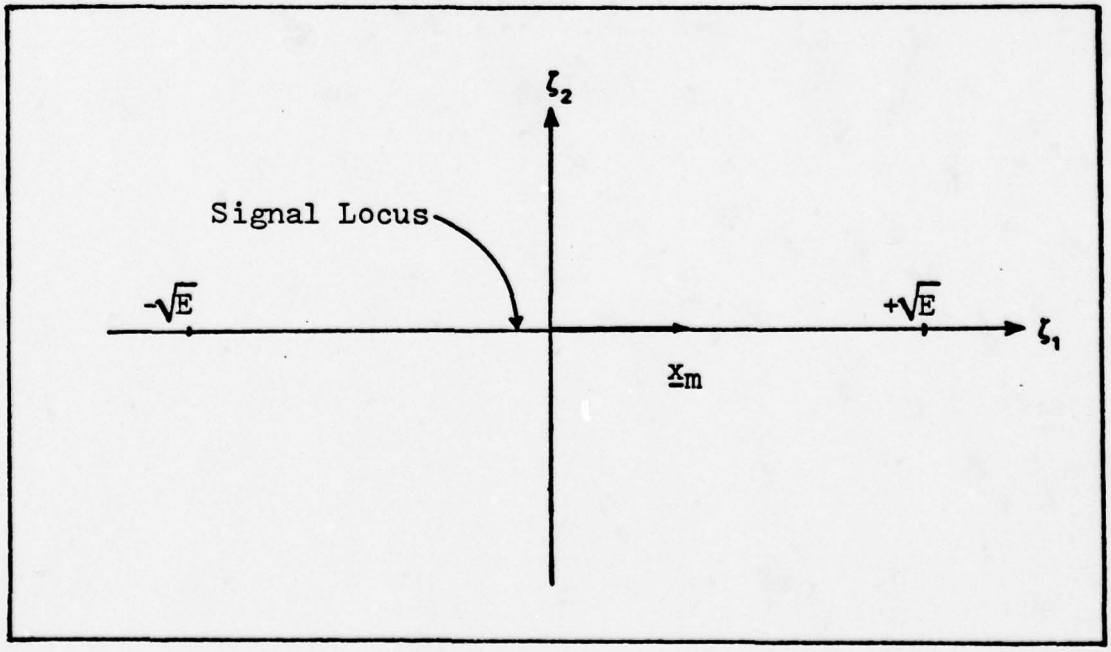

Fig 4. Locus of Transmitted Signal Vector

The simplest modulation format considered will use one pseudonoise code or bases function to traverse the channel. The signal space representation of this modulation scheme is shown in Figure 4. Allowing m_i to range over the interval $[-1,+1]$ causes the tip of the transmitted vector $\underline{x}_m$ to move along the ζ_1 axis from $-\sqrt{E}$ to $+\sqrt{E}$. The modulation technique just described in signal space is antipodal pulse-width modulation and will be analyzed in the next chapter.

III. Antipodal Pulse-Width Modulation

The use of signal formats similar to antipodal pulse-width modulation have been envisioned for more than ten years as an efficient method of communicating between terminals in ranging systems using pseudonoise tracking links (Ward, 1967: 69). When used solely to provide a robust communication system, antipodal pulse-width modulation (PWM) is a simple direct sequence method of transmitting analog speech information.

Modulation Technique

Antipodal PWM requires only one code waveform $c_1(t)$, assumed to be a pseudonoise code and the ability to employ a phase coherent receiver. The transmitted antipodal PWM signal $x(t)$ is given by

$$x(t) = \sqrt{P}\, d(t)\cos(\omega_0 t) \tag{10}$$

where the data waveform, $d(t)$, is defined by

$$d(t) = P(m,t)c_1(t) \tag{11}$$

and the pulse-width modulation is represented mathematically as

$$P(m,t) = \sum_{k=-\infty}^{\infty} \text{sgn}'\left(t-kT-\frac{T}{2}-\frac{m_k T}{2}\right) \tag{12}$$

with $\text{sgn}'(t)$ defined as the inverted signum function

$$\text{sgn}'(t) = \begin{cases} -1, & t \geq 0 \\ +1, & t < 0 \end{cases}$$

Combining equations (1) and (12) results in the expression

$$d(t) = \sum_{k=-\infty}^{\infty} a_k P_{T_c}(t-kT_c) \sum_{\substack{i=-\infty \\ i=\lceil k/N \rceil}}^{\infty} \text{sgn}'\left(t-iT-\frac{T}{2}-\frac{m_i T}{2}\right) \qquad (13)$$

where $\lceil k/N \rceil$ denotes the greatest integer value. Physically each analog sample is mapped into a code period by the pulse-width modulation signal that inverts the required final portion of the period. The kth analog sample value, m_k, determines the point where code inversion begins during the interval $kT \leq t \leq (k+1)T$, which corresponds to the kth code period. The start of both the code period and PWM signal are synchronized and no dead time is allowed between PWM signals. Figure 5 illustrates typical segments from the code and PWM signals before they are mixed and applied to the radio frequency (RF) carrier for transmission. The general correspondence between sample values and the alteration produced in the transmitted code segment is shown in Table I.

Transmission through the channel described in Chapter II results in a received signal represented by

$$\underset{\sim}{R}(t) = \sqrt{P}\, d(t)\cos(\omega_0 t) + \underset{\sim}{n}(t) + \underset{\sim}{J}(t)\cos(\omega_0 t - \underset{\sim}{\theta}) \qquad (14)$$

The channel disturbances were shown to be approximately

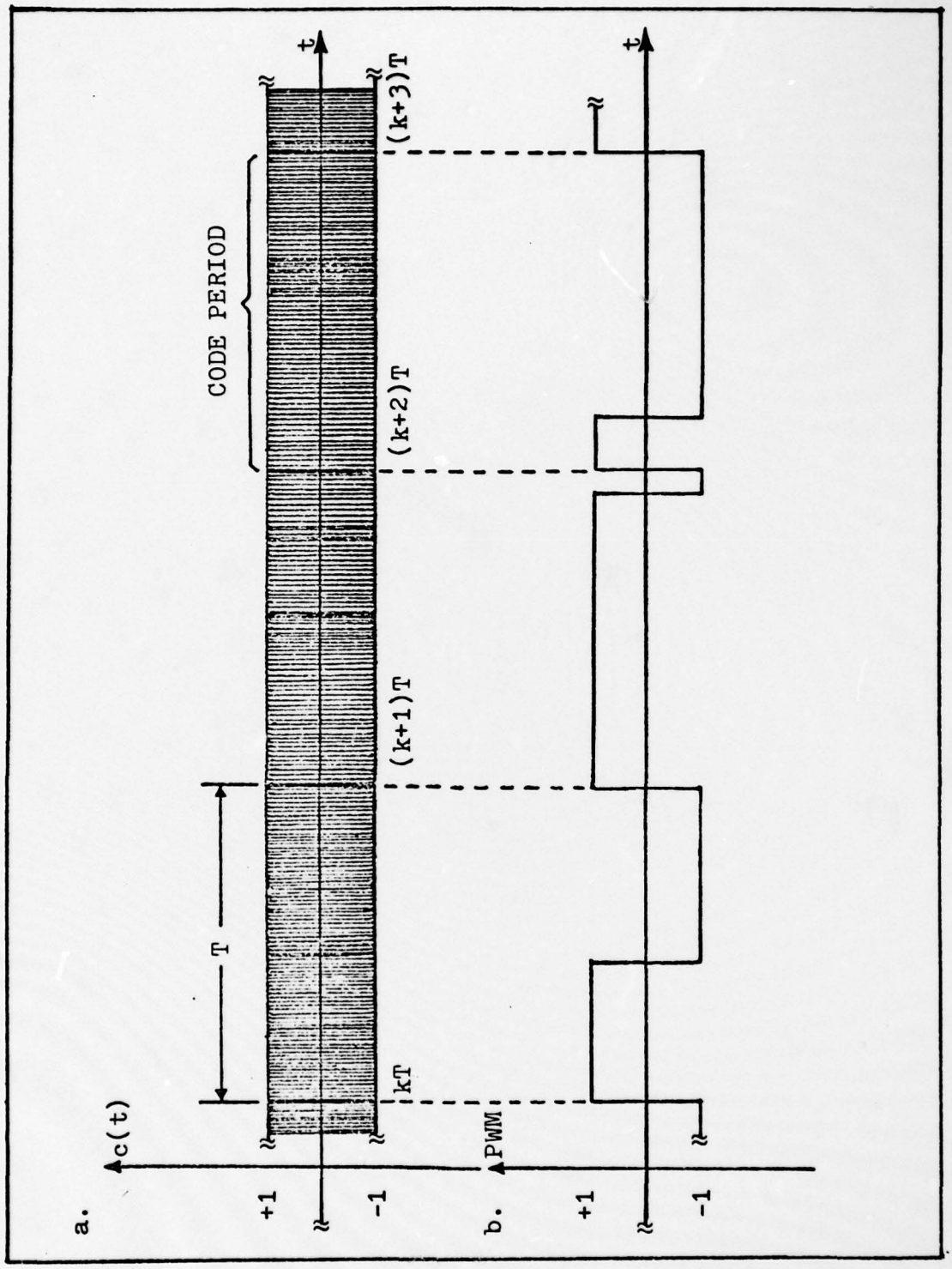

Fig 5. Antipodal Pulse-width Modulation Format
a) Code-waveform b) PWM Waveform

TABLE I

Mapping from Sample Value to Altered Code Segment

m	Upright Interval	Inverted Interval
-1.0	0	0 to T
-0.5	0 to T/4	T/4 to T
0	0 to T/2	T/2 to T
+0.5	0 to 3/4T	3/4T to T
+1.0	0 to T	0

Gaussian and represent thermal noise and a narrow band jammer operating at the receive frequency.

Receiver Structure

The coherent receiver's structure shown in Figure 6 represents a charge coupled device (CCD) configured as an analog correlator (Melen, 1977). The sample output from the CCD correlator matched to $c_1(t)$ can be written as

$$\underset{\sim}{Z} = 2\int_0^T \underset{\sim}{R}(t)c_1(t)\cos(\omega_0 t)dt \qquad (15)$$

inserting $\underset{\sim}{R}(t)$ into the integrand gives

$$\underset{\sim}{Z} = 2\sqrt{P}\int_0^T d(t)c_1(t)\cos^2(\omega_0 t)dt + 2\int_0^T \underset{\sim}{n}_f(t)c_1(t)\cos(\omega_0 t)dt + \qquad (16)$$

$$2\int_0^T \underset{\sim}{J}(t)\cos(\omega_0 t-\underset{\sim}{\theta})c_1(t)\cos(\omega_0 t)dt$$

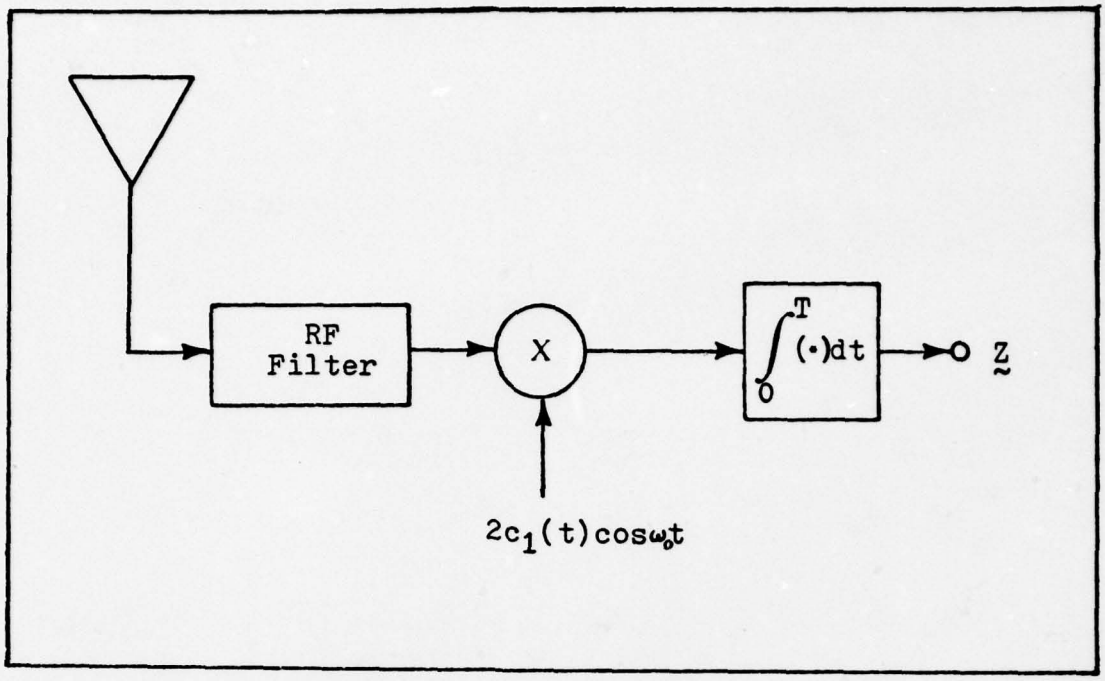

Fig. 6. Coherent Antipodal Pulse-Width Modulation Receiver (Ziemer, 1976:321)

The narrow-band noise process $n_f(t)$ which appears after the RF filter in the receiver can be represented by an in-phase component $n_c(t)$ and a quadrature component $n_s(t)$. Thus

$$n_f(t) = n_c(t)\cos(\omega_0 t) - n_s(t)\sin(\omega_0 t) \tag{17}$$

where both the in-phase component $n_c(t)$ and quadrature component $n_s(t)$ are statistically independent Gaussian random variables with zero-mean and variance σ^2 (Papoulis, 1965: 373).

Using the trigonometric identity $\cos(\omega_0 t = \frac{1}{2}(1+\cos(2\omega_0 t))$ the sample output can be written

$$\underset{\sim}{Z} = \sqrt{P}\int_0^T d(t)c_1(t)(1+\cos(2\omega_0 t))dt + \int_0^T \underset{\sim}{n}_c(t)c_1(t)(1+\cos(2\omega_0 t))dt -$$

$$2\int_0^T \left(\underset{\sim}{n}_s(t)c_1(t)\sin(\omega_0 t)\right)\left(\cos(\omega_0 t)\right)dt + 2\int_0^T c_1(t)\cos(\omega_0 t) \qquad (18)$$

$$\left[\underset{\sim}{J}_x(t)\cos(\omega_0 t) + \underset{\sim}{J}_y(t)\sin(\omega_0 t)\right]dt$$

The terms with $[\sin(\omega_0 t)][\cos(\omega_0 t)]$ in the integrand reduce to zero since the sin and cos are approximately orthogonal over the interval 0 to T . Also with $\omega_0 >> 2\pi/T$ the double frequency component of the first term can be ignored. The assumption is valid in any realistic hardware implementation of the correlation receiver since the frequency response is such that the double frequency term will be blocked. The correlator output reduces to

$$\underset{\sim}{Z} = \sqrt{P}\int_0^T d(t)c_1(t)dt + \int_0^T \underset{\sim}{n}_c(t)c_1(t)dt + \int_0^T c_1(t)\underset{\sim}{J}_x(t)dt \qquad (19)$$

At time kT the sample output from the analog correlator can be written as

$$\underset{\sim}{Z}_k = \sqrt{P}T\, m_k + \underset{\sim}{J} + \underset{\sim}{n} \qquad (20)$$

where m_k is a fixed but unknown quantity and both $\underset{\sim}{n}$ and $\underset{\sim}{J}$ are independent Gaussian random variables. The density function describing the random variables $\underset{\sim}{Z}_k$ is also Gaussian

with mean

$$E\{Z_k\} = E\{\sqrt{P}\ T\ m_k\} + E\{J\} + E\{n\} \qquad (21)$$

$$= \sqrt{P}\ T\ m_k$$

Since the random variables J and n are independent with zero-mean, the variance of Z_k is found from

$$\sigma_z^2 = E\{n^2\} + E\{J^2\} \qquad (22)$$

$$= \int_0^T\int_0^T R_{n_c}(\alpha-\beta)R_c(\alpha-\beta)d\alpha d\beta + \int_0^T\int_0^T R_c(\alpha-\beta)$$

$$R_J(\alpha-\beta)d\alpha d\beta$$

Using an integral transformation where $\tau=\alpha-\beta$ (Papoulis, 1965:325) and the approximation that $R_{n_c}(\alpha-\beta) \simeq \frac{N_0}{2}\delta(\alpha-\beta)$ when compared to the code auto-correlation function, the variance can be approximated by

$$\sigma_z^2 \simeq \frac{N_0}{2}\int_0^T d\beta + \int_{-T}^{T}(T-|\tau|)R_c(\tau)R_J(\tau)d\tau \qquad (23)$$

The power spectral densities of the code waveform and narrow-band jammer are compared in Figure 7. Examination of the spectral densities shows $B<<1/T_c$ and that $S_c(f)$ is approximately flat when compared to the jammers power spectral density. Therefore, $R_c(\tau)$ can be written as an impulse function with weight T_c . Thus

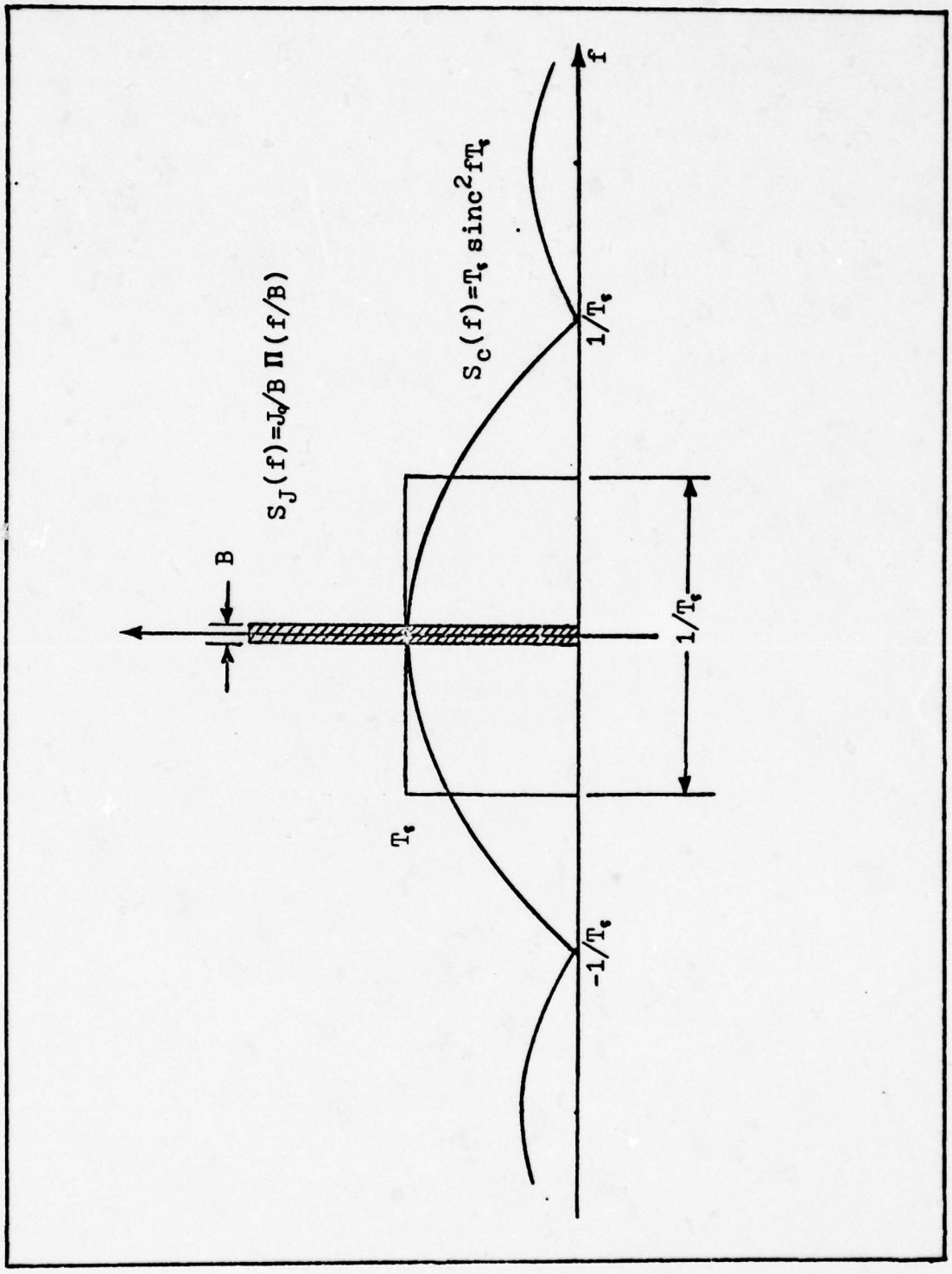

Fig 7. Baseband Comparison of Code and Narrow-Band Jammer Power Spectral Densities

$$\sigma_z^2 \simeq \frac{N_0 T}{2} + \int_{-T}^{T} (T-|\tau|)T_c \delta(\tau) J_0 \text{sinc}(B\tau) d\tau \qquad (24)$$

The sample variance is then approximately given by

$$\sigma_z^2 \simeq \frac{N_0 T}{2} + \frac{J_0 T^2}{N} \qquad (25)$$

Signal Processing Performance

The output of the analog correlator is thus a Gaussian random variable with mean $\sqrt{P}Tm$ and variance $\frac{N_0 T}{2} + \frac{J_0 T^2}{N}$. The receiver will estimate the parameter m based on the observed sample value Z_c which is corrupted by additive noise. Since m is a constant, but unknown value, a logical method (Van Trees, 1968:63) of determining m is to find $\hat{m}_{ml}$, the value of m that maximizes the density function $f(Z|m)$. The quantity $\hat{m}_{ml}$ is the maximum likelihood estimate or the value of m which most probably gave rise to the observed quantity $\underset{\sim}{Z}$. Thus the maximum likelihood estimate of the parameter m is given by

$$\hat{m}_{ml} = \frac{Z}{\sqrt{P}T} \qquad (26)$$

The receiver performance can now be predicted by evaluating the quality of the estimator structure employed. The first measure of quality is the expectation of the estimate

$$E\{\hat{m}_{ml}\} = \int_{-\infty}^{\infty} \hat{m}_{ml} f(Z|m) dZ = m \qquad (27)$$

which demonstrates that the estimate is conditionally unbiased. A second measure of quality is the variance of the estimation error

$$\mathrm{Var}\left\{(\hat{m}_{ml}-m)\,|\,m\right\} = E\left\{(\hat{m}_{ml}-m)^2\,|\,m\right\}$$

$$= \frac{\sigma_Z^2}{PT^2} \tag{28}$$

The Cramér-Rao bound (Van Trees, 1968:66) represents a lower bound on the variance of any unbiased estimate of m and is given by

$$\mathrm{Var}\{(\hat{m}-m)\,|\,m\} \geq \left[E\left\{\left[\frac{\partial \ln f(Z|m)}{\partial m}\right]^2 \,\middle|\, m\right\}\right]^{-1} \tag{29}$$

Solving for the Cramér-Rao bound gives

$$\mathrm{Var}\{(\hat{m}-m)\,|\,m\} \geq \left[E\left\{\left[\frac{Z-\sqrt{P}Tm}{\sigma_Z^2}\sqrt{P}T\right]^2\right\}\right]^{-1} \tag{30}$$

$$\geq \frac{\sigma_Z^2}{PT^2} = \frac{N_0/2 + J_0T/N}{PT}$$

The estimate satisfies the bound with equality and is termed an efficient estimate of m.

Since a closed form expression for the density function $f(Z|m)$ cannot be obtained for all receiver configurations, a second equivalent measure of system performance will be defined for future comparisons. The signal-to-noise ratio (S/N)

will be defined as (Wozencraft, 1965:588)

$$\frac{S}{N} = \frac{E^2\{Z\}}{\sigma_Z^2} \tag{31}$$

Thus antipodal PWM results in a signal-to-noise ratio given by

$$\frac{S}{N} = \frac{PT\ m^2}{N_0/2 + J_0 T/N} = \frac{m^2}{\mathrm{Var}\{(\hat{m}_{ml} - m)|m\}} \tag{32}$$

The geometrical ideas associated with signal space give added insight into the performance of various pulse-width modulation formats. As discussed in the last chapter, the locus of the transmitted vector can be written as

$$\underline{X}_m = m\sqrt{E}\underline{\zeta}_2 \tag{33}$$

where the parameter m is allowed to range over the interval $[1,+1]$. The transmitter is effectively "stretching" the interval $[-1,+1]$ onto the larger interval $[-\sqrt{E},+\sqrt{E}]$ in signal space. The "stretching" is uniform in the sense that (Wozencraft, 1965:611)

$$\left|\frac{d\underline{X}_m}{dm}\right| = \sqrt{E} \quad ; \text{ for all } m \ . \tag{34}$$

The effect of maximum-likelihood reception is to undo the "stretching" performed by the transmitter. Therefore the signal "stretching" is related to the receiver performance. Defining the stretch factor S by

$$S = \frac{d\underline{X}_m}{dm} \tag{35}$$

The antipodal PWM signal-to-noise ratio can now be written as

$$\frac{S}{N} = \frac{S^2 m^2}{N_0 + 2J_0 T/N} \tag{36}$$

where $S=\sqrt{E}=\sqrt{\frac{PT}{2}}$

This expression for S/N shows that the signal energy must be increased to improve performance in the antipodal PWM system.

The next logical step in signal space would be a signal format with two bases functions. Figure 8 shows the signal space representation for a noncoherent signal format with two pseudonoise codes or bases functions. The locus of the transmitted signal vector can be written as

$$\underline{X}_m = \left(\frac{1+m}{2}\right)\sqrt{E}\ \underline{\zeta}_1 + \left(\frac{1-m}{2}\right)\sqrt{E}\ \underline{\zeta}_2 \tag{37}$$

where the parameter m is allowed to range over the interval $[-1,+1]$. The signal format just described in signal space is bi-orthorgonal word PWM and will be analyzed in the next chapter.

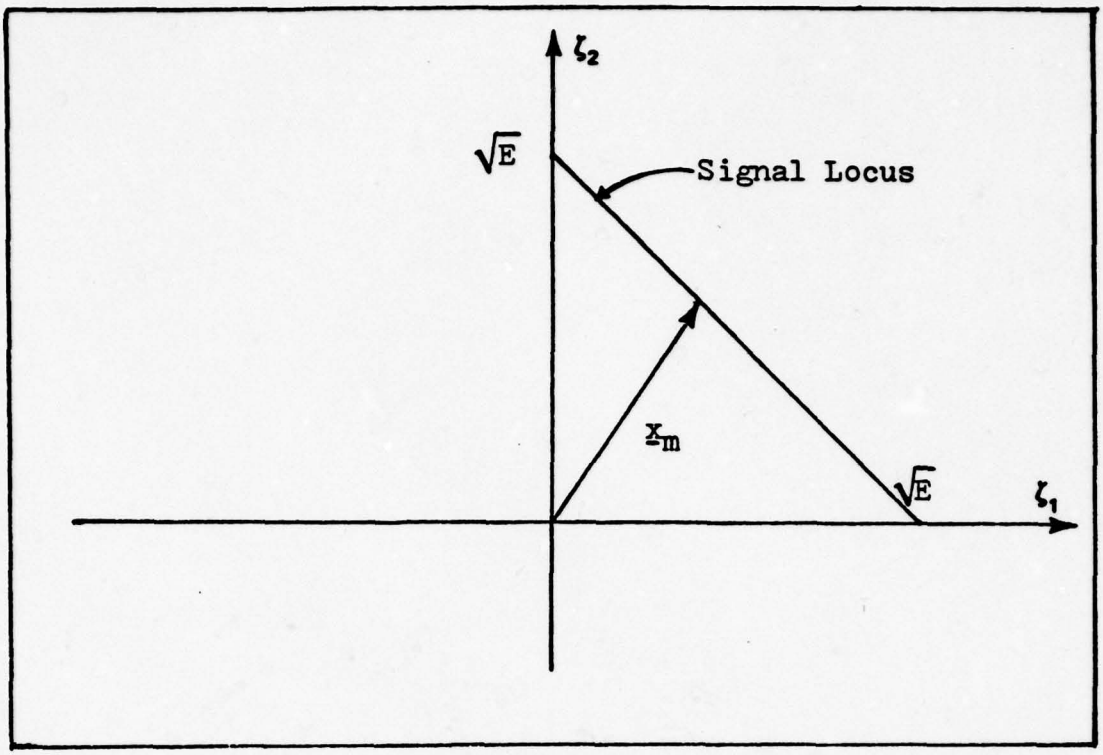

Fig 8. Locus of Transmitted Signal Vector

IV. Bi-Orthogonal Word Pulse-Width Modulation

The second technique for information transmission in a spread spectrum system is similar to antipodal PWM. The analog sample value controls the modulating signal as before, but now varying portions of two orthogonal codes are interleaved in each T second transmission interval. The analysis of both a coherent and noncoherent system will be given in this chapter.

Modulation Format

The generic code transmitted in bi-orthogonal word PWM, $c(t)$ is composed of segments from two orthogonal pseudo-noise waveforms each with T second periods. Every T second interval of the generic code begins with $c_1(t)$ and at the point determined by the PWM signal, switches to $c_2(t)$ for the remaining portion of the interval. The duration of each sequence portion corresponds to the analog sample m_i, such that when m_i is $+1$, only $c_1(t)$ is sent, when it is -1, only $c_2(t)$ is sent; and when m_i is 0, $c_1(t)$ is sent for the first half of the interval and $c_2(t)$ is sent for the second. There is no dead time between the two sequences. The data waveform is represented mathematically as

$$d(t) = \sum_{k=-\infty}^{\infty} \left| c_1(t)\left[u(t-kT)-u(t-kT-\frac{T}{2}-\frac{m_k T}{2})\right] \right. \tag{38}$$

$$\left. +c_2(t)\left[u(t-kT-\frac{T}{2}-\frac{m_k T}{2})-u(t-(k+1)T)\right] \right|$$

where

$$u(t) = \begin{cases} 1, & t \geq 0 \\ 0, & t < 0 \end{cases}$$

The transmitted spread spectrum signal is given by

$$x(t) = \sqrt{P}\, d(t)\cos(\omega_0 t) \tag{39}$$

Phase Coherent System

After propagating through the channel, the resulting received signal in a phase coherent bi-orthogonal word PWM system is the same as the antipodal PWM system with an alternate representation for $d(t)$, the data signal. Thus the received signal is given by

$$\underset{\sim}{R}(t) = \sqrt{P}\, d(t)\cos(\omega_0 t) + \underset{\sim}{n}(t) + \underset{\sim}{J}(t)\cos(\omega_0 t - \underset{\sim}{\theta}) \tag{40}$$

Receiver Structure. The required phase coherent receiver structure is shown in Figure 9. The output from the ith leg correlator matched to codeword $c_i(t)$ can be written as

$$\underset{\sim}{I}_i = 2\int_0^T \underset{\sim}{R}(t)c_i(t)\cos(\omega_0 t)dt \tag{41}$$

Now working with I_1, the output from the upper leg correlator, matched to codeword $c_1(t)$ and expanding the integrand gives (42)

$$\underset{\sim}{I}_1 = 2\sqrt{P}\int_0^T d(t)c_1(t)\cos^2(\omega_0 t)dt + 2\int_0^T \underset{\sim}{n}_f(t)c_1(t)\cos(\omega_0 t)dt + 2\int_0^T \underset{\sim}{J}_x(t)c_1(t)\cos^2(\omega_0 t)dt$$

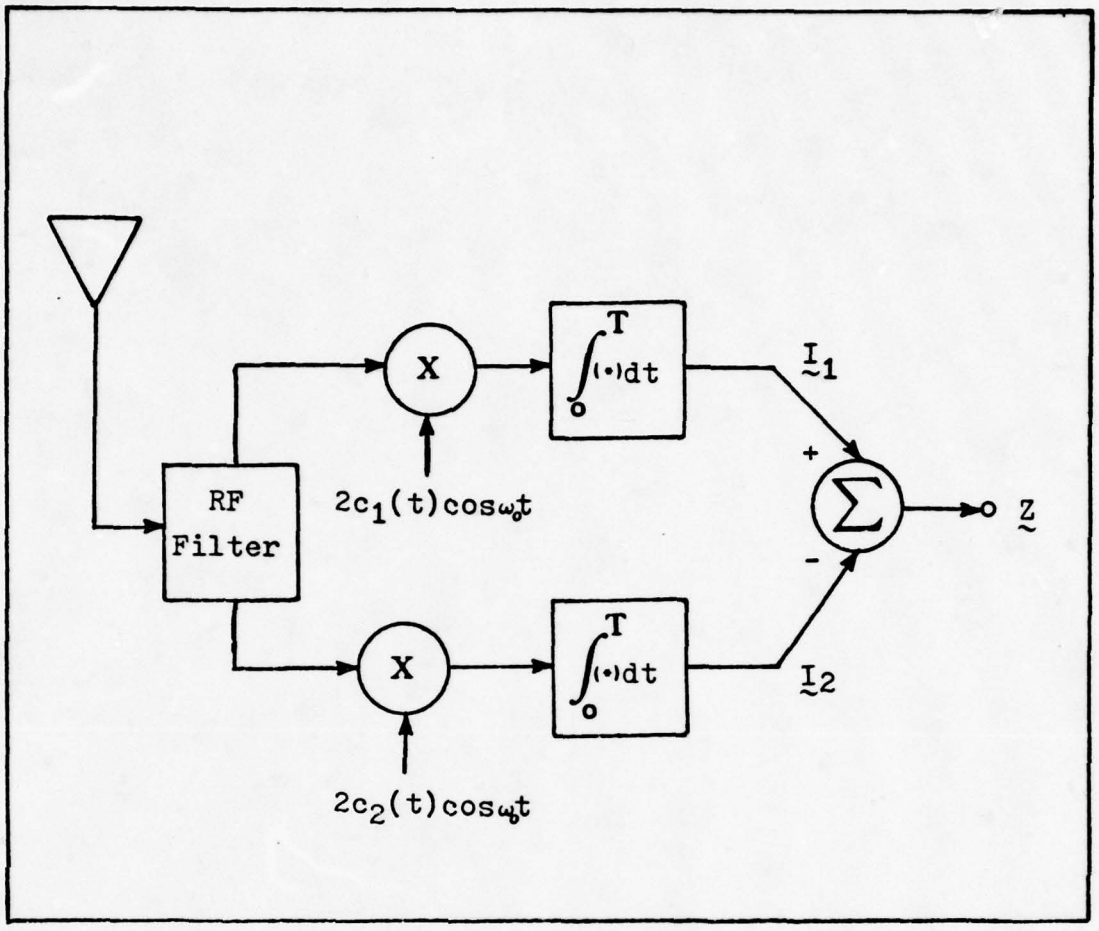

Fig 9. Phase Coherent Bi-Orthogonal Word Pulse-Width Modulation Receiver.

Following the same logic presented in the chapter on anti-podal PWM results in the expression

$$\underset{\sim}{I}_1 = \sqrt{P}\int_0^T d(t)c_1(t)dt + \int_0^T \underset{\sim}{n}_c(t)c_1(t)dt + \int_0^T \underset{\sim}{J}_x(t)c_1(t)dt \quad (43)$$

Expanding the data signal $d(t)$ appearing in first term of equation 43 results in

$$\underset{\sim}{I}_1 = \sqrt{P}\int_0^{\left(\frac{1+m}{2}\right)T} c_1(t)c_1(t)dt+\sqrt{P}\int_{\left(\frac{1+m}{2}\right)T}^{T} c_1(t)c_2(t)dt+\int_0^T \underset{\sim}{n}_c(t)c_1(t)$$

$$dt + \int_0^T c_1(t)\underset{\sim}{J}_x(t)dt \qquad (44)$$

The second term in equation 44 is a partial cross-correlation function of pseudonoise codewords $c_1(t)$ and $c_2(t)$ over the final segment of the generic code period. The codes are selected to be approximately orthogonal when the cross-correlation occurs over a complete T second period, however, cross-correlation over a partial code period will not, in general, be zero. The partial cross-correlation function then represents an additional signal dependent interference term for the receiver. Chapter VI provides an analysis of this signal dependent noise and shows that the partial cross-correlation in channel one will produce an additional Gaussian noise term $\underset{\sim}{\varepsilon}(m)$ which is distributed $N(o,\Psi^2(M))$. Then at time KT, the sample output from the correlator in the upper leg can be written as

$$\underset{\sim}{I}_1 = \sqrt{P}T\left(\frac{1+m_k}{2}\right) + \underset{\sim}{n}+\underset{\sim}{J}+\underset{\sim}{\varepsilon}(m) \qquad (45)$$

where m_k is a fixed but unknown quantity, $\underset{\sim}{n}$ is distributed $N(o,N_oT/2)$, $\underset{\sim}{J}$ is distributed $N(o,J_oT^2/N)$ and $\underset{\sim}{\varepsilon}(m)$ is the signal dependent noise.

Following the same logic used to find the output produced

in channel one, the output from the correlator matched to $c_2(t)$ in the lower receiver leg is given by

$$\underset{\sim}{I}_2 = \sqrt{P}\int_0^{\left(\frac{1+m}{2}\right)T} c_1(t)c_2(t)dt+\sqrt{P}\int_{\left(\frac{1+m}{2}\right)T}^{T} c_2(t)c_2(t)dt+ \tag{46}$$

$$\int_0^T \underset{\sim}{n}_c(t)c_2(t)dt+\int_0^T c_2(t)\underset{\sim}{J}_x(t)dt$$

The first term in equation 46 is the partial cross-correlation function of pseudonoise codewords $c_1(t)$ and $c_2(t)$ over the initial segment of the generic code period. Again the partial cross-correlation function represents a signal dependent noise to the receiver. The partial cross-correlation in channel two will produce an additional Gaussian noise term $\underset{\sim}{\xi}(m)$ which is distributed $N(o,\Lambda^2(m))$. The noise produced in each receiver channel, however, has a symmetric relationship such that total cross-correlation variance $\sigma_c^2 \triangleq \Psi^2(m)+\Lambda^2(m)$ is not signal dependent. Again at time kT the sample output from the correlator in the lower leg can be written as

$$\underset{\sim}{I}_2 = \sqrt{P}T\left(\frac{1-m_k}{2}\right)+\underset{\sim}{n}+\underset{\sim}{J}+\underset{\sim}{\xi}(m) \tag{47}$$

where m_k is the fixed but unknown parameter, $\underset{\sim}{n}$ is distributed $N(o,N_oT/2)$, $\underset{\sim}{J}$ is distributed $N(o,J_oT^2/N)$ and $\underset{\sim}{\xi}(m)$

is the signal dependent noise in channel two.

The final ad hoc receiver output is formed by subtracting the output of receiver channel two from the output of channel one to produce the Gaussian random variable $\underset{\sim}{Z}$.

$$\underset{\sim}{Z} = \underset{\sim}{I}_1 - \underset{\sim}{I}_2 \tag{48}$$

The expected value of $\underset{\sim}{Z}$ is given by

$$\begin{aligned} E\{Z\} &= E\{I_1\} - E\{I_2\} \\ &= \sqrt{P}Tm \end{aligned} \tag{49}$$

Since the noises in each channel's sample output are independent random variables, the variance of $\underset{\sim}{Z}$ is easily computed as

$$\begin{aligned} \sigma_z^2 &= N_0 T + \frac{2J_0 T^2}{N} + \Psi^2(m) + \Lambda^2(m) \\ &= N_0 T + \frac{2J_0 T^2}{N} + \sigma_c^2 \end{aligned} \tag{50}$$

Signal Processing Performance. The observed receiver sample output can be described by the conditional probability density function $f(z|m)$ as

$$f(z|m) = \frac{1}{\sqrt{2\pi}\sigma_z} \exp\left[- \frac{(z-\sqrt{P}Tm)^2}{2\sigma_z^2} \right] \tag{51}$$

The estimate of the parameter m is again given by

$$\hat{m} = \frac{z}{\sqrt{P}T} \tag{52}$$

The estimate is conditionally unbiased with the variance of the estimation error given by

$$\begin{aligned} \mathrm{Var}\{(\hat{m}-m)|m\} &= \frac{\sigma_z^2}{PT^2} \\ &= \frac{N_0T+2J_0T^2/N+\sigma_c^2}{PT^2} \end{aligned} \tag{53}$$

Neglecting the cross-correlation noise, the variance of the estimation error is double that seen in the antipodal PWM system. Namely,

$$\mathrm{Var}\{(\hat{m}-m)|m\} \approx \frac{N_0+2J_0T/N}{PT} \tag{54}$$

The corresponding signal-to-noise ratio reveals the same 3db degradation in system performance

$$\frac{S}{N} = \frac{PTm^2}{N_0+2J_0T/N} \tag{55}$$

Phase Noncoherent System

Noncoherent bi-orthogonal word PWM will be employed when a phase offset exists between the received signal and the local oscillator in the receiver. The phase offset may be due to doppler shift, oscillator drift and other common disturbances. The transmitted signal is now given by

$$x(t) = \sqrt{P}d(t)\cos(\omega_0 t+\phi) \tag{56}$$

where ϕ is the phase difference between the received signal and the receiver local reference.

Receiver Structure. The noncoherent bi-orthogonal word PWM receiver is shown in Figure 10. The complete received signal is given by

$$\underset{\sim}{R}(t) = \sqrt{P}d(t)\cos(\omega_0 t+\phi)+\underset{\sim}{n}(t)+\underset{\sim}{J}(t)\cos(\omega_0 t-\underset{\sim}{\theta}) \tag{57}$$

The receiver now produces inphase and quadrature signal components at the output of the correlator matched to $c_k(t)$. The correlator outputs are given by

$$\underset{\sim}{I}_k = 2\int_0^T \underset{\sim}{R}(t)c_k(t)\cos(\omega_0 t)dt, \qquad k=1,2 \tag{58}$$

and

$$\underset{\sim}{Q}_k = 2\int_0^T \underset{\sim}{R}(t)c_k(t)\sin(\omega_0 t)dt, \qquad k=1,2 \tag{59}$$

Following steps similar to those required in the coherent receiver analysis and using the trignometric identity $\sin^2(\omega_0 t)=\frac{1}{2}(1-\cos(2\omega_0 t))$ results in an inphase signal given by

$$\underset{\sim}{I}_k = \sqrt{P}\cos\phi\int_0^T d(t)c_k(t)dt+\int_0^T \underset{\sim}{n}_c(t)c_k(t)dt+ \tag{60}$$

$$\int_0^T \underset{\sim}{J}_x(t)c_k(t)dt \quad ; \; k=1,2$$

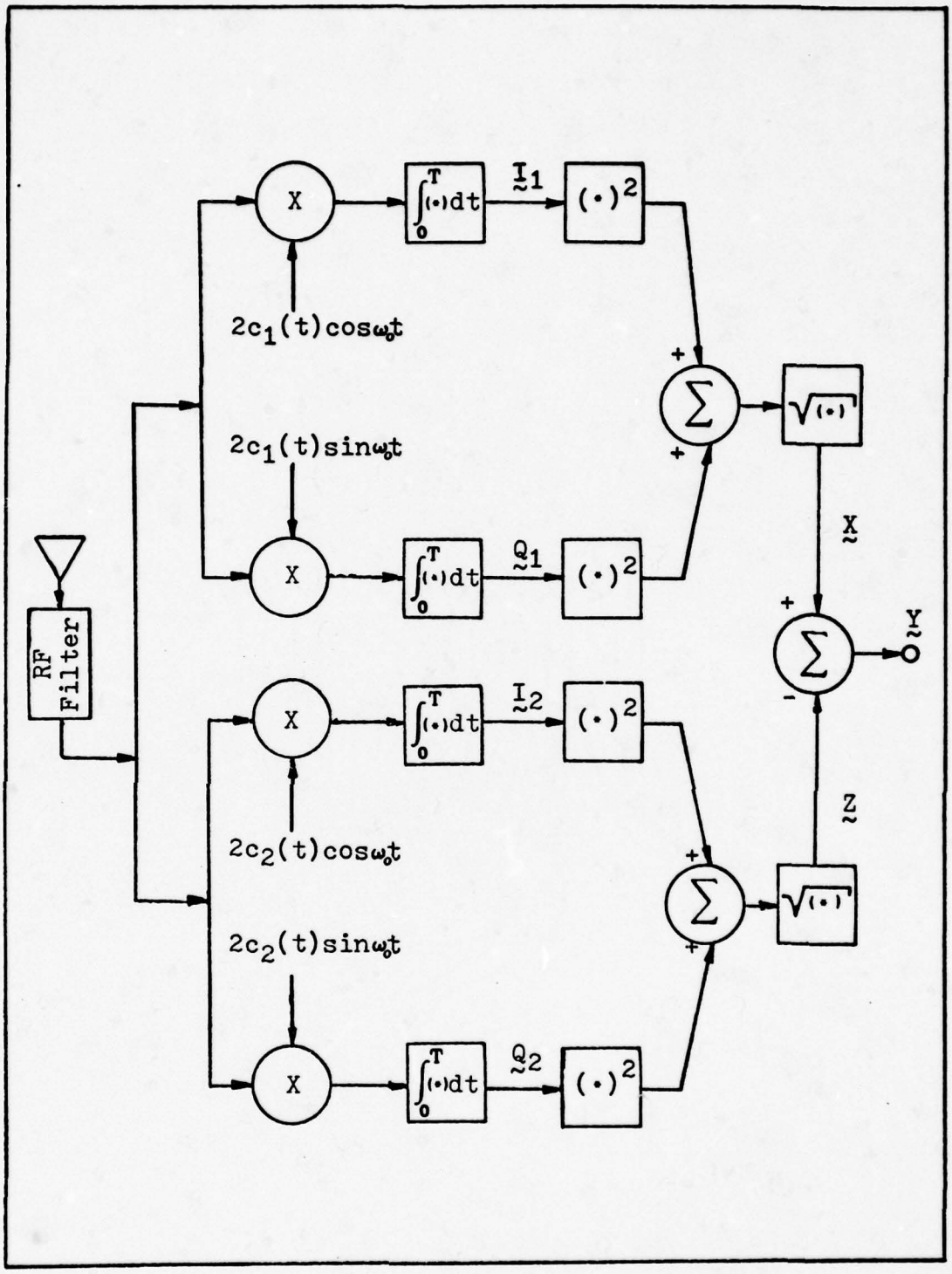

Fig 10. Phase Noncoherent Bi-Orthogonal Word Pulse-Width Modulation Receiver.

and a quadrature signal given by

$$\underset{\sim}{Q}_k = \sqrt{P}\sin\phi\int_0^T d(t)c_k(t)dt - \int_0^T \underset{\sim}{n}_s(t)c_k(t)dt + \int_0^T \underset{\sim}{J}_y(t)c_k(t)dt \quad ;k=1,2 \tag{61}$$

Now applying the definition of the data signal d(t) forces the use of all four correlator outputs. The equations for outputs produced by the correlators matched to codeword one are

$$\underset{\sim}{I}_1 = \sqrt{P}\cos\phi\int_0^{\left(\frac{1+m}{2}\right)T} c_1(t)c_1(t)dt + \sqrt{P}\cos\phi\int_{\left(\frac{1+m}{2}\right)T}^T c_1(t)c_2(t)dt + \int_0^T \underset{\sim}{n}_c(t)c_1(t)dt + \int_0^T c_1(t)\underset{\sim}{J}_x(t)dt \tag{62}$$

and

$$\underset{\sim}{Q}_1 = \sqrt{P}\sin\phi\int_0^{\left(\frac{1+m}{2}\right)T} c_1(t)c_1(t)dt + \sqrt{P}\sin\phi\int_{\left(\frac{1+m}{2}\right)T}^T c_1(t)c_2(t)dt - \int_0^T \underset{\sim}{n}_s(t)c_1(t)dt + \int_0^T \underset{\sim}{J}_y(t)c_1(t)dt \tag{63}$$

The corresponding equations for the outputs produced by the correlators matched to codeword two are

$$\underset{\sim}{I}_2 = \sqrt{P}\cos\phi\int_0^{\left(\frac{1+m}{2}\right)T} c_1(t)c_2(t)dt + \sqrt{P}\cos\phi\int_{\left(\frac{1+m}{2}\right)T}^{T} c_2(t)c_2(t)dt + \tag{64}$$

$$\int_0^T \underset{\sim}{n}_c(t)c_2(t)dt + \int_0^T \underset{\sim}{J}_x(t)c_2(t)dt$$

and

$$\underset{\sim}{Q}_2 = \sqrt{P}\sin\phi\int_0^{\left(\frac{1+m}{2}\right)T} c_1(t)c_2(t)dt + \sqrt{P}\sin\phi\int_{\left(\frac{1+m}{2}\right)T}^{T} c_2(t)c_2(t)dt - \tag{65}$$

$$\int_0^T \underset{\sim}{n}_s(t)c_2(t)dt + \int_0^T \underset{\sim}{J}_y(t)c_2(t)dt$$

Then at time kT the sample outputs from the correlators matched to codeword one can be written as

$$\underset{\sim}{I}_1 = \sqrt{P}T\left(\frac{1+m_k}{2}\right)\cos\phi + \underset{\sim}{n} + \underset{\sim}{J}+\cos\phi\underset{\sim}{\varepsilon}(m) \tag{66}$$

and

$$\underset{\sim}{Q}_2 = \sqrt{P}T\left(\frac{1+m_k}{2}\right)\sin\phi - \underset{\sim}{n} + \underset{\sim}{J} + \sin\phi\underset{\sim}{\varepsilon}(m) \tag{67}$$

The corresponding sample outputs from the correlators matched to codeword two can be written as

$$\underset{\sim}{I}_2 = \sqrt{P}T\left(\frac{1-m_k}{2}\right)\cos\phi + \underset{\sim}{n} + \underset{\sim}{J} + \cos\phi\underset{\sim}{\xi}(m) \tag{68}$$

and

$$\underset{\sim}{Q}_2 = \sqrt{P}T\left(\frac{1-m_k}{2}\right)\sin\phi - \underset{\sim}{n} + \underset{\sim}{J} + \sin\phi\underset{\sim}{\xi}(m) \tag{69}$$

where as in the phase coherent receiver m_k is a fixed, but unknown quantity, $\underset{\sim}{n}$ is distributed $N(o,N_oT/2)$, $\underset{\sim}{J}$ is distributed $N(o,J_oT^2/N)$, and $\underset{\sim}{\xi}(m)$ and $\underset{\sim}{\xi}(m)$ are the signal dependent cross-correlation noises distributed $N(o,\Psi^2(m))$ and $N(o,\Lambda^2(m))$ respectively.

The correlator sample outputs are therefore independent Gaussian random variables that can be totally characterized with knowledge of their mean and variance. Table II provides the mean and variance associated with each of the four correlator sample outputs. The receiver then produces random variables $\underset{\sim}{x}$ and $\underset{\sim}{z}$ as shown in Figure 10 which are defined by

$$\underset{\sim}{x} = \sqrt{(\underset{\sim}{I}_1)^2 + (\underset{\sim}{Q}_1)^2} \tag{70}$$

$$\underset{\sim}{z} = \sqrt{(\underset{\sim}{I}_2)^2 + (\underset{\sim}{Q}_2)^2} \tag{71}$$

The probability density functions for $\underset{\sim}{x}$ and $\underset{\sim}{z}$ cannot be obtained with the correlator output variances defined as

TABLE II

Correlator Output Statistics

Correlator Output	Mean	Variance
I_1	$\sqrt{P}T(\frac{1+m}{2})\cos\phi$	$\frac{N_0T}{2} + \frac{J_0T^2}{N} + \cos^2\phi\Psi^2(m)$
Q_1	$\sqrt{P}T(\frac{1+m}{2})\sin\phi$	$\frac{N_0T}{2} + \frac{J_0T^2}{N} + \sin^2\phi\Psi^2(m)$
I_2	$\sqrt{P}T(\frac{1-m}{2})\cos\phi$	$\frac{N_0T}{2} + \frac{J_0T^2}{N} + \cos^2\phi\Lambda^2(m)$
Q_2	$\sqrt{P}T(\frac{1-m}{2})\sin\phi$	$\frac{N_0T}{2} + \frac{J_0T^2}{N} + \sin^2\phi\Lambda^2(m)$

signal dependent and unique to each receiver channel. However, Chapter VI shows that the total cross-correlation noise $\sigma_c^2=\Psi^2(m)+\Lambda^2(m)$ is not signal dependent and in this case the total cross-correlation noise is

$$\sigma_c^2 = \sin^2\phi\Lambda^2(m)+\cos^2\phi\Lambda^2(m)+\sin^2\phi\Psi^2(m)+\cos^2\phi\Psi^2(m)$$

$$= \Psi^2(m) + \Lambda^2(m) \qquad (72)$$

Then to obtain a closed form expression for the conditional densities $f(x|m)$ and $f(z|m)$, the cross-correlation noise in each channel will be assumed to be approximately $\sigma_c^2/4$. All four correlator sample outputs now have an approximate variance given by $N_0T/2+J_0T^2/N+\sigma_c^2/4$.

The random variables I_1 and Q_1 are independent and

jointly normal, with the means given in Table II and the variance in each channel approximately

$$\beta^2 = \frac{N_0 T}{2} + \frac{J_0 T^2}{N} + \frac{\sigma_c^2}{4} \tag{73}$$

The conditional density of $\underset{\sim}{x} = \sqrt{(\underset{\sim}{I}_1)^2+(\underset{\sim}{Q}_1)^2}$ is given by (Papoulis, 1965:498)

$$f(x|m) = \frac{x}{\beta^2} \exp\left[-\frac{x^2+\eta^2}{2\beta^2}\right] I_0\left(\frac{x\eta}{\beta^2}\right) \tag{74}$$

where

$$\eta^2 = T^2 P\left[\frac{1+m}{2}\right]^2$$

and $I_0(w)$ is the modified Bessel function of order zero defined in Papoulis.

The conditional density of $\underset{\sim}{z} = \sqrt{(\underset{\sim}{I}_2)^2+(\underset{\sim}{Q}_2)^2}$ is obtained in the same manner and is given by

$$f(z|m) = \frac{z}{\beta^2} \exp\left[-\frac{z^2+s^2}{2\beta^2}\right] I_0\left(\frac{zs}{\beta^2}\right) \tag{75}$$

where

$$s^2 = T^2 P\left[\frac{1-m}{2}\right]^2$$

Signal Processing Performance. The random variables $\underset{\sim}{x}$ and $\underset{\sim}{z}$ were shown to have a Rice-Nakagami or Rician conditional probability density functions in the last section. The

final ad hoc receiver output is obtained by differencing these two Rician random variables or the final output $\underset{\sim}{y}$ is given by

$$\underset{\sim}{y} = \underset{\sim}{x} - \underset{\sim}{z} \tag{76}$$

Given the ad hoc receiver structure shown in Figure 10, the ideal result would be to obtain $f(y|m)$, the conditional probability density function for the random variable $\underset{\sim}{y}$. The desired density could be obtained from the convolution of $f(x|m)$ and $f(z|m)$ as

$$f_y(y|m) = \int_{-\infty}^{\infty} f_x(y-u) f_z(-u)\,du \tag{77}$$

$$= \int_{-\infty}^{\infty} \left(\frac{y-u}{\beta^2}\right)\left(\frac{-u}{\beta^2}\right) \exp\left[-\frac{(y-u)^2+\eta^2}{2\beta^2}\right] I_0\left(\frac{(y-u)\eta}{\beta^2}\right)$$

$$\exp\left[-\frac{u^2+s^2}{2\beta^2}\right] I_0\left(\frac{-us}{\beta^2}\right) du$$

However, this integral proved formidable and this route was abandoned. The second approach was to use the characteristic function defined as

$$\Phi(\omega) = \int_{-\infty}^{\infty} e^{j\omega x} f(x)\,dx \tag{78}$$

The characteristic function for the random variable $\underset{\sim}{y}$ is then given by (Van Trees, 1968:396)

$$\Phi_Y(\omega) = \Phi_X(\omega)\Phi_Z(-\omega)$$

$$= \frac{\exp\left[\frac{j\omega\eta^2}{1-2j\omega\beta^2}\right]}{(1-2j\omega\beta^2)^{\frac{1}{2}}} \quad \frac{\exp\left[\frac{-j\omega s^2}{1+2j\omega\beta^2}\right]}{(1+2j\omega\beta^2)^{\frac{1}{2}}} \tag{79}$$

The density function is obtained by the inversion formula

$$f(y|m) = \frac{1}{2\pi}\int_{-\infty}^{\infty} \frac{\exp\left[\frac{j\omega\eta^2}{1-2j\omega\beta^2}\right]}{(1-2j\omega\beta^2)^{\frac{1}{2}}} \quad \frac{\exp\left[\frac{-j\omega s^2}{1+2j\omega\beta^2}\right]}{(1+2j\omega\beta^2)^{\frac{1}{2}}} e^{-j\omega y} d\omega \tag{80}$$

The inversion could not be completed and the conditional density $f(y|m)$ was not obtained; therefore the estimate for m and its associated error variance could not be found for the given ad hoc noncoherent receiver.

The alternate signal-to-noise ratio analysis requires the first two moments of the output random variable. The nth order moments are found for the random variables $\underset{\sim}{x}$ and $\underset{\sim}{z}$ directly to be (Middleton, 1960:414)

$$E\{x^N\} = \int_0^{\infty} \frac{x^{N+1}}{\beta^2} e^{\left[-(x^2+\eta^2)/2\beta^2\right]} I_0\left(\frac{x\eta}{\beta^2}\right) dx$$

$$= (2\beta^2)^{\frac{N}{2}}\Gamma\left(\frac{N}{2}+1\right){}_1F_1\left(-\frac{N}{2}\,;\,1;\,a_0^2\right) \tag{81}$$

where

$$a_0^2 = \frac{\eta^2}{2\beta^2}$$

and ${}_1F_1(\alpha;\beta;\pm x)$ is the confluent hypergeometric function discussed in Appendix B.

The mean is therefore given by

$$E\{x\} = \sqrt{\frac{\pi}{2}}\,\beta\,{}_1F_1(-\tfrac{1}{2};1;-a_0^2)$$

$$= \sqrt{\frac{\pi}{2}}\,\beta e^{-\eta^2/4\beta^2}\left[(1+\frac{\eta^2}{2\beta^2})I_0(\frac{\eta^2}{4\beta^2}) + \frac{\eta^2}{2\beta^2}\,I_1\left(\frac{\eta^2}{4\beta^2}\right)\right] \tag{82}$$

The "large" signal approximation for the expected value is valid when $\eta^2 >> \beta^2$ is given by (Papoulis, 1965:499)

$$E\{x\}_{l.s.} \simeq \eta(1+\frac{\beta^2}{2\eta^2}) \tag{83}$$

Similarly the "small" signal approximation is given by (Papoulis, 1965:500)

$$E\{x\}_{s.s.} \simeq \sqrt{\frac{\pi}{2}}\,\beta(1+\frac{\eta^2}{4\beta^2}) \tag{84}$$

Following the exact same logic for the random variable $\underset{\sim}{z}$ results in a "large" signal approximation for the expected value of

$$E\{z\}_{l.s.} \simeq s(1+\frac{\beta^2}{2s^2}) \tag{85}$$

and a "small" signal approximation given by

$$E\{z\}_{s.s.} \simeq \sqrt{\frac{\pi}{2}}\,\beta\left(1+\frac{s^2}{4\beta^2}\right) \tag{86}$$

The expected value of the random variable that defines the receiver sample value output is found from $E\{y\} = E\{x\}-E\{z\}$. The "large" signal case is given by

$$\begin{aligned} E\{y\}_{l.s.} &\simeq \eta\left(1+\frac{\beta^2}{2\eta^2}\right) - s\left(1+\frac{\beta^2}{2s^2}\right) \\ &= (\eta-s)+\frac{\beta^2}{2}\left(\frac{1}{\eta}-\frac{1}{s}\right) \\ &= \sqrt{PT}m-\frac{\beta^2}{\sqrt{PT}}\left(\frac{m}{1-m^2}\right) \end{aligned} \tag{87}$$

The expected value of the random variable $\underset{\sim}{y}$ in the "small" signal region is given by

$$\begin{aligned} E\{y\}_{s.s.} &\simeq \sqrt{\frac{\pi}{2}}\left(\frac{\eta^2}{4\beta}-\frac{s^2}{4\beta}\right) \\ &= \sqrt{\frac{\pi}{2}}\,\frac{PT^2}{4\beta}\,m \end{aligned} \tag{88}$$

Comparing the results obtained here for the noncoherent receiver with the expected value of $\Gamma=\sqrt{PT}m$ obtained for the coherent receiver structure indicates some distortion effects are introduced by the noncoherent receiver. The "large"

signal approximation can be written with $K=\frac{\sqrt{P}T}{\beta}$ as

$$E\{y\}_{l.s.} \simeq \Gamma - \frac{\beta^2}{\sqrt{P}T}\left(\frac{m}{1-m^2}\right)$$

$$= \Gamma - \frac{\Gamma}{K^2}\left(\frac{1}{1-m^2}\right) \qquad (89)$$

$$\simeq \Gamma - \frac{\Gamma}{K^2}(1+m^2)$$

where the last approximation results from keeping only the first two terms of the geometric series $\sum_{n=0}^{\infty} R^n = \frac{1}{1-R}$ and imposing the condition $|m^2|<1$ on the modulation sample values. The "small" signal approximation can also be written in terms of the coherent receiver's expected value

$$E\{y\}_{s.s.} \simeq \sqrt{\frac{\pi}{2}}\ \frac{\sqrt{P}T}{4\beta}\ \Gamma \qquad (90)$$

$$= (0.313)K\Gamma$$

The distortion effects are shown in Figure 11 where the expected value of the coherent receiver is compared to the noncoherent receiver expected value approximations. The approximations are given as a function of K, the square root of the signal power to noise power ratio and show the effect of variations in m.

The second central moments are obtained from Middleton's result (Equation 81) and reduce to

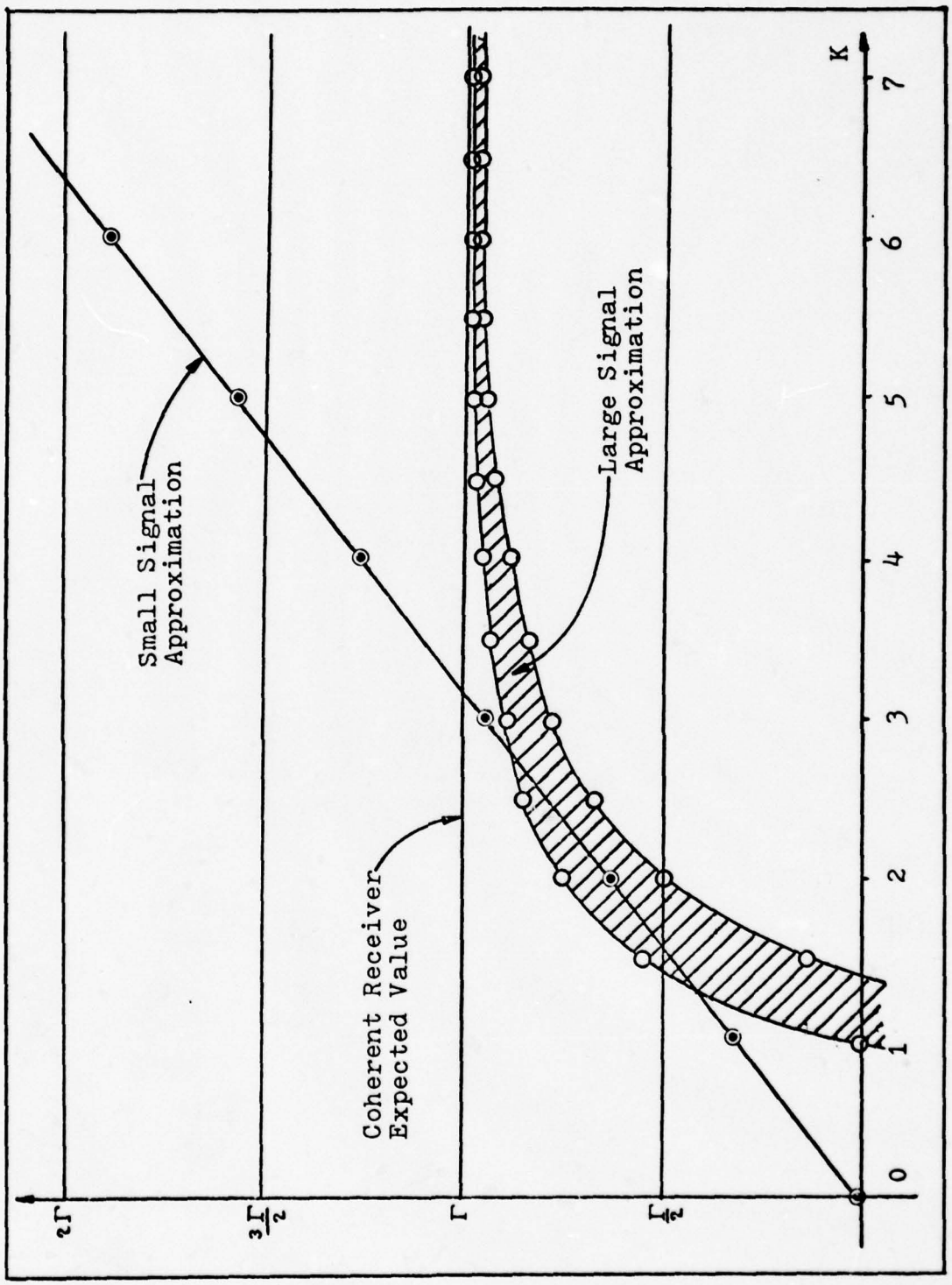

Fig 11. Noncoherent Receiver Expected Value Approximations Compared to Coherent Receiver Expected Value $(K = \frac{\sqrt{P}T}{\beta})$.

$$E\{x^2\} = 2\beta^2+\eta^2 \tag{91}$$

and

$$E\{z^2\} = 2\beta^2+s^2 \tag{92}$$

The variance is the required parameter for the signal-to-noise ratio comparison. The variance is found from $\sigma_x^2 = E(x^2)-E^2(x)$ as

$$\sigma_x^2=2\beta^2+\eta^2- \frac{\pi}{2}\beta^2 e^{-\eta^2/2\beta^2}\left[\left[1+ \frac{\eta^2}{2\beta^2}\right]I_0\left(\frac{\eta^2}{4\beta^2}\right)+ \frac{\eta^2}{2\beta^2}\ I_1\left(\frac{\eta^2}{4\beta^2}\right)\right]^2 \tag{93}$$

The "large" signal approximation for the mean results in a corresponding "large" signal approximation for the variance given by $(K=\sqrt{P}T/\beta)$

$$\begin{aligned}\sigma^2_{xl.s.} &\simeq 2\beta^2+\eta^2-\left(\eta+\frac{\beta^2}{2\eta}\right)^2 \\ &= \beta^2\left[1- \frac{1}{K^2}\left(\frac{1}{1+m}\right)^2\right] \qquad (94) \\ &\simeq \beta^2\left[1- \frac{1}{K^2}(1-m)^2\right]\end{aligned}$$

where the last equation results from keeping only the first two terms of the geometric series $\sum_{n=0}^{\infty}(-m)^n= \frac{1}{1-(-m)}$ and imposing the condition $|m|<1$ on the modulation sample values.

The "small" signal approximation for the variance is given by

$$\sigma^2_{x_{s.s.}} = 2\beta^2+\eta^2-\frac{\pi}{32}\left(\frac{1}{\beta^2}\right)(4\beta^2+\eta^2)^2$$

$$\simeq (2-\frac{\pi}{2})\beta^2+(1-\frac{\pi}{4})\eta^2 \qquad (95)$$

$$\simeq \beta^2((0.429)+(0.054)K^2(1+m)^2)$$

The same analysis shows that the random variable $\underset{\sim}{z}$ has a "large" signal approximation for the variance given by

$$\sigma^2_{z_{l.s.}} \simeq \beta^2(1-\frac{1}{K^2}(1+m)^2) \qquad (96)$$

and a "small" signal approximation for the variance given by

$$\sigma^2_{z_{s.s.}} \simeq \beta^2((0.429)+(0.054)K^2(1-m)^2) \qquad (97)$$

The total variance of the receiver output random variable $\underset{\sim}{y}$ can now be obtained. Because the receiver channels produce independent random variables, the total variance is given by

$$\sigma^2_y = \sigma^2_x + \sigma^2_z \qquad (98)$$

and for the "large" signal region

$$\sigma^2_{y_{l.s.}} \simeq 2\beta^2-\frac{\beta^2}{K^2}(1+m^2) \qquad (99)$$

and the "small" signal region has the approximation

$$\sigma^2_{y_{s.s.}} \simeq (0.858)\beta^2+(0.108)\beta^2K^2(1+m^2) \qquad (100)$$

The coherent receiver variance and both approximations for the noncoherent receiver variance are shown in Figure 12.

The signal-to-noise ratio for the "small" signal region or where K is less than three as shown in Figures 11 and 12 can now be computed. The S/N is given by

$$\left(\frac{S}{N}\right)_{s.s.} = \frac{E^2\{y\}_{s.s.}}{\sigma^2_{y_{s.s.}}} \tag{101}$$

$$= \frac{1.94PT^2 \left(\frac{S}{N}\right)_{coherent}}{8.58\beta^2+1.08PT^2(1+m^2)}$$

When this result is written in terms of $K^2 = \frac{PT^2}{\beta^2}$, which is the signal to noise ratio without the modulation parameter, the impact of the envelope detectors is better understood. The signal-to-noise is then expressed by

$$\left(\frac{S}{N}\right)_{s.s.} = \frac{1.94\ K^2\left(\frac{S}{N}\right)_{coherent}}{8.58 + 1.08\ K^2\ (1+m^2)}$$

$$= \frac{1.94\ K^2\left(\frac{S}{N}\right)_{coherent}}{8.58 + 2.16\ K^2} \tag{102}$$

Both the "small" signal and "large" signal approximations for the signal-to-noise ratio are plotted in Figure 13. The signal-to-noise ratio plots compared to the coherent signal-to-noise ratio isolated the distortion produced by the enveloped detectors.

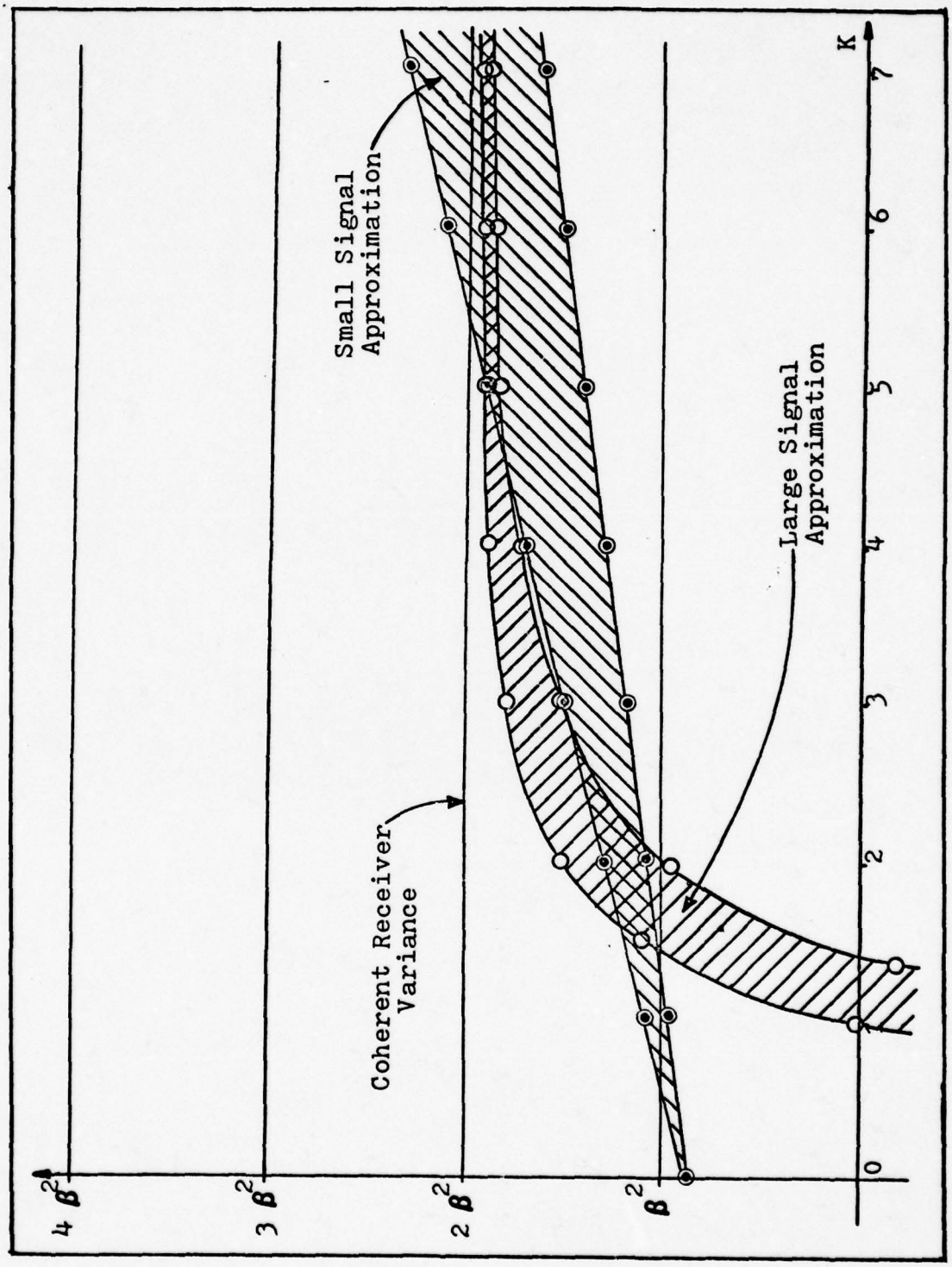

Fig 12. Noncoherent Receiver Variance Approximations Compared to Coherent Receiver Variance $(K=\frac{\sqrt{PT}}{\beta})$.

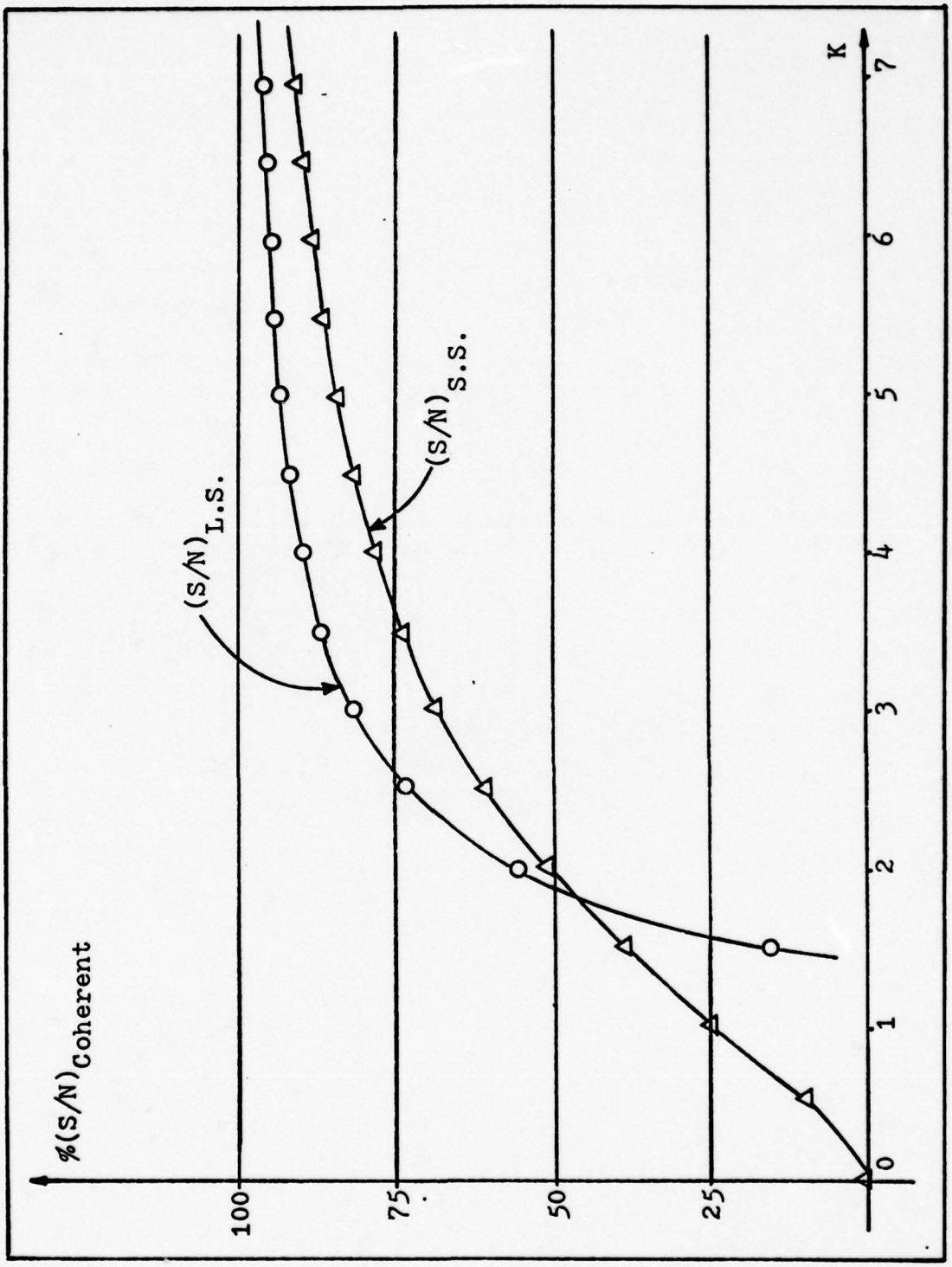

Fig 13. Noncoherent (S/N) Approximations versus Coherent (S/N)

In the "large" signal region or where K is greater than three the signal-to-noise ratio is given by

$$\left(\frac{S}{N}\right)_{l.s.} = \frac{E^2\{y\}_{l.s.}}{\sigma^2_{y_{l.s.}}}$$

$$= \frac{\left[1-\left(\frac{\beta^2}{PT^2}\right)_{m(1+m^2)}\right]}{\left[1-\left(\frac{\beta^2}{2PT^2}\right)(1+m^2)\right]}\left(\frac{S}{N}\right)_{coherent} \qquad (103)$$

$$\simeq \frac{\left[1-\frac{2}{K^2}\right]}{\left[1-\frac{1}{2K^2}\right]}\left(\frac{S}{N}\right)_{coherent}$$

The "large" signal region signal-to-noise ratio converges to the same (S/N) obtained in the coherent receiver structure. In the region of operation where $K=\frac{\sqrt{P}T}{\beta}>5$, both the coherent and noncoherent bi-orthogonal word PWM receivers produce approximately the same performance.

The fact that the noncoherent receiver's S/N approaches the performance obtained with the coherent receiver can be shown by an alternate method. The density function describing the sample outputs from either envelope detector has the form

$$f(x|m) = \frac{x}{\beta^2}\exp\left[-\frac{x^2+\alpha^2}{2\beta^2}\right] I_0\left(\frac{x\alpha}{\beta^2}\right) \qquad (104)$$

with $\alpha x >> \beta^2$ this density function can be approximated by (Davenport, 1958:166)

$$f(x|m) = \frac{1}{\beta}\left(\frac{x}{2\pi\alpha}\right)^{\frac{1}{2}} \exp\left[-\frac{(x-\alpha)^2}{2\beta^2}\right] \tag{105}$$

Hence, when the magnitude α of the signal component is large compared to β (signal standard deviation) and when $\underset{\sim}{x}$ is near α, the probability density function of the envelope of the sum process is approximately Gaussian. Then with $x \simeq \alpha$

$$f(x|m) \simeq \frac{1}{\sqrt{2\pi}\beta} \exp\left[-\frac{(x-\alpha)^2}{2\beta^2}\right] \tag{106}$$

The envelope detectors produce independent random variables $\underset{\sim}{x}$ and $\underset{\sim}{z}$ which are differenced to produce the receiver output $\underset{\sim}{y}$ can now be approximated $(\alpha x >> \beta^2)$ by a Gaussian density

$$\begin{aligned} f(y|m) &\simeq \frac{1}{\sqrt{2\pi}\sqrt{2\beta^2}} \exp\left[-\frac{|y-(\eta-s)|^2}{2(2\beta^2)}\right] \\ &= \frac{1}{\sqrt{2\pi}\sqrt{2\beta^2}} \exp\left[-\frac{(y-\sqrt{P}Tm)^2}{2(2\beta^2)}\right] \end{aligned} \tag{107}$$

The expected value and variance are given immediately by

$$E\{y\}_{l.s.} = \sqrt{P}Tm \tag{108}$$

and

$$\sigma^2_{y_{l.s.}} = 2\beta^2 \tag{109}$$

The S/N ratio is then given by

$$\left(\frac{S}{N}\right)_{l.s.} \simeq \frac{PT^2m^2}{2\beta^2} \qquad (110)$$

This S/N result is the same obtained by both the original "large" signal approximation and the coherent bi-orthogonal word receiver.

The signal-to-noise ratio can again be defined in terms of the stretch factor introduced in the last chapter. Since equal increments in m_i correspond to equal increments in the distance measured along the signal locus shown in Figure 8, the stretch factor is also given by $S=L/2$, where L is the total length of the locus traversed by $\underline{x}_m$ as m increases from -1 to $+1$. The length in the bi-orthogonal PWM format is $\sqrt{2E}$, a factor of $\sqrt{2}$ decrease in the stretch factor seen in the antipodal PWM format. The signal-to-noise is therefore

$$\frac{S}{N} = \frac{(S^2/2)m^2}{N_0+2J_0T/N} \qquad (111)$$

The signal space concept of signal locus length then shows the same 3db degradation in performance and points toward the fact that the signal energy must be increased to improve the bi-orthogonal word system. A logical alternative would seem to call for an increase in the dimension of the signal space to produce a longer signal locus and corresponding

performance enhancement. Figure 14 shows a three dimensional signal space where the signal locus has been increased to $2\sqrt{2E}$ which projects a 3db improvement in system performance over the antipodal PWM format. Figure 14 is the signal space representation for tri-orthogonal word PWM that will be discussed in the next chapter.

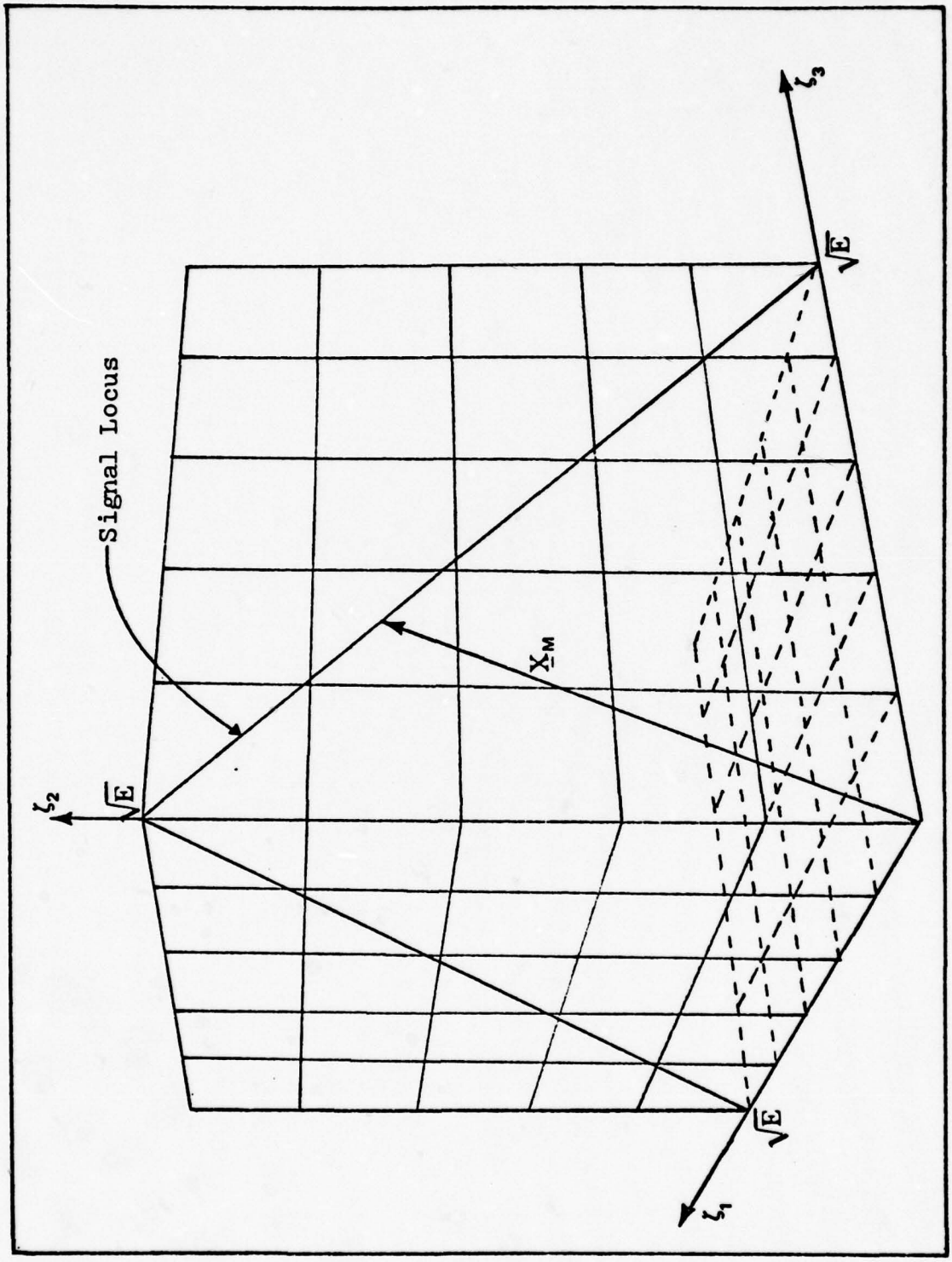

Fig 14. Locus of Transmitted Signal Vector

V. Tri-Orthogonal Word Pulse-Width Modulation

The final technique for spread spectrum modulation requires segments from three orthogonal pseudonoise waveforms. Tri-orthogonal word PWM is bi-orthogonal word PWM with one main alteration to the modulation format. The new feature seen in this signal format is the selection of the initial code sequence being determined by the polarity of m_i , the modulation sample value. The analysis of both a coherent and noncoherent system will be given in this chapter.

Modulation Format

The generic code transmitted in tri-orthogonal word PWM, $c(t)$, is composed of segments from three orthogonal pseudonoise waveforms each with T second periods. Every T second interval of the generic code begins with $c_1(t)$ when m_i is a positive quantity or begins with $c_3(t)$ when m_i is a negative quantity and at the point determined by the magnitude of the sample value switches to $c_2(t)$ for the remaining portion of the interval. The duration of each sequence portion corresponds to the analog sample m_i such that when m_i is +1, only $c_1(t)$ is sent, when it is -1, only $c_3(t)$ is sent, and when m_i is 0 only $c_2(t)$ is sent. There is no dead time between any of the transmitted sequence segments. The data waveform is represented mathematically by

$$d(t) = \sum_{k=-\infty}^{\infty} \Big[c_1(t) \Big[u(t-kT) - u(t-kT-|m_k|T) \Big] + c_2(t) \Big[u(t-kT-|m_k|T) - u(t-(k+1)T) \Big] \Big] \quad (112)$$

for positive m_k $(0 \leq m_k \leq +1)$

and

$$d(t) = \sum_{k=-\infty}^{\infty} \Big[c_3(t) \Big[u(t-kT) - u(t-kT-|m_k|T) \Big] + c_2(t) \Big[u(t-kT-|m_k|T) - u(t-(k+1)T \Big] \Big] \quad (113)$$

for negative m_k $(-1 \leq m_k < 0)$

Figure 15 illustrates how positive and negative sample values control the interleaving of code segments to form the transmitted generic code waveform. The transmitted spread spectrum signal is given

$$x(t) = \sqrt{P}\, d(t)\cos(\omega_0 t) \quad (114)$$

Phase Coherent System

Using the same channel model presented in Chapter II results in a received signal of the form

$$\underset{\sim}{R}(t) = \sqrt{P}\, d(t)\cos(\omega_0 t) + \underset{\sim}{n}(t) + \underset{\sim}{J}(t)\cos(\omega_0 t - \underset{\sim}{\theta}) \quad (115)$$

The channel has introduced both a white Gaussian noise process and narrowband jammer.

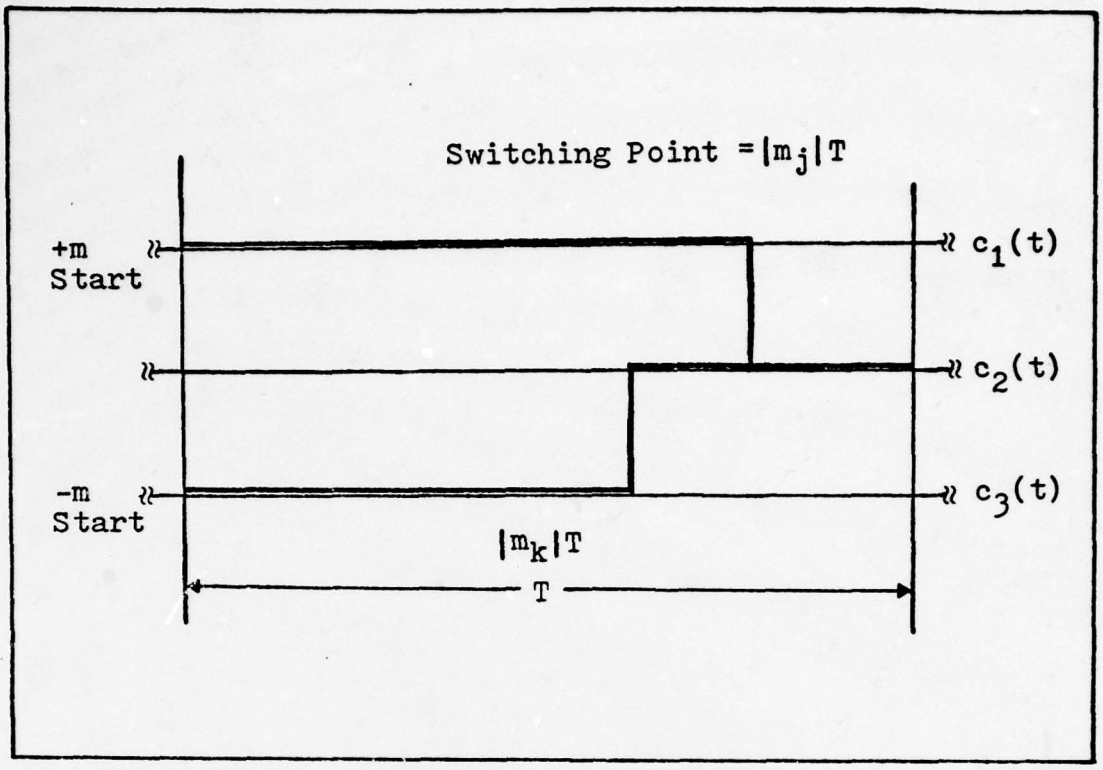

Fig 15. Code Sequence Selection for Positive and Negative Sample Values

Receiver Structure. The phase coherent receiver structure for tri-orthogonal word PWM is shown in Figure 16. The output from the ith leg correlator matched to codeword $c_i(t)$ can be written as

$$I_i = 2\int_0^T R(t)c_i(t)\cos(\omega_0 t)dt \qquad (116)$$

During each T second transmission interval, either the output I_1 or I_3 produces just a noise and interference component with no signal contribution. Given that m_i is positive, the correlator outputs are given by

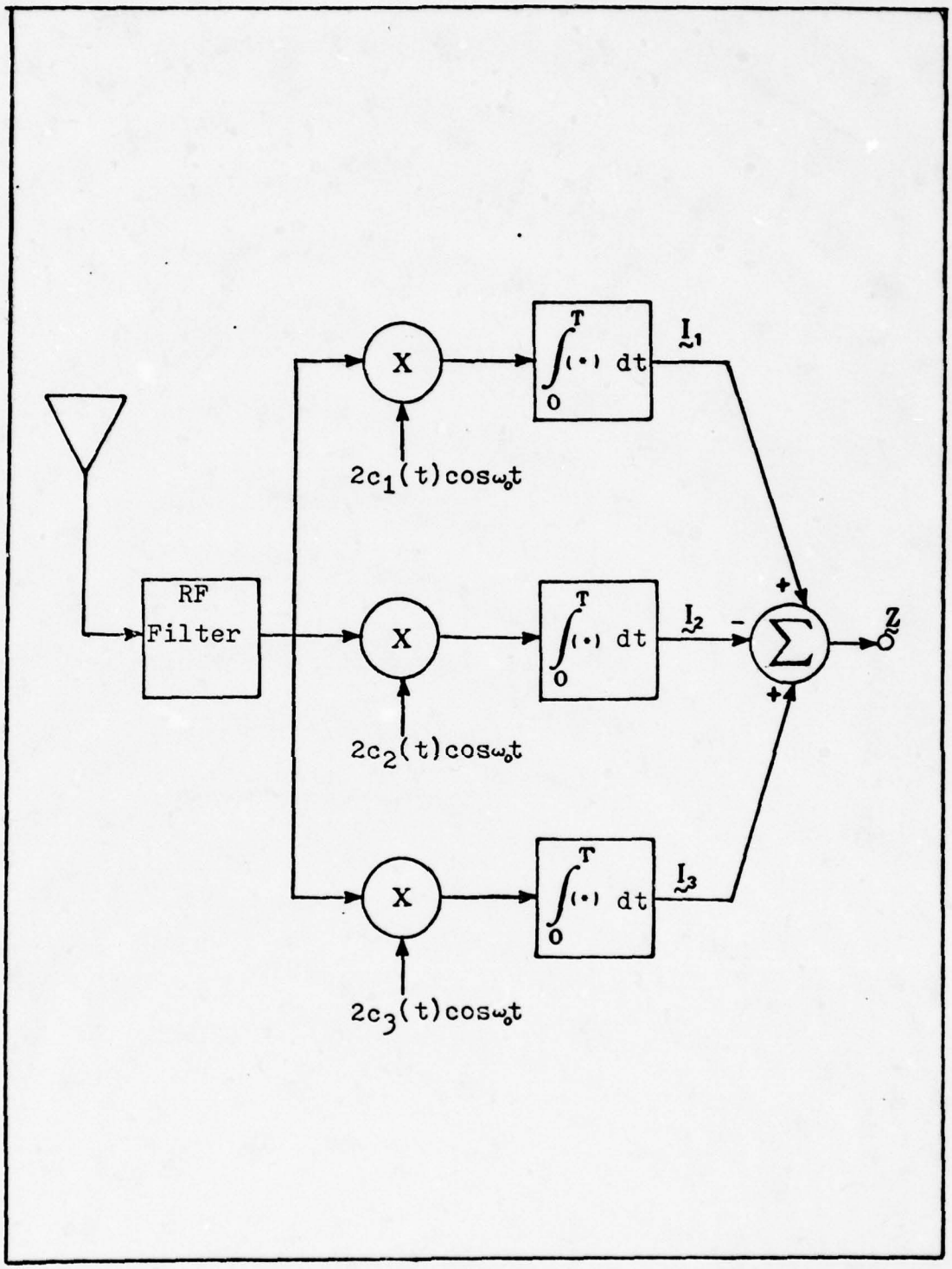

Fig 16. Phase Coherent Tri-Orthogonal Word Pulse-Width Modulation Receiver

$$\underline{I}_1 = \sqrt{P}\int_0^T d(t)c_1(t)dt + \int_0^T \underline{n}_c(t)c_1(t)dt + \int_0^T \underline{J}_x(t)c_1(t)dt \tag{117}$$

$$\underline{I}_2 = \sqrt{P}\int_0^T d(t)c_2(t)dt + \int_0^T \underline{n}_c(t)c_2(t)dt + \int_0^T \underline{J}_x(t)c_2(t)dt \tag{118}$$

and

$$\underline{I}_3 = \int_0^T \underline{n}_c(t)c_3(t)dt + \int_0^T \underline{J}_x(t)c_3(t)dt +$$

$$\sqrt{P}\int_0^{|m|T} c_1(t)c_3(t)dt + \sqrt{P}\int_{|m|T}^T c_2(t)c_3(t)dt \tag{119}$$

When m_i is negative there is a symmetrical result where the correlator outputs are given by

$$\underline{I}_1 = \int_0^T \underline{n}_c(t)c_1(t)dt + \int_0^T \underline{J}_x(t)c_1(t)dt + \sqrt{P}\int_0^{|m|T} c_3(t)c_1(t)dt$$

$$+ \sqrt{P}\int_{|m|T}^T c_2(t)c_1(t)dt \tag{120}$$

$$\underline{I}_2 = \sqrt{P}\int_0^T d(t)c_2(t)dt + \int_0^T \underline{n}_c(t)c_2(t)dt + \int_0^T \underline{J}_x(t)c_2(t)dt \tag{121}$$

and

$$\underset{\sim}{I}_3 = \sqrt{P}\int_0^T d(t)c_3(t)dt + \int_0^T \underset{\sim}{n}_c(t)c_3(t)dt + \int_0^T \underset{\sim}{J}_x(t)c_3(t)dt \quad (122)$$

Following the logic used to evaluate the coherent bi-orthogonal word receiver structure produces a representation for positive and negative sample values that has a symmetrical structure. The sample outputs at time kT from the analog correlators can be written as

$$\underset{\sim}{I}_1 = \sqrt{P}T\left(\frac{1+m_k \operatorname{sgn} m_k}{2}\right)\operatorname{sgn} m_k + \underset{\sim}{n} + \underset{\sim}{J} + \underset{\sim}{\xi}(m) \quad (123)$$

$$\underset{\sim}{I}_2 = \sqrt{P}T\left(\frac{1-m_k \operatorname{sgn} m_k}{2}\right)\operatorname{sgn} m_k + \underset{\sim}{n} + \underset{\sim}{J} + \underset{\sim}{\xi}(m) \quad (124)$$

$$\underset{\sim}{I}_3 = \underset{\sim}{n} + \underset{\sim}{J} + \underset{\sim}{\xi}(m) + \underset{\sim}{\xi}(m) \quad (125)$$

where m_k is a positive quantity.

When m_k is a negative quantity the analog correlators produce

$$\underset{\sim}{I}_1 = \underset{\sim}{n} + \underset{\sim}{J} + \underset{\sim}{\xi}(m) + \underset{\sim}{\xi}(m) \quad (126)$$

$$\underset{\sim}{I}_2 = \sqrt{P}T\left(\frac{1-m_k \operatorname{sgn} m_k}{2}\right)\operatorname{sgn} m_k + \underset{\sim}{n} + \underset{\sim}{J} + \underset{\sim}{\xi}(m) \quad (127)$$

$$\underset{\sim}{I}_3 = \sqrt{P}T\left(\frac{1+m_k \operatorname{sgn} m_k}{2}\right)\operatorname{sgn} m_k + \underset{\sim}{n} + \underset{\sim}{J} + \underset{\sim}{\xi}(m) \quad (128)$$

Where in both cases m_k is a fixed, but unknown quantity, $\underset{\sim}{n}$

is distributed $N(o,N_0T/2)$, $\underset{\sim}{J}$ is distributed $N(o,J_0T^2/N)$, $\underset{\sim}{\xi}(m)$ is distributed $N(o,\Psi^2(m))$ and $\underset{\sim}{\xi}(m)$ is the complementary signal dependent noise distributed $N(o,\Lambda^2(m))$.

The final receiver output as shown in Figure 16 is a linear combination of the three Gaussian random variables that are the correlator outputs and is therefore also a Gaussian random variable. The receiver output $\underset{\sim}{Z}$ is given by

$$\underset{\sim}{Z} = \underset{\sim}{I}_1 + \underset{\sim}{I}_3 - \underset{\sim}{I}_2 \tag{129}$$

The expected value of $\underset{\sim}{Z}$ for both positive and negative sample values is given by

$$\begin{aligned} E\{Z\} &= E\{I_1\} + E\{I_3\} - E\{I_2\} \\ &= \sqrt{P}Tm \end{aligned} \tag{130}$$

Because the correlator outputs are also independent random variables the variance is given by

$$\begin{aligned} \lambda^2 &= \mathrm{Var}\{I_1\} + \mathrm{Var}\{I_2\} + \mathrm{Var}\{I_3\} \\ &= 3\beta^2 + \frac{5}{4}\sigma_c^2 \end{aligned} \tag{131}$$

where

$$\beta^2 = \frac{N_0T}{2} + \frac{J_0T^2}{N} + \frac{\sigma_c^2}{4}$$

σ_c^2 = total cross-correlation noise=$\Psi^2(m)+\Lambda^2(m)$

Signal Processing Performance. The symmetry seen in the receiver output relations insures that the expected value and variance of the random variable Z_k are constant over time. The observed receiver sample output can therefore be described by the conditional probability density function $f(z|m)$ as

$$f(Z|m) = \frac{1}{\sqrt{2\pi}\lambda} \exp\left[-\frac{(Z-\sqrt{P}Tm)^2}{2\lambda^2}\right] \tag{132}$$

The maximum likelihood estimate of the parameter m is given by

$$\hat{m}_{ml} = \frac{Z}{\sqrt{P}T} \tag{133}$$

The estimate is conditionally unbiased with the variance of the estimation error given by

$$\begin{aligned} \mathrm{Var}\{(\hat{m}_{ml}-m)|m\} &= \frac{\lambda^2}{PT^2} \\ &= \frac{3N_0T/2 + 3J_0T^2/N + 2\sigma_c^2}{PT^2} \end{aligned} \tag{134}$$

Neglecting the cross-correlation noise the variance of the estimation error is triple that seen in the antipodal PWM system. Namely

$$\mathrm{Var}\{(\hat{m}_{ml}-m)|m\} = \frac{3N_0/2 + 3J_0T/N}{PT} \tag{135}$$

The corresponding signal-to-noise ratio reveals the same

4.77db degradation in system performance.

$$\frac{S}{N} = \left(\frac{1}{3}\right) \frac{PTm^2}{\frac{N_0}{2} + \frac{J_0 T}{N}} \tag{136}$$

Phase Noncoherent System

Noncoherent tri-orthogonal word PWM will be employed when a phase offset exists between the received signal and the local oscillator in the receiver. The transmitted signal is then given by

$$x(t) = \sqrt{P}\, d(t)\cos(\omega_0 t+\phi) \tag{137}$$

where ϕ is the phase difference between the received signal and the receiver local reference.

Receiver Structure. The noncoherent tri-orthogonal word PWM receiver is shown in Figure 17. The complete received signal is given by

$$\underset{\sim}{R}(t) = \sqrt{P}d(t)\cos(\omega_0 t+\phi)+\underset{\sim}{n}(t)+\underset{\sim}{J}(t)\cos(\omega_0 t-\underset{\sim}{\theta}) \tag{138}$$

The receiver now produces inphase and quadrature signal components at the output of the correlator matched to $c_k(t)$. The correlator outputs are given by

$$\underset{\sim}{I}_k = 2\int_0^T \underset{\sim}{R}(t)c_k(t)\cos(\omega_0 t)dt, \quad k=1,2,3 \tag{139}$$

and

$$\underset{\sim}{Q}_k = 2\int_0^T \underset{\sim}{R}(t)c_k(t)\sin(\omega_0 t)dt, \quad k=1,2,3 \tag{140}$$

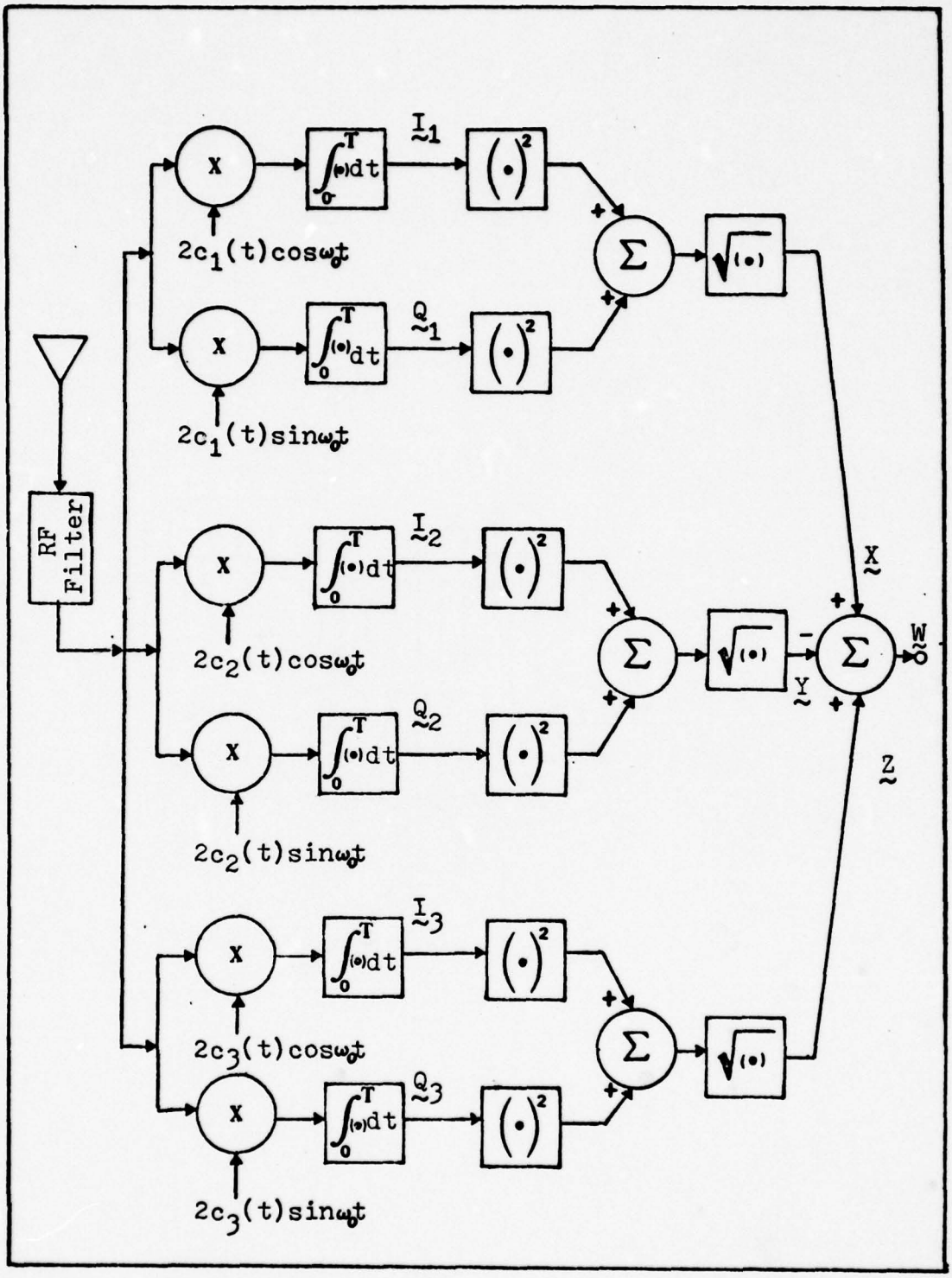

Fig 17. Phase Noncoherent Tri-Orthogonal Word Pulse-Width Modulation Receiver

Following the steps outlined in the noncoherent bi-orthogonal word receiver analysis results in an inphase signal given by

$$\underset{\sim}{I}_k = \sqrt{P}\cos\phi \int_0^T d(t)c_k(t)dt + \int_0^T \underset{\sim}{n}_c(t)c_k(t)dt + \int_0^T \underset{\sim}{J}_x(t)c_k(t)dt \qquad (141)$$

$$; \; k=1,2,3$$

and a quadrature signal given by

$$\underset{\sim}{Q}_k = \sqrt{P}\sin\phi \int_0^T d(t)c_k(t)dt - \int_0^T \underset{\sim}{n}_s(t)c_k(t)dt + \int_0^T \underset{\sim}{J}_y(t)c_k(t)dt \qquad (142)$$

$$; \; k=1,2,3$$

The representation for positive and negative sample values has the same symmetrical character seen in the analysis of the coherent receiver structure. When m_k is positive the sample value outputs at time kT of the correlators matched to $c_1(t)$ are given by

$$\underset{\sim}{I}_1 = \sqrt{P}T\cos\phi\left(\frac{1+m_k \operatorname{sgn} m_k}{2}\right) \operatorname{sgn} m_k + \underset{\sim}{n} + \underset{\sim}{J} + \cos\phi\,\underset{\sim}{\xi}(m) \qquad (143)$$

and

$$\underset{\sim}{Q}_1 = \sqrt{P}T\sin\phi\left(\frac{1+m_k \operatorname{sgn} m_k}{2}\right) \operatorname{sgn} m_k - \underset{\sim}{n} + \underset{\sim}{J} + \sin\phi\,\underset{\sim}{\xi}(m) \qquad (144)$$

The sample outputs from the correlators matched to codeword two can be written as

$$\underset{\sim}{I}_2 = \sqrt{P}T\cos\phi\left(\frac{1-m_k \operatorname{sgn} m_k}{2}\right) \operatorname{sgn} m_k + \underset{\sim}{n} + \underset{\sim}{J} + \cos\phi\,\underset{\sim}{\xi}(m) \qquad (145)$$

and

$$\underset{\sim}{Q}_2 = \sqrt{P}T\sin\phi\left(\frac{1-m_k \operatorname{sgn} m_k}{2}\right) \operatorname{sgn} m_k - \underset{\sim}{n} + \underset{\sim}{J} + \sin\phi\,\underset{\sim}{\xi}(m) \qquad (146)$$

The corresponding sample outputs with positive m_k for channel three are given by

$$\underset{\sim}{I}_3 = \underset{\sim}{n} + \underset{\sim}{J} + \cos\phi\,\underset{\sim}{\xi}(m) + \cos\phi\,\underset{\sim}{\xi}(m) \qquad (147)$$

and

$$\underset{\sim}{Q}_3 = -\underset{\sim}{n} + \underset{\sim}{J} + \sin\phi\,\underset{\sim}{\xi}(m) + \sin\phi\,\underset{\sim}{\xi}(m) \qquad (148)$$

When m_k is a negative quantity the outputs from channel one and channel three are interchanged. The sample outputs from the correlators matched to codeword one are thus

$$\underset{\sim}{I}_1 = \underset{\sim}{n} + \underset{\sim}{J} + \cos\phi\,\underset{\sim}{\xi}(m) + \cos\phi\,\underset{\sim}{\xi}(m) \qquad (149)$$

and

$$\underset{\sim}{Q}_1 = -\underset{\sim}{n} + \underset{\sim}{J} + \sin\phi\,\underset{\sim}{\xi}(m) + \sin\phi\,\underset{\sim}{\xi}(m) \qquad (150)$$

The correlator matched to codeword two produce outputs defined by

$$\underset{\sim}{I}_2 = \sqrt{P}T\cos\phi\left(\frac{1-m_k \operatorname{sgn} m_k}{2}\right) \operatorname{sgn} m_k + \underset{\sim}{n} + \underset{\sim}{J} + \cos\phi\,\underset{\sim}{\xi}(m) \qquad (151)$$

and

$$\underset{\sim}{Q}_2 = \sqrt{P}T \sin\phi\left(\frac{1-m_k \operatorname{sgn} m_k}{2}\right)\operatorname{sgn} m_k - \underset{\sim}{n} + \underset{\sim}{J} + \sin\phi\,\underset{\sim}{\xi}(m) \qquad (152)$$

The corresponding outputs from the correlators in channel three are given by

$$\underset{\sim}{I}_3 = \sqrt{P}T \cos\phi\left(\frac{1+m_k \operatorname{sgn} m_k}{2}\right)\operatorname{sgn} m_k + \underset{\sim}{n} + \underset{\sim}{J} + \cos\phi\,\underset{\sim}{\xi}(m) \qquad (153)$$

and

$$\underset{\sim}{Q}_3 = \sqrt{P}T \sin\phi\left(\frac{1+m_k \operatorname{sgn} m_k}{2}\right) \operatorname{sgn} m_k - \underset{\sim}{n} + \underset{\sim}{J} + \sin\phi\,\underset{\sim}{\xi}(m) \qquad (154)$$

Where in both cases m_k is a fixed but unknown quantity, $\underset{\sim}{n}$ is distributed $N(o,N_oT/2)$, $\underset{\sim}{J}$ is distributed $N(o,\frac{J_oT^2}{N})$, $\underset{\sim}{\xi}(m)$ is distributed $N(o,\Psi^2(m))$, and $\xi(m)$ is the complementary signal dependent noise distributed $N(o,\Lambda^2(m))$.

The correlator sample outputs are thus Gaussian random variables that can be totally characterized with knowledge of their mean and variance. Table III provides the mean and variance associated with each correlator output and sample parameter polarity. The receiver then uses envelope detectors to produce intermediate outputs $\underset{\sim}{x}$, $\underset{\sim}{y}$ and $\underset{\sim}{z}$ as shown in Figure 17. The envelope detector outputs are defined by

$$\underset{\sim}{x} = \sqrt{(\underset{\sim}{I}_1)^2 + (\underset{\sim}{Q}_1)^2} \qquad (155)$$

Table III

Correlator Output Statistics

Correlator Output		Mean	Variance
POSITIVE M	I_1	$\sqrt{P}T\left[\frac{1+m}{2}\right]\cos\phi$	$\frac{N_0T}{2} + \frac{J_0T^2}{N} + \cos^2\phi\Psi^2(m)$
	Q_1	$\sqrt{P}T\left[\frac{1+m}{2}\right]\sin\phi$	$\frac{N_0T}{2} + \frac{J_0T^2}{N} + \sin^2\phi\Psi^2(m)$
	I_2	$\sqrt{P}T\left[\frac{1-m}{2}\right]\cos\phi$	$\frac{N_0T}{2} + \frac{J_0T^2}{N} + \cos^2\phi\Lambda^2(m)$
	Q_2	$\sqrt{P}T\left[\frac{1-m}{2}\right]\sin\phi$	$\frac{N_0T}{2} + \frac{J_0T^2}{N} + \sin^2\phi\Lambda^2(m)$
	I_3	0	$\frac{N_0T}{2} + \frac{J_0T^2}{N} + \cos^2\phi\sigma_c^2$
	Q_3	0	$\frac{N_0T}{2} + \frac{J_0T^2}{N} + \sin^2\phi\sigma_c^2$
NEGATIVE M	I_1	0	$\frac{N_0T}{2} + \frac{J_0T^2}{N} + \cos^2\phi\sigma_c^2$
	Q_1	0	$\frac{N_0T}{2} + \frac{J_0T^2}{N} + \sin^2\phi\sigma_c^2$
	I_2	$\sqrt{P}T\left[\frac{1-m}{2}\right]\cos\phi$	$\frac{N_0T}{2} + \frac{J_0T^2}{N} + \cos^2\phi\Lambda^2(m)$
	Q_2	$\sqrt{P}T\left[\frac{1-m}{2}\right]\sin\phi$	$\frac{N_0T}{2} + \frac{J_0T^2}{N} + \sin^2\phi\Lambda^2(m)$
	I_3	$\sqrt{P}T\left[\frac{1+m}{2}\right]\cos\phi$	$\frac{N_0T}{2} + \frac{J_0T^2}{N} + \cos^2\phi\Psi^2(m)$
	Q_3	$\sqrt{P}T\left[\frac{1+m}{2}\right]\sin\phi$	$\frac{N_0T}{2} + \frac{J_0T^2}{N} + \sin^2\phi\Psi^2(m)$

$$\underset{\sim}{y} = \sqrt{(I_2)^2 + (Q_2)^2} \tag{156}$$

$$\underset{\sim}{z} = \sqrt{(I_3)^2 + (Q_3)^2} \tag{157}$$

The probability density functions for $\underset{\sim}{x}$, $\underset{\sim}{y}$ and $\underset{\sim}{z}$ cannot be obtained with the correlator output variances defined as signal dependent and unique to each receiver channel. Chapter VI shows that the total cross-correlation noise $\sigma_c^2=\Lambda^2(m)+\Psi^2(m)$ is not signal dependent and as shown in Chapter IV each envelope detector channel produces approximately $\sigma_c^2/4$ cross-correlation noise. Using this approximation, the correlator outputs with non-zero means all have a variance equal to $\frac{N_0T}{2} + \frac{J_0T^2}{N} + \frac{\sigma_c^2}{4}$ and the correlator outputs with zero means have a variance equal to $\frac{N_0T}{2} + \frac{J_0T^2}{N} + \frac{\sigma_c^2}{2}$. The probability density functions can now be defined using the approximate channel variances.

Signal Processing Performance. The final receiver output $\underset{\sim}{w}$ is formed from a linear combination of the envelope detector outputs. The receiver output is defined by

$$\underset{\sim}{w} = \underset{\sim}{x} + \underset{\sim}{z} - \underset{\sim}{y} \tag{158}$$

The symmetry seen in the envelope detector outputs insures that the expected value and variance of the random variable $\underset{\sim}{w}$ are constant over time since interchanging the roles of $\underset{\sim}{x}$ and $\underset{\sim}{z}$ has no impact on $\underset{\sim}{w}$. Therefore, throughout the

remainder of this section z will be assumed to be the envelope detector output with zero mean.

The random variables I_1 and Q_1 are independent and jointly normal with means given in Table III and the variance in each channel approximately

$$\beta^2 = \frac{N_0 T}{2} + \frac{J_0 T^2}{N} + \frac{\sigma_c^2}{4} \tag{159}$$

The conditional density of $x=\sqrt{(I_1)^2+(Q_1)^2}$ is given by (Papoulis, 1965:498)

$$f(x|m) = \frac{x}{\beta^2} \exp\left[-\frac{x^2+\eta^2}{2\beta^2}\right] I_0\left(\frac{x\eta}{\beta^2}\right) U(x) \tag{160}$$

where

$$\eta^2 = T^2 P \left(\frac{1+m}{2}\right)^2$$

$$U(x) = \text{the unit step function}$$

The conditional density of $y=\sqrt{(I_2)^2+(Q_2)^2}$ is obtained in the same fashion and is given by

$$f(y|m) = \frac{y}{\beta^2} \exp\left[-\frac{y^2+s^2}{2\beta^2}\right] I_0\left(\frac{ys}{\beta^2}\right) U(y) \tag{161}$$

where

$$s^2 = T^2 P \left(\frac{1-m}{2}\right)^2$$

The conditional density $\underset{\sim}{Z} = \sqrt{(\underset{\sim}{I}_3)^2+(\underset{\sim}{Q}_3)^2}$ is obtained when both $\underset{\sim}{I}_3$ and $\underset{\sim}{Q}_3$ are zero mean as a simplification of the usual Rician density function (Raemer, 1969:85). The resulting envelope is distributed Rayleigh with the probability density function given by

$$f(z|m) = \frac{Z}{(\beta^2 + \frac{\sigma_c^2}{2})} \exp\left[-\frac{z^2}{2(\beta^2 + \frac{\sigma_c^2}{2})}\right] U(Z) \tag{162}$$

Thus, the random variables $\underset{\sim}{x}$ and $\underset{\sim}{y}$ have a Rician conditional density function while the third channel $\underset{\sim}{z}$ has a Rayleigh density function. The final receiver output is formed by

$$\underset{\sim}{w} = \underset{\sim}{x} + \underset{\sim}{z} - \underset{\sim}{y} \tag{163}$$

The density function $f(w|m)$ could not be obtained as shown in Chapter IV. Thus, an estimate for m and its associated error variance could not be found for the given ad hoc noncoherent receiver. The alternate signal-to-noise ratio requires only the first two moments of the output random variable. The expected value is found from

$$E\{w\} = E\{x\} + E\{z\} - E\{y\} \tag{164}$$

The results derived in Chapter IV and $E\{Z\} = \sqrt{\frac{\pi}{2}(\beta^2+\sigma_c^2/2)}$ immediately provide the expected value of the receiver output. Thus, in the "large" signal region ($PT^2m^2 >> \beta^2$)

$$E\{w\}_{l.s.} = \sqrt{P}Tm - \frac{\beta^2}{\sqrt{P}T}\left[\frac{m}{1-m^2}\right] + \sqrt{\frac{\pi}{2}\left[\beta^2 + \frac{\sigma_c^2}{2}\right]} \qquad (165)$$

and in the corresponding "small" signal region

$$E\{w\}_{s.s.} = \sqrt{\frac{\pi}{2}}\ \frac{PT^2}{4\beta}\ m + \sqrt{\frac{\pi}{2}\left[\beta^2 + \frac{\sigma_c^2}{2}\right]} \qquad (166)$$

Comparing the results obtained here for the noncoherent receiver with an expected value of $\Gamma = \sqrt{P}Tm$ obtained for the coherent receiver structure indicates some distortion effects are introduced by the noncoherent receiver. Neglecting the cross-correlation noise, the "large" signal approximation can be written with $K = \frac{\sqrt{P}T}{\beta}$ as

$$E\{w\}_{l.s.} \simeq \Gamma - \frac{\Gamma}{K^2}(1+m^2) + \frac{\Gamma}{K}\sqrt{\frac{\pi}{2}}\left[\frac{1}{m}\right] \qquad (167)$$

The "small" signal approximation can also be written in terms of the coherent receivers expected value

$$E\{w\}_{s.s.} \simeq 0.313K\Gamma + \frac{\Gamma}{Km}\sqrt{\frac{\pi}{2}} \qquad (168)$$

The distortion effects are shown in Figure 18, where the expected value of the coherent receiver is compared to the noncoherent receiver expected value approximations. The approximations are plotted as a function of K , the square root of the signal power to noise power ratio. The distortion caused

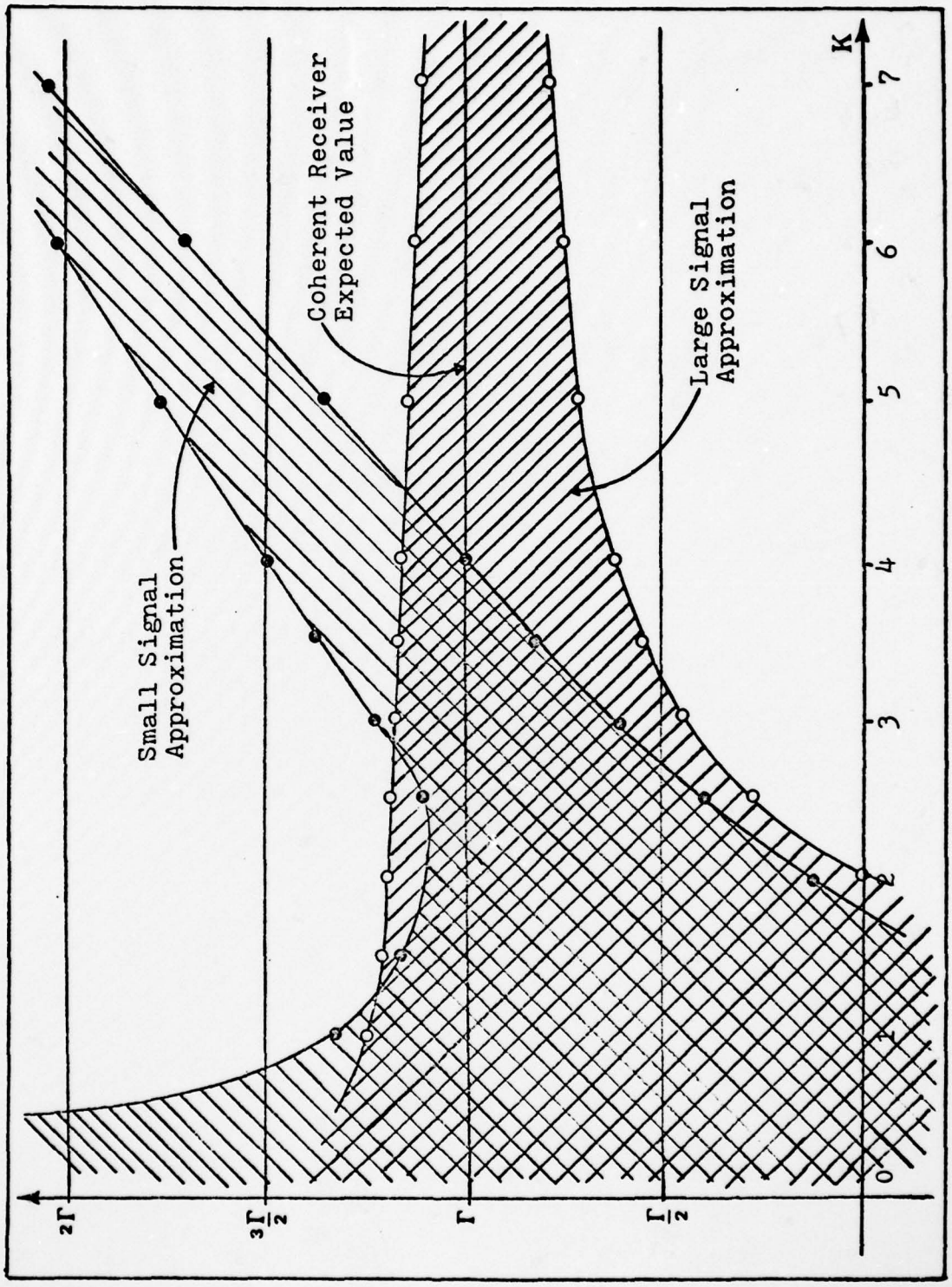

Fig 18. Noncoherent Receiver Expected Value Approximations Compared to Coherent Receiver Expected Value $(K=\frac{\sqrt{PT}}{\beta})$

by the direct feed-through of noise in one channel is very severe when the signal-to-noise ratio is small. The receiver should perform poorly in a high noise environment.

The corresponding "large" signal approximation for the receiver output variance is given by

$$\sigma^2_{w_{l.s.}} \simeq 2\beta^2 - \frac{\beta^2}{K^2}(1+m^2)+(2-\frac{\pi}{2})\beta^2 \tag{169}$$

and the "small" signal region has the approximation

$$\sigma^2_{w_{s.s.}} \simeq (0.858)\beta^2 + (0.108)\beta^2K^2(1+m^2)+(2-\frac{\pi}{2})\beta^2 \tag{170}$$

The coherent receiver variance and both approximations for the noncoherent receiver variance are shown in Figure 19.

The signal-to-noise ratio for the "small" signal region or where K is less than three as shown in Figures 18 and 19 can now be computed. The S/N is given by

$$\left(\frac{S}{N}\right)_{s.s.} \simeq \frac{E^2\{w\}_{s.s.}}{\sigma^2_{w\ s.s.}}$$

$$= \frac{5\pi\left[\frac{PT^2}{4\beta}m + \beta\right]^2}{12.9\beta^2+1.08\beta^2K^2(1+m^2)} \tag{171}$$

$$= \frac{15\pi(\sqrt{P}T/4\beta+\beta/\sqrt{P}Tm)^2}{12.9+1.08PT^2(1+m^2)/\beta^2} \left(\frac{S}{N}\right)_{\text{coherent}}$$

In the "large" signal region or where K is greater than three

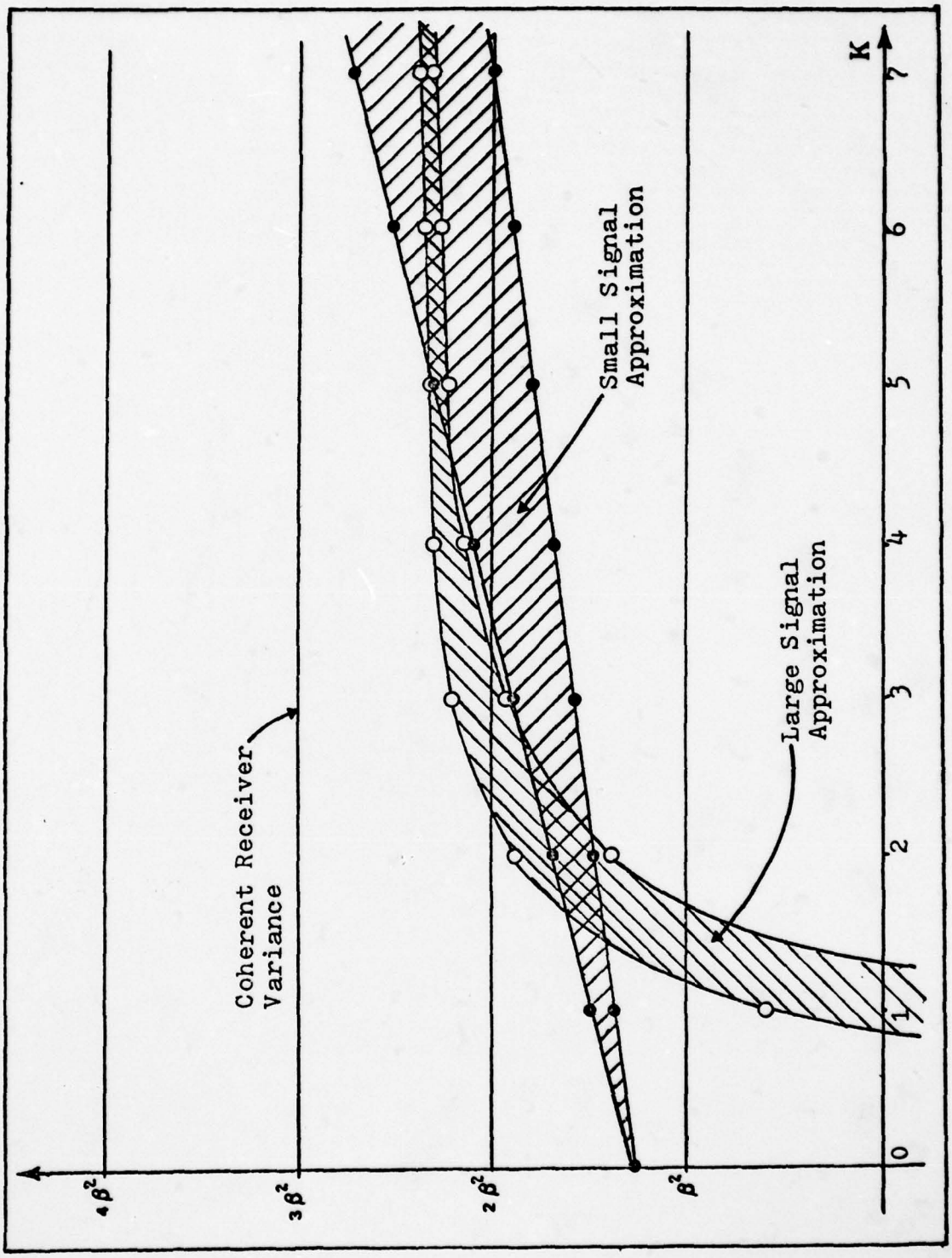

Fig 19. Noncoherent Receiver Variance Approximation Compared to Coherent Receiver Variance $(K=\frac{\sqrt{P}T}{\beta})$

the signal-to-noise ratio is given by

$$\left(\frac{S}{N}\right)_{l.s.} \simeq \frac{\left[\sqrt{PT}m-(\beta^2/\sqrt{PT})(1+m^2)+\sqrt{\frac{\pi}{2}}\,\beta\right]^2}{2.43\beta^2-(\beta^4/PT^2)(1+m^2)}$$

$$= \frac{3\left[1-\frac{\beta^2}{PT^2m}(1+m^2)+\sqrt{\frac{\pi}{2}}\,\frac{\beta}{\sqrt{PT}m}\right]^2}{\left[2.43-\frac{\beta^2}{PT^2}(1+m^2)\right]}\left(\frac{S}{N}\right)_{\text{coherent}} \tag{172}$$

The "large" signal region signal-to-noise ratio does not converge to the S/N obtained for the coherent structure due to the distortion introduced by the third channel feed through. Both the "large" and "small" signal approximations for the signal-to-noise ratio are plotted in Figure 20. The signal-to-noise ratio approximation plots compared to the coherent signal-to-noise ratio isolates the distortion produced by the envelope detectors. The third curve shows the true performance when the distortion terms are removed.

The signal space model also predicts the same 4.77db degradation in system performance seen in the coherent tri-orthogonal word receiver when viewed correctly. The stretch factor for any sample value is $\sqrt{E/2}$ rather than the expected $\sqrt{2}E$ value. Also an additional noise term is introduced through the third bases function to give

$$\frac{S}{N} = \left(\frac{1}{3}\right)\frac{s^2}{N_0+2J_0T/N} \tag{173}$$

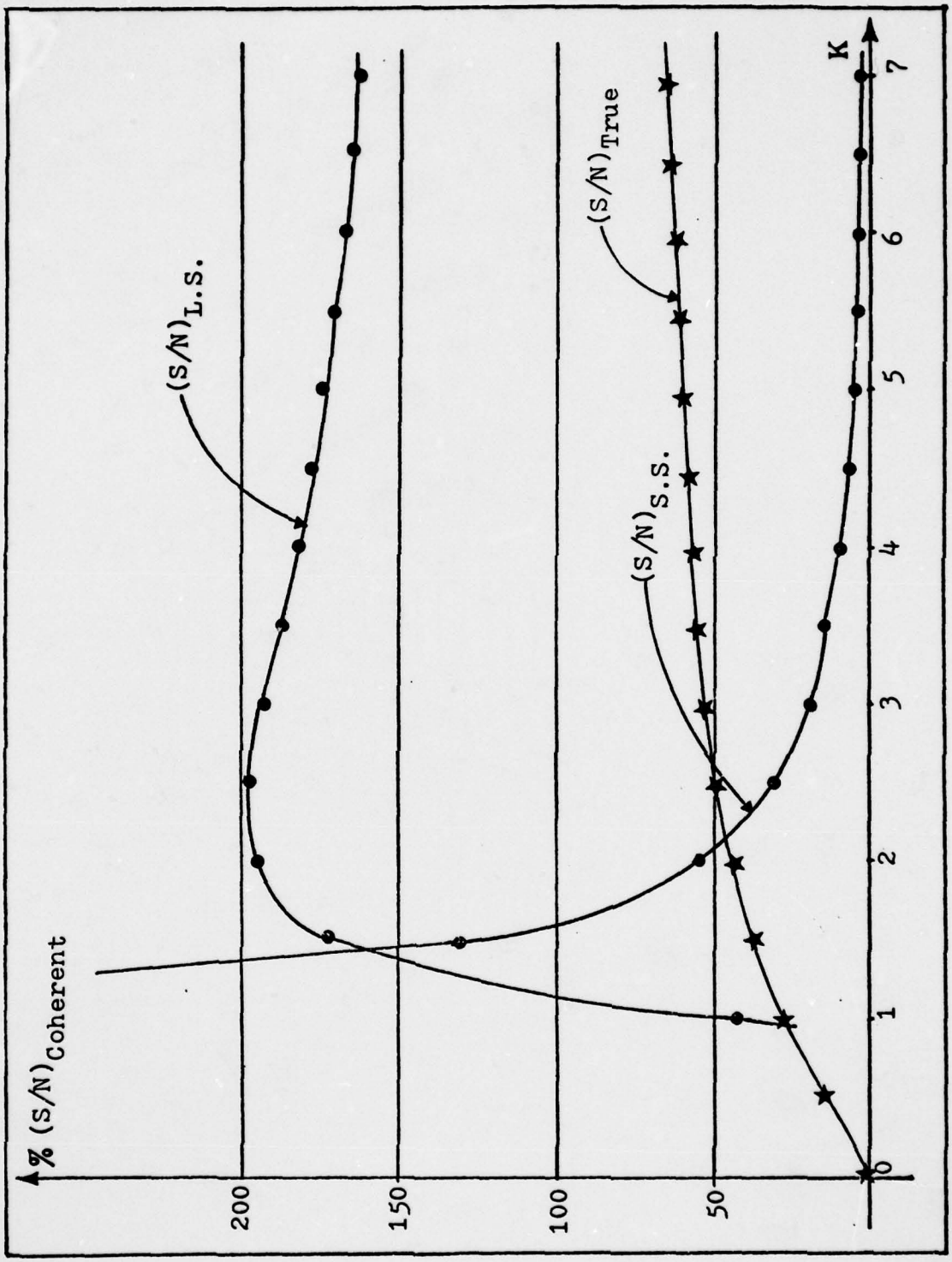

Fig 20. Noncoherent (S/N) Approximations Versus Coherent (S/N)

Thus the additional noise seen in the tri-orthogonal word format degrades the expected system performance below that provided by the earlier modulation formats. Because of the severe impact of additional noise sources in any modulation format, the next chapter will examine signal dependent noise produced in the multiple code word receivers.

VI. Code Noise

All multiple codeword pulse-width modulation schemes produce a partial cross-correlation function in addition to the desired signal. The code cross-correlation function will represent a signal dependent noise source to the receiver. This chapter will examine code cross-correlation noise in both the single and multiple user environment. The random binary wave discussed in Appendix A will be used to set bounds on the performance of any deterministic code sequence used in an actual communication system.

Self Noise

The coherent bi-orthogonal word PWM system will be used to develope the partial cross-correlation noise results that apply to all multiple codeword modulation formats. The output of just the signal component from the analog correlators was given in Chapter IV as

$$I_1 = \sqrt{P}\int_0^{\left\{\frac{1+m}{2}\right\}T} c_1(t)c_1(t)dt + \sqrt{P}\int_{\left\{\frac{1+m}{2}\right\}T}^{T} c_1(t)c_2(t)dt \tag{174}$$

and

$$I_2 = \sqrt{P}\int_0^{\left\{\frac{1+m}{2}\right\}T} c_1(t)c_2(t)dt + \sqrt{P}\int_{\left\{\frac{1+m}{2}\right\}T}^{T} c_2(t)c_2(t)dt \tag{175}$$

Both receiver channels produce a desired signal term and an unwanted signal dependent noise term. Figure 21 illustrates for a typical transmitted code sequence the formation of both the desired term and cross-correlation noise in the receiver channels. The correlator outputs reduce to

$$\underset{\sim}{I}_1 = \sqrt{P}\left\{\frac{1+m}{2}\right\}T + \underset{\sim}{\xi}(m) \tag{176}$$

and

$$\underset{\sim}{I}_2 = \underset{\sim}{\xi}(m) + \sqrt{P}\left\{\frac{1-m}{2}\right\}T \tag{177}$$

The output from channel I is then a signal term and partial cross-correlation function. The partial cross-correlation function is given by

$$\underset{\sim}{\xi}(m) = \sqrt{P}\int_{\left\{\frac{1+m}{2}\right\}T}^{T} c_2(t)c_1(t)dt \tag{178}$$

Assuming that both $c_1(t)$ and $c_2(t)$ are random binary waves composed of equally likely pulses of amplitude ± 1 and duration T_c seconds, their temporally aligned product $c_1(t)$ $c_2(t)$ will produce another random binary wave $c_3(t)$ with the same characteristics.

The partial cross-correlation function is then expressed by

$$\underset{\sim}{\xi}(m) = \sqrt{P}\int_{\left\{\frac{1+m}{2}\right\}T}^{T} c_3(t)dt \tag{179}$$

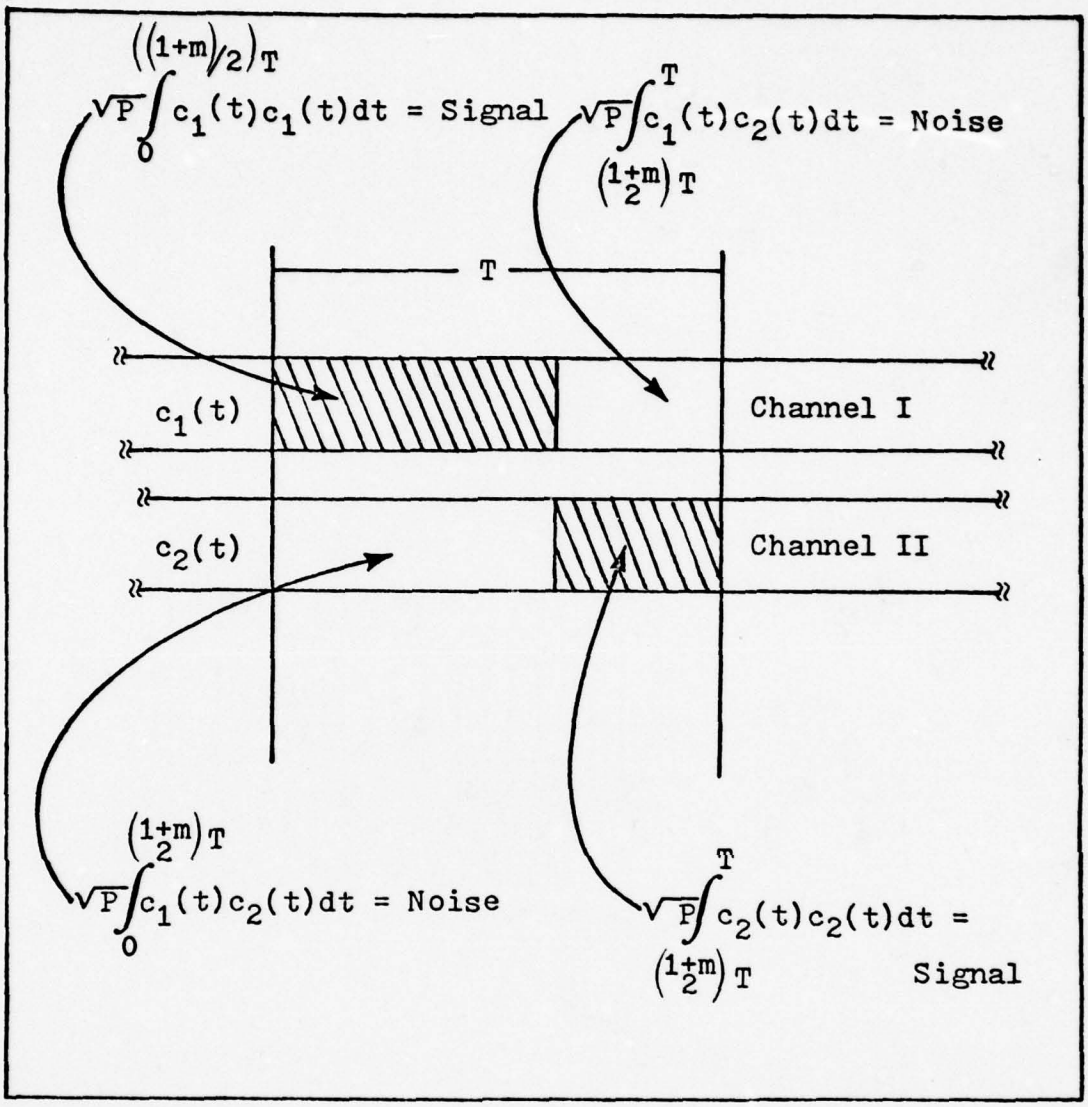

Fig 21. Origin of Signal Dependent Noise in Multiple Codeword Systems

The first two moments of the signal dependent noise can now be computed. The expected value of $\underset{\sim}{\varepsilon}(m)$ is given by

$$E\{\varepsilon(m)\} = \sqrt{P} \int_{\left\{\frac{1+m}{2}\right\}T}^{T} E\{c_3(t)\}dt \qquad (180)$$

$$= 0$$

The variance of the signal dependent noise is then found from

$$E\{\varepsilon^2(m)\} = P \int_{\left\{\frac{1+m}{2}\right\}T}^{T} \int_{\left\{\frac{1+m}{2}\right\}T}^{T} E\left\{c_3(t_1)c_3(t_2)\right\}dt_1dt_2$$

$$= P \int_{T\left\{\frac{1+m}{2}\right\}}^{T} \int_{\left\{\frac{1+m}{2}\right\}T}^{T} R_c(t_1-t_2)dt_1dt_2 \qquad (181)$$

Defining the variable $\tau=t_1-t_2$, the double integral can be transformed into a single integral in τ as shown in Figure 22 (Papoulis, 1965:335). The variance is then

$$E\{\varepsilon^2(m)\} = P \int_{-A}^{A} (A-|\tau|)R_c(\tau)d\tau \qquad (182)$$

where $R_c(\tau)$ is the autocorrelation function of the random binary wave defined in Appendix A and $A=T(\frac{1-m}{2})$.

Substituting the expression for $R_c(\tau)$ into the integrand results in

$$E\{\varepsilon^2(m)\} = P \int_{-T\left\{\frac{1-m}{2}\right\}}^{T\left\{\frac{1-m}{2}\right\}} \left[T\frac{(1-m)}{2} - |\tau| \right]\left[1- \frac{|\tau|}{T_c}\right] d\tau \qquad (183)$$

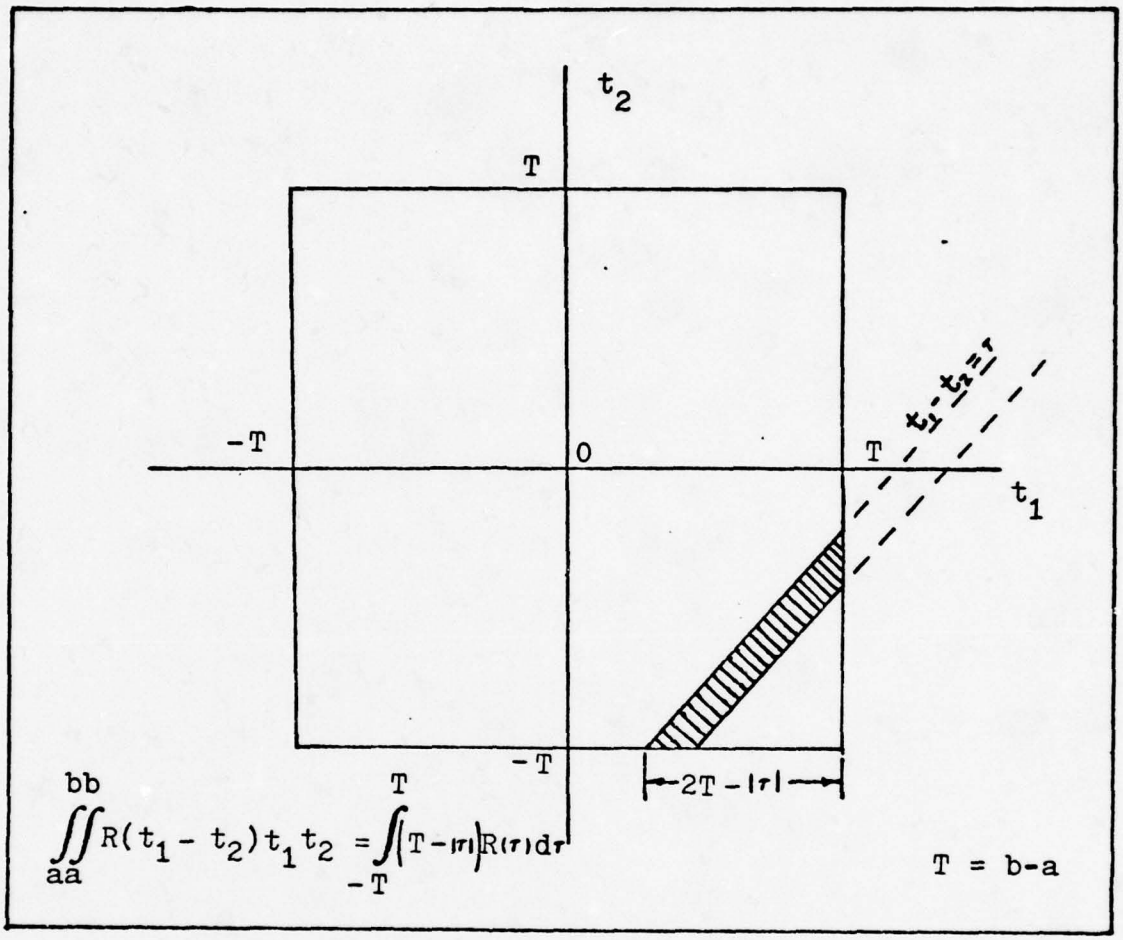

Fig 22. Double Integral Transformation

$$\simeq 2P \int_0^{T_c} \left[T\left|\frac{1-m}{2}\right| - \tau \right]\left[1 - \frac{\tau}{T_c}\right] d\tau$$

$$= \frac{PTT_c}{2}\left|(1-m)\right| - \frac{PT_c^{\,2}}{3}$$

The second channel also produces a partial cross-correlation term defined in Equation 175 and given by

$$\underset{\sim}{\xi}(m) = \sqrt{P} \int_0^{\left\{\frac{1+m}{2}\right\}T} c_3(t)dt \tag{184}$$

The expected value is found to be

$$E\{\xi(m)\} = \sqrt{P} \int_0^{\left\{\frac{1+m}{2}\right\}T} E\{c_3(t)\}dt$$

$$= 0 \tag{185}$$

The variance of the signal dependent noise in the second channel is found from

$$E\{\xi^2(m)\} = P \int_0^{\left\{\frac{1+m}{2}\right\}T} \int_0^{\left\{\frac{1+m}{2}\right\}T} E\left\{c_3(t_1)c_3(t_2)\right\}dt_1dt_2$$

$$= P \int_0^{\left\{\frac{1+m}{2}\right\}T} \int_0^{\left\{\frac{1+m}{2}\right\}T} R_c(t_1-t_2)dt_1dt_2 \tag{186}$$

Using the same integral transformation required for channel I results in a single integral expression. The variance in channel II is given by

$$E\{\xi^2(m)\} = P \int_{-\left\{\frac{1+m}{2}\right\}T}^{\left\{\frac{1+m}{2}\right\}T} \left[T\left|\frac{1+m}{2}\right| - |\tau| \right] R_c(\tau)\, d\tau$$

AD-A080 158 AIR FORCE INST OF TECH WRIGHT-PATTERSON AFB OH SCHOO--ETC F/G 17/2.1
PULSE-WIDTH MODULATION OF SPREAD SPECTRUM CARRIERS.(U)
DEC 79 F D TILLER
UNCLASSIFIED AFIT/GE/EE/79-39 NL

2 OF 2
AD
A080158

END
DATE FILMED
2-80
DDC

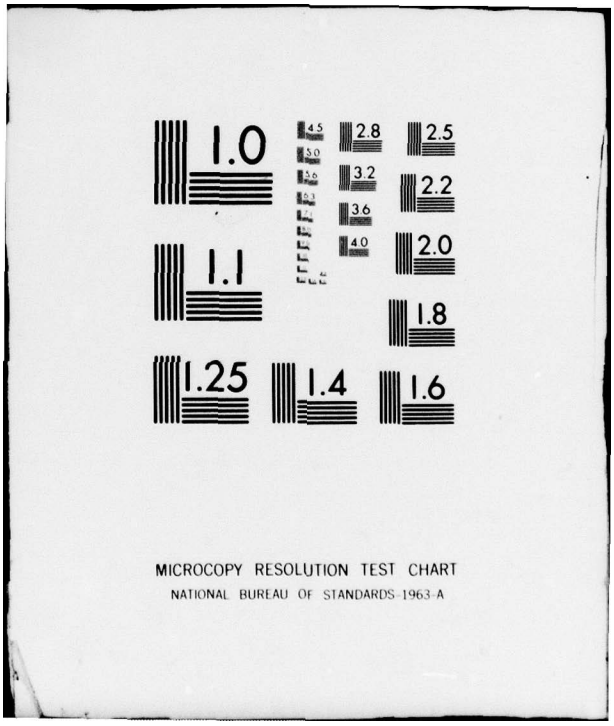
1.0
1.1
1.25
1.4
1.6
1.8
2.0
2.2
2.5
2.8
3.2
3.6
4.0
4.5
5.0
MICROCOPY RESOLUTION TEST CHART
NATIONAL BUREAU OF STANDARDS-1963-A

$$\simeq 2P \int_0^{T_c} \left[T\left\{\frac{1+m}{2}\right\} - \tau \right]\left[1 - \frac{\tau}{T_c}\right] d\tau \qquad (187)$$

$$= \frac{PTT_c}{2}(1+m) - \frac{PT_c^2}{3}$$

Defining the variance in channel I as $\Psi^2(m)$ and the variance in channel II as $\Lambda^2(m)$ allows the total cross-correlation variance σ_c^2 to be defined since the channel outputs are temporally juxtaposed and therefore are independent random variables. The total cross-correlation variance is not signal dependent and is defined by

$$\sigma_c^2 = \Lambda^2(m) + \Psi^2(m)$$

$$= PTT_c - \frac{2PT_c^2}{3} \qquad (188)$$

The partial cross-correlation noise is formed by adding (integrating) the contributions of a large number of random "chips" in the random binary waveform. The central-limit theorem then insures that the resulting cross-correlation noise will be approximately Gaussian.

Multiple User Code Noise

The results derived in the last section can be extended to multiple users operating in a conferencing mode. The

correlator outputs in the coherent bi-orthogonal word receiver now contain the superposition of the K users in the conference. The correlator outputs are given by

$$\underset{\sim}{I}_1 = \sum_{i=1}^{K} \sqrt{P}_i \left\{\frac{1+m_i}{2}\right\} T + \sum_{i=1}^{K} \underset{\sim}{\xi}_i(m) \tag{189}$$

and

$$\underset{\sim}{I}_2 = \sum_{i=1}^{K} \sqrt{P}_i \left\{\frac{1-m_i}{2}\right\} T + \sum_{i=1}^{K} \underset{\sim}{\xi}_i(m) \tag{190}$$

The expected value of the partial cross-correlation noise is given by

$$E\left\{\sum_{i=1}^{K} \varepsilon_i(m)\right\} = \sum_{i=1}^{K} E\{\varepsilon_i(m)\} \tag{191}$$

$$= 0$$

and

$$E\left\{\sum_{i=1}^{K} \xi_i(m)\right\} = \sum_{i=1}^{K} E\{\xi_i(m)\} \tag{192}$$

$$= 0$$

The partial cross-correlation variance produced in

channel I of the receiver is found from

$$E\left\{\sum_{i=1}^{K}\sum_{N=1}^{K}\epsilon_i(m)\epsilon_N(m)\right\} = \sum_{i=1}^{K}\sum_{N=1}^{K}E\{\varepsilon_i(m)\varepsilon_N(m)\}$$

$$= \sum_{i=1}^{K}\sum_{N=1}^{K}\sqrt{P}_i\sqrt{P}_N \int_{T\left\{\frac{1+m_i}{2}\right\}}^{T}\int_{T\left\{\frac{1+m_N}{2}\right\}}^{T} R_c(t_1-t_2)dt_1dt_2 \qquad (193)$$

The sample values $m_1, m_2, m_3 \ldots m_i, m \ldots m_K$ can be assumed to occur as increasing algebraic numbers in the interval $[-1,+1]$ without loss of generality. This result occurs since any other ordering of the K sample values is only a permutation of this ordering and all permutations sum to the same quantity. Now assuming that $P_i \simeq P_N = P$ and $m_i < m_N$, the double integral given in equation 193 can be transformed to (Papoulis, 1965:335)

$$E\left\{\sum_{i=1}^{K}\sum_{n=1}^{K}\varepsilon_i(m)\varepsilon_n(m)\right\} = \sum_{n=1}^{K}(2n-1)P \int_{-T\left\{\frac{1-m_n}{2}\right\}}^{T\left\{\frac{1-m_n}{2}\right\}} \left[T\left\{\frac{1-m_n}{2}\right\} - |\tau|\right] R_c(\tau)d\tau$$

$$= \sum_{n=1}^{K}(2n-1)2P \int_{o}^{T_c} (T(\tfrac{1-m_n}{2})-\tau)(1-\tfrac{\tau}{T_c})d\tau \qquad (194)$$

$$= \sum_{n=1}^{K} (2n-1)\left[\frac{PTT_c}{2}(1-m_n) - \frac{PT_c^2}{3}\right]$$

The partial cross-correlation variance produced in channel II of the receiver is found using the same approximations. The variance is then given by

$$E\left\{\sum_{i=1}^{K}\sum_{n=1}^{K}\xi_i(m)\xi_n(m)\right\} = \sum_{i=1}^{K}\sum_{n=1}^{K}\sqrt{P_i}\sqrt{P_n}\int_0^{T\left\{\frac{1+m_i}{2}\right\}}\int_0^{T\left\{\frac{1+m_n}{2}\right\}} R_c(t_1-t_2)dt_1dt_2 \tag{195}$$

The sample values again occur as increasing algebraic numbers in the interval $[-1,+1]$ where $m_i<m_N$ and $P_i \simeq P_N = P$. The double integral in equation 195 can now be transformed to

$$E\left\{\sum_{i=1}^{K}\sum_{n=1}^{K}\xi_i(m)\xi_n(m)\right\} = \sum_{i=1}^{K}(2K-2i+1)P\int_{-T\left\{\frac{1+m_i}{2}\right\}}^{T\left\{\frac{1+m_i}{2}\right\}}\left[T\left(\frac{1+m_i}{2}\right)-|\tau|\right]\left[1-\frac{|\tau|}{T_c}\right]d\tau \tag{196}$$

$$= \sum_{i=1}^{K}(2K-2i+1)\left[\frac{PTT_c}{2}(1+m_i) - \frac{PT_c^2}{3}\right]$$

The results for the multiple user code noise reduce to those obtained for the self noise produced by a single user. The total cross-correlation noise produced in the multiple user system is however more complicated than the single user case since the noise terms produced are now not independent.

The total cross-correlation noise produced in the receiver is then given by

$$\Xi^2 = E\left\{\sum_{i=1}^{K}\sum_{n=1}^{K}\varepsilon_i(m)\varepsilon_n(m)\right\} + E\left\{\sum_{i=1}^{K}\sum_{n=1}^{K}\xi_i(m)\xi_n(m)\right\} - 2E\left\{\sum_{i=1}^{K}\sum_{n=1}^{K}\varepsilon_i(m)\xi_n(m)\right\}$$

(197)

$$= \sum_{i=1}^{K}(K-2i+1)PTT_c m_i + K^2PT_cT - \frac{2K^2PT_c^2}{3} - 2E\left\{\sum_{i=1}^{K}\sum_{n=1}^{K}\varepsilon_i(m)\xi_n(m)\right\}$$

The cross product terms in equation 197 only occur when

$$\left\{\frac{1-m_i}{2}\right\} > 1-\left\{\frac{1+m_n}{2}\right\}$$

or (198)

$$m_i < m_n$$

The assumed ordering of the sample values allows the cross product terms to be expressed as

$$2E\left\{\sum_{i=1}^{K}\sum_{n=1}^{K}\varepsilon_i(m)\xi_n(m)\right\} = 2\sum_{i=1}^{K}\sum_{n=i+1}^{K}P\int_{-T\left\{\frac{m_n-m_i}{2}\right\}}^{T\left\{\frac{m_n-m_i}{2}\right\}}\left[T\left\{\frac{m_n-m_i}{2}\right\}-|\tau|\right]$$

$$\left[1-\frac{|\tau|}{T_c}\right]d\tau \qquad (199)$$

$$= PTT_c\sum_{i=1}^{K}\sum_{n=i+1}^{K}(m_n-m_i)-\frac{(K^2-K)2PT_c^2}{3}$$

The total code noise produced in a receiver with K users can be found as

$$\Xi^2 = \sum_{i=1}^{K}(K-2i+1)PTT_cm_i - \sum_{i=1}^{K}\sum_{n=i+1}^{K}PTT_c(m_n-m_i) \qquad (200)$$

$$+K^2PT_cT-\frac{2KPT_c^2}{3}$$

The impact of this code noise can be better seen when the sample values are viewed as random variables. Since the sample values are constrained to the interval $[-1,+1]$, the logical mean for any probability distribution associated with the sample values is zero. Therefore, the "average" code noise produced in a receiver with K users is given by

$$\overline{\Xi^2} = K^2 PT_c T - \frac{2}{3} KPT_c^2 \qquad (201)$$

where the bar denotes an average over the voice ensembles.

The approximation suggests that the performance obtained from multiple codeword modulation formats will degrade with large numbers of users in conference. The additional noise will tend to degrade performance in the "large" signal region to a point that could be unacceptable in a strong signal environment. The performance degradation produced is seen in the noncoherent bi-orthogonal word PWM signal-to-noise ratio approximations. The "large" signal region approximation with code noise from K users introduced into the system is given by $(\Omega^2 = PT^2/\beta^2)$

$$\left(\frac{S}{N}\right)_{l.s.} = \frac{(1-2/\Omega^2)}{(1-\frac{1}{2}\Omega^2 + \Omega^2(K^2/2N - K/N^2))} \left(\frac{S}{N}\right)_{coherent} \qquad (202)$$

The "small" signal S/N approximation with K users producing code noise is given by

$$\left(\frac{S}{N}\right)_{s.s.} = \frac{1.94\Omega^2}{8.54+2.16\Omega^2+\Omega^2(K^2/2N - K/N^2)} \left(\frac{S}{N}\right)_{coherent} \qquad (203)$$

With $K<<N$ the dominant factor introduced by the code noise is $K^2/2N$, the number of users squared, divided by twice the number of "chips" per period. The impact of code noise on system performance can be seen by letting $K^2/2N = 1/20$, which

corresponds to four or five users in a multiple user net and approximately 200-250 "chips" per period. The "small" signal region expression for signal-to-noise ratio does not appreciably change with the introduction of the code noise. The expression for the signal-to-noise ratio in a strong signal environment, however, is altered to

$$\left(\frac{S}{N}\right)_{l.s.} = \frac{(1- 2/\Omega^2)}{(1- \frac{1}{2}\Omega^2 + \Omega^2/20} \left(\frac{S}{N}\right)_{coherent} \quad (204)$$

Figure 23 demonstrates the impact of code noise produced by multiple users as the signal strength is increased. The signal-to-noise ratio plots show that a 3db degradation in system performance can be expected when operating in this configuration.

The coherent bi-orthogonel word PWM signal-to-noise ratio is also altered with introduction of multiple user code noise. The coherent system S/N with K users producing code noise is given by

$$\left(\frac{S}{N+\text{Code Noise}}\right)_{coherent} = \frac{PT^2m^2}{2\beta^2+K^2PTT_c - \frac{2}{3} KPT_c^2} \quad (205)$$

Using only the dominant factor $K^2/2N = 1/20$ as in the non-coherent analysis results in

$$\left(\frac{S}{N+\text{Code Noise}}\right)_{coherent} = \frac{1}{1+\Omega^2/20} \left(\frac{S}{N}\right)_{coherent} \quad (206)$$

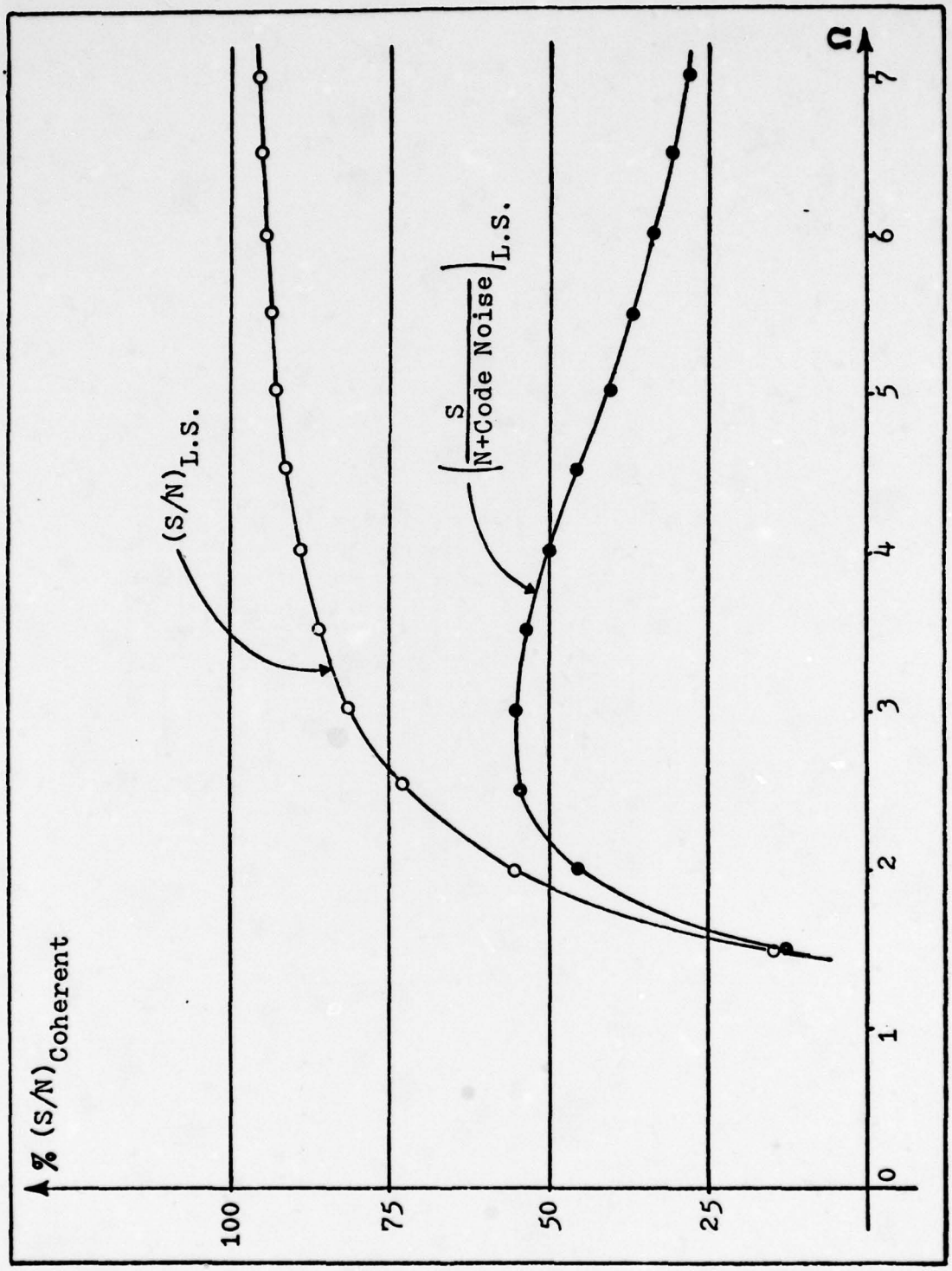

Fig. 23. Signal-to-Noise Degradation with Multiple User Code Noise

In a strong signal environment this is approximately the same result seen in the noncoherent "large" signal expression. The coherent system suffers a 3db degradation at $\Omega \approx 4.5$ and performance continues to degrade with increased signal power.

The exact reduction in system performance is a function of the number of users in a net. Performance will not seriously degrade with the introduction of self noise from a signal user. However, many users in a common net could have a severe impact on system performance. All modulation formats should be tested to determine the exact impact of this code noise phenomenon on pulse-width modulation systems.

VII. Conclusions and Recommendations

Conclusions

Three techniques for pulse-width modulating a spread spectrum carrier have been explored in this paper. These techniques are forms of linear modulation and thus provide both the inherent advantage associated with spread spectrum communications and the capability to superimpose several desired signals. However, linear modulation and maximum-likelihood reception produce a signal-to-noise ratio that can be improved in general only by increasing the transmitted energy.

Antipodal pulse-width modulation is the simplest of the three signal formats and also provides the best expected performance. In signal space this format uses one pseudo-noise code as a bases function and provides a signal locus of length $2\sqrt{E}$. The length of the signal locus was seen to determine the system performance. Antipodal pulse-width modulation, however, requires a phase coherent receiver which will significantly increase the overall system complexity.

Bi-orthogonal word pulse-width modulation increases the signal space dimensions to provide the capability to operate with a noncoherent receiver. This format uses two orthogonal pseudonoise codes as bases function and provides a signal locus length of $\sqrt{2E}$. All performance criteria pointed to

this same 3db degradation in performance from the benchmark antipodal format. When operating in a strong signal region where the S/N>2.0, both the noncoherent and coherent receivers provided approximately the same performance. The noncoherent system, however, exhibited a threshold effect, defined as 3db below coherent performance, around S/N = 1.5 below which performance degraded rapidly.

The final format is tri-orthogonal word pulse-width modulation which attempts to increase the signal locus length to $2\sqrt{2E}$ by adding a third dimension to the signal space. The effective signal locus length, however, was shown to be $\sqrt{2E}$ with the third bases function only adding an additional noise term. The result was a 4.77 db degradation in system performance with a phase coherent receiver and severe distortion in the noncoherent version. This modulation format has unused potential that suggests an alteration could increase the effective signal locus and allow tri-orthogonal word PWM performance to surpass the other formats.

The orthogonality of the bases functions used in the multiple codeword formats was also examined. Using the properties of random binary waveforms the codes were shown to be only approximately orthogonal and actually introduce a code noise into the receiver. The self noise introduced by a single user was shown to have almost no impact on system performance. However, the effects of code noise grows with

both the number of users squared and the signal strength at the receiver. Figure 23 demonstrates how as few as four users in a net can degrade theoretical system performance. The exact impact of code noise in a multiple user net can only be found through carefully constructed performance tests.

Recommendations

It is the recommendation of the author that three aspects of pulse-width modulation be pursued as areas of further study. First, investigate through simulation or experimentation the impact of code noise in multiple user systems. Since theory suggests that code noise grows as the number of users squared, a dense user environment could jeopardize the effectiveness of pulse-width modulation formats. An analysis should also be performed to define the optimum receiver structure in the signal dependent code noise environment (Froelich, 1978:1665). Finally, an analysis of possible methods of improving the tri-orthogonal word PWM format should be explored. This analysis should examine both methods of increasing the effect length of the signal locus in the present linear format and the possible use of a twisted modulation formation that would provide additional noise suppression (Wozencraft, 1965:611).

Bibliography

Davenport, Wilbur B., Jr. and William L. Root. An Introduction to the Theory of Random Signal Noise. New York: McGraw-Hill Book Company, Inc., 1958.

Dixon, Robert C. Spread Spectrum Systems. New York: John Wiley and Sons, Inc., 1976.

Easterling, Mahlon F. "Modulation by Pseudo-Random Sequences," Digital Communications with Space Applications, edited by S.W. Golomb, et al. Englewood Cliffs: Prentice-Hall, Inc., 1964.

Froelich, Gray K., et al. "Optimal Estimation in Signal-Dependent Noise," Journal of the Optical Society of America, Vol. 68, No. 12, pp. 1665-1672, December, 1978.

Haykin, Simon. Communication Systems. New York: John Wiley and Sons, Inc., 1978.

Judge, W.J. "Multiplexing Using Quasiorthogonal Binary Functions," Spread Spectrum Techniques, edited by Robert C. Dixon. New York: IEEE Press, 1976.

Melen, R. and D. Buss. Change Coupled Devises: Technology and Applications. New York: IEEE Press, 1977.

Middleton, David. An Introduction to Statistical Communication Theory. New York: McGraw-Hill Book Company, 1960.

Papoulis, A. Probability, Random Variables and Stochastic Processes. New York: McGraw-Hill Book Company, 1965.

Raemer, Harold R. Statistical Communication Theory and Applications. Englewood Cliffs: Prentice Hall, Inc., 1969.

Van Trees, H.L. Detection, Estimation and Modulation Theory. New York: John Wiley and Sons, Inc., 1968.

Ward, Robert B. "Digital Communications on a Pseudonoise Tracking Link Using Sequence Inversion Modulation," Spread Spectrum Techniques, edited by Robert C. Dixon. New York: IEEE Press, 1976.

Wozencraft, J.M. and I.M. Jacobs. Principles of Communications Engineering. New York: John Wiley and Sons, Inc., 1965.

Ziemer, R.E. and W.H. Tranter. Principles of Communications Systems, Modulation and Noise. Boston: Houghton Mifflin Company, 1976.

Appendix A

Correlation Properties of Binary Waveforms

The sequences which are dealt with in this paper are important because of their correlation properties. The (unnormalized) correlation between two sequences of the same length is defined as (Easterling, 1964:68):

R = number of agreements - number of disagreements (A-1)

The (unnormalized) cross-correlation function of two sequences of the same length is the set of correlation values of the one sequence with all of the cyclic permutations of the other sequence. The autocorrelation function of a sequence is the set of correlation values of the sequence with all cyclic permutations of itself.

These correlation concepts may be applied to binary waveforms. In contra-distinction to sequences, binary waveforms are periodic functions of time that extend indefinitely far along the time axis. The correlation of two binary waveforms that have the same period T is defined as:

$$R = \int_0^T c_1(t)c_2(t)dt \qquad \text{(A-2)}$$

The normalized cross-correlation function is defined as:

$$R_{12}(\tau) = \frac{1}{T} \int_0^T c_1(t)c_2(t+\tau)dt \qquad \text{(A-3)}$$

The normalized autocorrelation function of a binary waveform is defined as:

$$R(\tau) = \frac{1}{T} \int_0^T c_1(t)c_1(t+\tau)dt \qquad \text{(A-4)}$$

The random binary wave (Papoulis, 1965:294) which simulates the tossing of a fair coin an infinite number of times is the standard to which other deterministic codes are compared. The random binary wave is defined by the process $\underset{\sim}{y}(t)=\underset{\sim}{x}(t-\underset{\sim}{e})$ where the process $\underset{\sim}{x}(t)$ is

$$\underset{\sim}{x}(t) = \begin{cases} 1 \text{ if heads at kth toss} \\ -1 \text{ if tails at kth toss} \end{cases} \quad (k-1)T_c<t<k\ T_c \qquad \text{(A-5)}$$

and the random variable $\underset{\sim}{e}$ is uniformly distributed in the $[0,T]$ interval and independent of $\underset{\sim}{x}(t)$. The autocorrelation function $R(\tau)$ for the random binary wave is given by

$$R(\tau) = \begin{cases} \left(1-\frac{|\tau|}{T_c}\right), & |\tau| \leq T_c \\ 0 \quad , & |\tau| > T_c \end{cases} \qquad \text{(A-6)}$$

and the corresponding power spectral density (See figureA-1)

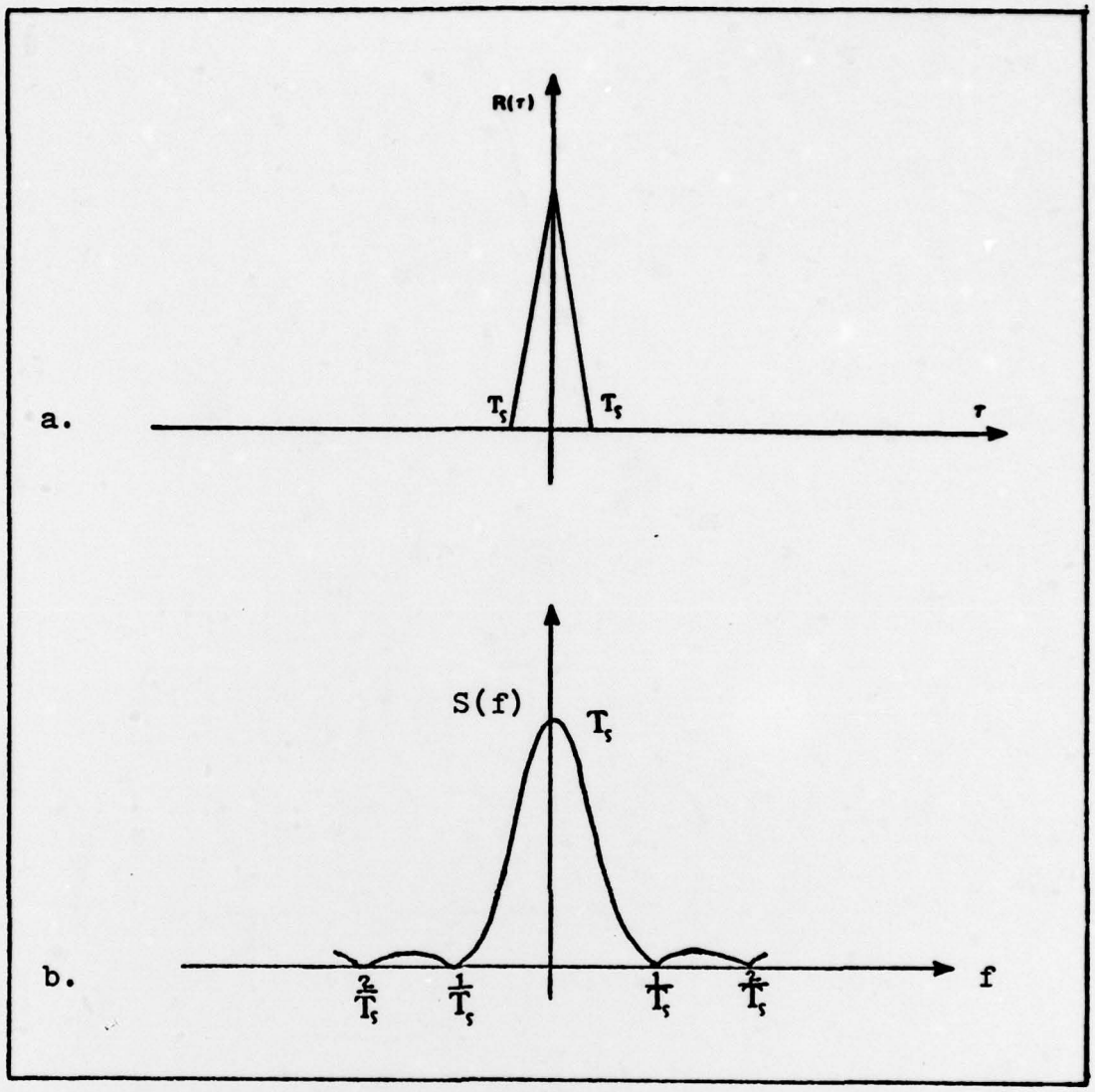

Fig. A-1. Characteristics of Random Binary Wave
(a) Autocorrelation Function (b) Spectral Density

is given by

$$S(f) = T_c \text{sinc}^2(fT_c) \qquad \text{(A-7)}$$

The normalized autocorrelation function $R(\tau)$ for a pseudo-noise binary waveform is given by

$$R(\tau) = \begin{cases} 1 - \frac{N+1}{NT_c} |\tau| , & |\tau| \leq T_c \\ \\ -\frac{1}{N} , & \text{for the remainder of the period} \end{cases} \quad \text{(A-8)}$$

The corresponding power spectral density for the pseudonoise wave is given by

$$S(f) = \frac{1}{N^2} \delta(f) + \left(\frac{1+N}{N^2}\right) \sum_{\substack{k=-\infty \\ k \neq 0}}^{\infty} \text{sinc}^2\left(\frac{k}{N}\right) \delta\left(f - \frac{k}{NT_c}\right) \quad \text{(A-9)}$$

Comparing the power spectral density characteristics for a pseudonoise waveform given in Figure 1 of the text with the random binary wave, they both have an envelope of the same form, namely, $\text{sinc}^2(fT)$, which depends only on the duration T_c . The fundamental difference is that whereas the random binary sequence has a continuous spectral density characteristic, the corresponding characteristic of linear maximal sequence consists of delta functions spaced $1/NT_c$ Hertz apart.

Easterling points out several characteristics of the pseudonoise power spectrum that should be noted. First, it is a line spectrum with frequencies at multiples of the fundamental frequency. Second, because the binary waveform is a constant amplitude square wave and hence has constant power, there is a scale factor inversely proportional to the period of the sequence. Thus if the period of the

sequence is doubled, the lines in the spectrum become twice as dense and the power of each is reduced by a factor of two. Third, there is an envelope of the spectrum which is determined by the digit or chip period of the waveform. The bandwidth required to transmit a waveform with a given fidelity is independent of the length of the sequence, but is determined solely by the digit or chip period. The pseudonoise sequences with very long periods are therefore excellent approximations of random sequences with equal chip duration.

Appendix B

The Confluent Hypergeometric Function

The confluent Hypergeometric function ${}_1F_1(\alpha;\beta;\pm x)$ is represented by

$$ {}_1F_1(\alpha;\beta;\pm x) = 1+ \frac{\alpha}{\beta}\frac{(\pm x)}{1!} + \frac{\alpha}{\beta}\frac{(\alpha+1)}{(\beta+1)}\frac{(\pm x)^2}{2!} + \ldots \frac{(\alpha)_n}{(\beta)_n}\frac{(\pm x)^n}{n!} + \ldots $$

$$ = \sum_{n=0}^{\infty} \frac{(a)_n}{(\beta)_n}\frac{(\pm x)}{n!} \qquad \text{(B-1)} $$

where $(\alpha)_n \triangleq \alpha(\alpha+1)\ldots(\alpha+n-1), (\alpha)_0 \triangleq 1$. This function is analytic (holomorphic) and is a solution of Kummer's differential equation

$$ x\frac{d^2F}{dx^2} + (\beta-x)\frac{dF}{dx} - \alpha F = 0 \qquad \text{(B-2)} $$

A useful asymptotic development is

$$ {}_1F_1(\alpha;\beta;-x) \simeq \frac{\Gamma(\beta)x^{-x}}{\Gamma(\beta-\alpha)} \sum_{m=0}^{\infty} \frac{(\alpha)_m(\alpha-\beta)+1)m}{m!x^m} \qquad \mathrm{Re}x>0 $$

$$ \frac{\Gamma(\beta)x^{-\alpha}}{\Gamma(\beta-\alpha)} \left[1+ \frac{(\alpha)(\alpha-\beta+1)}{1!x} x \ldots \right] \qquad \text{(B-3)} $$

while functions of positive and negative argument are related by Kummer's transformation

$$ {}_1F_1(\alpha;\beta;x) = e^{x}\,{}_1F_1(\beta-\alpha;\beta;-x) \qquad \text{(B-4)} $$

$$ {}_1F_1(\alpha;\beta;-x) = e^{-x}\,{}_1F_1(\beta-\alpha;\beta;x) \qquad \text{(B-5)} $$

For special values of α and β, ${}_1F_1$ can be expressed in terms of other analytic functions. When $2\alpha=\beta=1,2,3,\ldots$, ${}_1F_1$ is given in terms of modified Bessel functions,

$$ {}_1F_1(\alpha;2\alpha;\pm x)=2^{2\alpha-1}\,\frac{\Gamma(2\alpha)}{(\pm x)^{\alpha-\frac{1}{2}}}\,e^{\pm x/2}\,I_{\alpha-\frac{1}{2}}\left(\frac{\pm x}{2}\right);\ 2\alpha=1,2\ldots \qquad \text{(B-6)} $$

Then when α is a half integer and β is a positive integer as used in expected value of the envelope density function, ${}_1F_1$ can be expressed in terms of modified Bessel functions of the first kind. The relationship required in the expected value expression is given by

$$ {}_1F_1(-\tfrac{1}{2};1;-x) = e^{-x/2}\left[(1+x)\,I_0(x/2)+xI_1(x/2)\right] \qquad \text{(B-7)} $$

Vita

Frank Davis Tiller was born on June 7, 1947, in Portsmouth, Virginia. After graduating from Amherst County High School in Amherst, Virginia in 1965, he attended Virginia Polytechnic Institute from which he received the degree of Bachelor of Science in Electrical Engineering in 1970. He was employed by the General Electric Company in Hickory, North Carolina until December 1970, when he entered Officer Training School and was commissioned in the USAF in April 1971. Captain Tiller has held assignments in European Communications Area, Rhein Main AB, Germany and Tactical Communications Area, Langley AFB, Virginia. In January 1978, Captain Tiller entered the Air Force Institute of Technology Graduate Electrical Engineering program at Wright-Patterson AFB, Ohio.

Permanent Address: Route 1 Box 281A
Madison Heights, VA 24572

UNCLASSIFIED
SECURITY CLASSIFICATION OF THIS PAGE (When Data Entered)

REPORT DOCUMENTATION PAGE		READ INSTRUCTIONS BEFORE COMPLETING FORM
1. REPORT NUMBER AFIT/GE/EE/79-39	2. GOVT ACCESSION NO.	3. RECIPIENT'S CATALOG NUMBER
4. TITLE (and Subtitle) PULSE-WIDTH MODULATION OF SPREAD SPECTRUM CARRIERS		5. TYPE OF REPORT & PERIOD COVERED MS Thesis 6. PERFORMING ORG. REPORT NUMBER
7. AUTHOR(s) Frank D. Tiller Captain, USAF		8. CONTRACT OR GRANT NUMBER(s)
9. PERFORMING ORGANIZATION NAME AND ADDRESS Air Force Institute of Technology (AFIT/EN) Wright-Patterson AFB, Ohio 45433		10. PROGRAM ELEMENT, PROJECT, TASK AREA & WORK UNIT NUMBERS 63727F/2277
11. CONTROLLING OFFICE NAME AND ADDRESS Rome Air Development Center/DCID Griffis AFB, New York 13441		12. REPORT DATE December 1979 13. NUMBER OF PAGES 120
14. MONITORING AGENCY NAME & ADDRESS(if different from Controlling Office)		15. SECURITY CLASS. (of this report) Unclassified 15a. DECLASSIFICATION/DOWNGRADING SCHEDULE

16. DISTRIBUTION STATEMENT (of this Report)
Approved for public release; distribution unlimited.

17. DISTRIBUTION STATEMENT (of the abstract entered in Block 20, if different from Report)

18. SUPPLEMENTARY NOTES
Approved for public release; IAW AFR 190-17

J.P.Hipps, Major,USAF
Director of Information

19. KEY WORDS (Continue on reverse side if necessary and identify by block number)
Spread Spectrum Communications
Pulse-Width Modulation
Code Noise
Antijam Communications

20. ABSTRACT (Continue on reverse side if necessary and identify by block number)
Spread spectrum techniques can produce results in communication and navigation systems that are not possible with standard signal formats. The results of particular interest are the ability to screen messages from eavesdroppers, high resolution ranging and the rejection of interference.

Three modulation schemes that exploit these spread spectrum properties are analyzed in this thesis. All three techniques use

DD FORM 1 JAN 73 1473 EDITION OF 1 NOV 65 IS OBSOLETE

UNCLASSIFIED
SECURITY CLASSIFICATION OF THIS PAGE (When Data Entered)

pulse-width modulation to encode sampled analog voice signals onto a digital phase coded carrier. The performance analysis assumes transmission in the presence of white Gaussian noise and CW jamming. The performance analysis uses maximum likelihood estimation to define the sample parameter estimate and associated error variance when probability density functions can be defined for the receiver sample outputs. When the density function is not available a second moment analysis is used to define the expected signal-to-noise ratio.

The results are extended to include the introduction of signal dependent code noise into the receiver resulting from the degradation of the orthogonal code word structure. The impact of code noise on system performance is seen to grow with the number of users squared and the received signal energy.